An Assessment of Deploying Advanced Pumped Storage Hydropower Technology in U.S. Electricity Markets

Mark Jacobson,[1†] Jin Tan,[1] Eduard Muljadi,[1]
Dave Corbus,[1] Zerui Dong,[2] Kim Jinho,[2] Eli Bailey,[3]
Matt Pevarnik,[4] Martin Racine,[4] Antoine St. Hilaire,[4]
and Chris Hodge[5]

1 National Renewable Energy Laboratory
2 Auburn University
3 Absaroka Energy
4 General Electric
5 Grid Dynamics

† Author deceased

NREL is a national laboratory of the U.S. Department of Energy
Office of Energy Efficiency & Renewable Energy
Operated by the Alliance for Sustainable Energy, LLC

This report is available at no cost from the National Renewable Energy Laboratory (NREL) at www.nrel.gov/publications.

Contract No. DE-AC36-08GO28308

Technical Report
NREL/TP-7A40-74775
July 2023

An Assessment of Deploying Advanced Pumped Storage Hydropower Technology in U.S. Electricity Markets

Mark Jacobson,[1†] Jin Tan,[1] Eduard Muljadi,[1]
Dave Corbus,[1] Zerui Dong,[2] Kim Jinho,[2] Eli Bailey,[3]
Matt Pevarnik,[4] Martin Racine,[4] Antoine St. Hilaire,[4]
and Chris Hodge[5]

1 National Renewable Energy Laboratory
2 Auburn University
3 Absaroka Energy
4 General Electric
5 Grid Dynamics

† Author deceased

Suggested Citation
Jacobson, Mark, Jin Tan, Eduard Muljadi, Dave Corbus, Zerui Dong, Kim Jinho, Eli Bailey, et al. 2023. *An Assessment of Deploying Advanced Pumped Storage Hydropower Technology in U.S. Electricity Markets*. Golden, CO: National Renewable Energy Laboratory. NREL/TP-7A40-74775. https://www.nrel.gov/docs/fy23osti/74775.pdf.

NREL is a national laboratory of the U.S. Department of Energy
Office of Energy Efficiency & Renewable Energy
Operated by the Alliance for Sustainable Energy, LLC

This report is available at no cost from the National Renewable Energy Laboratory (NREL) at www.nrel.gov/publications.

Contract No. DE-AC36-08GO28308

Technical Report
NREL/TP-7A40-74775
July 2023

National Renewable Energy Laboratory
15013 Denver West Parkway
Golden, CO 80401
303-275-3000 • www.nrel.gov

NOTICE

This work was authored by the National Renewable Energy Laboratory, operated by Alliance for Sustainable Energy, LLC, for the U.S. Department of Energy (DOE) under Contract No. DE-AC36-08GO28308. Funding provided by U.S. Department of Energy Office of Energy Efficiency and Renewable Energy Water Power Technologies Office. The views expressed herein do not necessarily represent the views of the DOE or the U.S. Government.

Cover Photos by Dennis Schroeder: (clockwise, left to right) NREL 51934, NREL 45897, NREL 42160, NREL 45891, NREL 48097, NREL 46526.

Acknowledgments

The National Renewable Energy Laboratory (NREL) would like to thank the Water Power Technologies Office of the U.S. Department of Energy not only for their funding but also for their active participation and guidance throughout this project.

NREL would like to thank Absaroka Energy for their continuous participation throughout the study process and for providing a Reference Project (their Gordon Butte project) from which our team could use current information on new siting and permitting techniques to expedite pumped storage hydropower development, updated installation costs, and various analytical studies and report preparation and review.

Additionally, NREL would like to extend its appreciation to GE Renewable Energy for their active participation in the areas of team meetings, modeling output review, costing data and technology performance data, and report preparation and review.

NREL would like to acknowledge Auburn University and their team for their strong participation in all meetings, modeling support, writing of journal articles, and report preparation and review.

NREL would like to thank Grid Dynamics for their participation in project meetings, market insight, and report preparation and review.

List of Acronyms

ALP	Alternative Licensing Process
AS-PSH	adjustable speed pumped storage hydropower
CAISO	California Independent System Operator
CapEx	capital expenditures
COI	center of inertia
C-PSH	conventional pumped storage hydropower
DFIG	doubly-fed induction generator
DLA	Draft License Application
DOE	U.S. Department of Energy
E3	Energy + Environmental Economics
EIA	U.S. Energy Information Administration
EPCL	Engineer's Program Control Language
ERCOT	Electric Reliability Council of Texas or Texas Interconnection
FACTS	flexible AC transmission system
FERC	Federal Energy Regulatory Commission
GE	General Electric
GW	gigawatt
HSC	hydraulic short circuit
IBR	inverter-based resources
IEEE	Institute of Electrical and Electronics Engineers
ILP	Integrated Licensing Process
ISO	independent system operator
ISO-NE	Independent System Operator–New England
kW	kilowatt
LCOE	levelized cost of energy
LGIA	Large Generator Interconnection Agreement
LSP	Light Spring
MW	megawatt
MWh	megawatt-hour
NEPA	National Environmental Policy Act
NERC	North American Electric Reliability Corporation
NREL	National Renewable Energy Laboratory
OpEx	operating expenditures
PI	proportional-integral
PSH	pumped storage hydropower
PSLF	positive sequence load flow
PV	photovoltaic(s)
Q-PSH	quaternary pumped storage hydropower
ROCOF	rate of change of frequency
SCADA	supervisory control and data acquisition
SCESS	supercapacitor energy storage system
STATCOM	static synchronous compensator
DTC	dynamic transmission control
TLP	traditional licensing process
T-PSH	ternary pumped storage hydropower

T/Q-PSH	ternary or quaternary pumped storage hydropower
TRL	technology readiness level
VSC	voltage source converter
WI	Western Interconnection
WPP	wind power plant

Executive Summary

Pumped storage hydropower (PSH) is a type of hydropower technology where energy can be stored and generated by moving water between two reservoirs of differing elevations. In addition to providing 97% of the total utility-scale hydropower storage in the United States, PSH plants have operational characteristics—such as high ramp rates and the ability to provide reserves—that contribute to greater flexibility and reliability of the power grid.[1] New PSH technologies can provide additional flexibility beyond existing, fixed-speed units. With the emergence of high levels of variable renewable energy resources (e.g., wind and solar), energy storage is expected to be crucial to the reliability and reliance of the power grid in a low-carbon future. At diurnal and longer durations, PSH plants have some of the lowest costs per unit of energy,[2] have been proven to be reliable and efficient, are not cycle-limited, and typically have long lives, often exceeding 50 years.

Approximately 70% of existing PSH projects were built to provide bulk storage (i.e., rated capacities greater than 100 megawatts [MW] and more than 4 hours of storage). Despite the important benefits that PSH offers, development stopped almost completely in the 1990s due to factors related to high capital costs, market and regulatory uncertainties, and the low price of natural gas.

The work presented here focuses on a new generation of PSH: ternary PSH (T-PSH) and quaternary PSH (Q-PSH; to simplify nomenclature, the term T/Q-PSH is used throughout this report when discussing topics that are applicable to both T-PSH and Q-PSH). Given recent experience with T/Q-PSH in Europe, grid operators in the United States and elsewhere are increasingly focusing their attention on T/Q-PSH as a proven, financeable technology that can offer utility-scale, long-duration, fast-acting energy storage capabilities and grid services. T/Q-PSH differs from conventional PSH in that it can provide fast-response ancillary services during both generating and pumping operations. This capability together with fast mode switching times are key attributes that make T/Q-PSH technologies attractive for managing and stabilizing electricity systems with high amounts of variable renewable energy.

This work was performed by the National Renewable Energy Laboratory (NREL), Absaroka Energy, GE Renewable Energy, Auburn University, and Grid Dynamics. Operational and cost information for this project comes from Absaroka Energy's research completed as part of their due diligence efforts in developing their 400-MW Gordon Butte Advanced Pumped Storage Hydro Project in central Montana, which is the reference project for this study and which was proceeding in parallel to this effort.

Motivated by the increasing need for PSH to provide reliability services to grid operation as the amount of variable generation increases across the United States, the team had the following objectives:

- Characterize how T/Q-PSH contributes to grid reliability and stability
- Understand the capital and development costs of T/Q-PSH.

To achieve the objectives, the team conducted a market study to investigate three classes of pumped storage hydropower technologies: fixed speed, hybrid, and adjustable speed, described in

[1] http://ceeesa.es.anl.gov/projects/psh/ANL-DIS-14-7_Advanced_PSH_Final_Report.pdf
[2] http://www.sandia.gov/ess/publications/SAND2015-1002.pdf

detail herein. A grid reliability and stability analysis evaluated the ability of T/Q-PSH, coupled with dynamic transmission, to provide a more cost-effective solution for the power system and greater grid stability. It also examined transients associated with the unique characteristics of T-PSH: rapid mode switching and hydraulic short-circuit operation, penstock sharing, and gate valve operation. Finally, a techno-economic analysis was completed, including a cost sensitivity analysis to determine which cost categories present the highest risk to the levelized cost of energy. The PSH unit under study is 1,276 MW in the small test system (a 5-gigawatt, 10-bus system) that was useful for characterizing the performance of T/Q-PSH under a wide variety of system contingencies. The study examined how T/Q-PSH performed while in each of its operating modes and when switching modes, and how the gate value and shared penstock design affected unit performance.

The main findings of the report are:

- Q-PSH can provide better frequency support than other PSH technologies.
- Q-PSH can provide frequency support similar to that of a conventional PSH unit twice its size.
- T/Q-PSH, when configured as part of a dynamic transmission control system, can provide congestion, power, and voltage control.
- The T/Q-PSH technology proposed for the Reference Project is approximately 40% less expensive than a traditional lithium-ion battery.

The analysis is summarized in Figure ES-1, which compares the capabilities of the various types of PSH.

Pumping Mode of Different PSH Technologies						
Service Types		C-PSH	AS-PSH DFIG	AS-PSH Full Conv.	T-PSH	Q-PSH
Ancillary Services	Inertial Response	🟢	🟡	🟡	🟢	🟢
	Primary Frequency Response	🔴	🟡	🟡	🟢	🟢
	Frequency Regulation	🔴	🟡	🟡	🟢	🟢
	Load Following	🔴	🟢	🟢	🟢	🟢
	Spinning Reserve	🔴	🟢	🟢	🟢	🟢
Others	Start-up (seconds [s])	300	280	40	120	120
	Pump-Generating (s)	190	190	190	25	30
	Synchronous Condenser-Generating (s)	100	100	100	20	30
	Pumping range (%)	100%	60%–100%	60%–100%	0%–100%	0%–100%

🔴 Uncapable 🟡 Capable with ancillary control 🟢 Capable

Figure ES-1. Pumped storage hydropower technology capability comparison (in pumping mode).

The "C" and "AS" prefixes to PSH stand for conventional and adjustable speed, respectively. DFIG stands for doubly-fed induction generator; Full Conv. stands for full converter.

Table of Contents

List of Figures

List of Tables

1 Introduction

The electrical grid in the United States is seeing a significant increase in new variable renewable energy generation, and at the same time a large amount of base-load thermal generation is being retired[3]. This dynamic is upending the traditional operation of the grid and is placing a premium on assets that can provide fast-ramping flexible capacity, and regulators, asset owners, and other market stakeholders are seeking information that will enable them to accurately quantify the value and benefits of new flexible capacity technologies. This will help stakeholders to make informed decisions and promote greater levels of future deployment.

Managing the electric grid with the higher penetration of renewables is currently handled by peaking units, namely gas turbines and hydrogeneration. For decades the hydrogeneration fleet has provided a cost-effective way to help keep the grid's supply and demand needs in balance. Recently, installed pumped storage and conventional hydropower facilities have started playing an increasingly important peaking role. Like gas turbine assets, hydropower assets are experiencing more rigorous operational demands, from greater ramping to additional stops and starts. This new operation results in shorter life cycles due to increased cycling fatigue and increased maintenance costs[4].

To address these challenges, industry has responded by developing innovative technologies designed to operate in this new paradigm. The latest peaking gas turbine fleet is not only larger in capacity but also more flexible, with improved ramp rates and operational hours as well as an increased number of allowable starts and stops between major overhauls. Similarly, advanced pumped storage hydropower will incorporate the latest technologies to increase the starting times, ramping rates, and overall longevity of the equipment.

The primary objective of this project was to assess the capabilities of flexible and fast-acting pumped storage hydropower, including ternary PSH (T-PSH) and quaternary PSH (Q-PSH) technologies (collectively known as T/Q-PSH). The technologies were compared to fixed-speed (i.e., conventional) PSH (C-PSH) and adjustable-speed PSH (AS-PSH).This work also examined how T/Q-PSH technology could be dynamically integrated into the transmission grid as part of an optimized control system to provide stability support to the grid (Figure 1). This combination was then applied to provide a systems solution to integration issues in a market with a high contribution of renewable energy.

This unique configuration has the potential to provide a cost-effective integration solution for renewable energy deployment, including grid stability, reliability, and ancillary and balancing services. Additionally, this proposed application has low technical risk, as T-PSH has already been successfully deployed outside the United States; however, an analysis of the benefits of the technology coupled with dynamic transmission has never been completed. Finally, if successfully deployed, this concept supports the U.S. Department of Energy's Hydropower Vision (U.S. Department of Energy 2016), which states that U.S. hydropower could grow from 101 gigawatts (GW) of capacity in 2015 to nearly 150 GW by 2050.

---

[3] See EIA Annual Energy Review, https://www.eia.gov/totalenergy/data/annual/

[4] P. J. Donalek, "Pumped Storage Hydro: Then and Now," in IEEE Power and Energy Magazine, vol. 18, no. 5, pp. 49-57, Sept.-Oct. 2020, doi: 10.1109/MPE.2020.3001418.

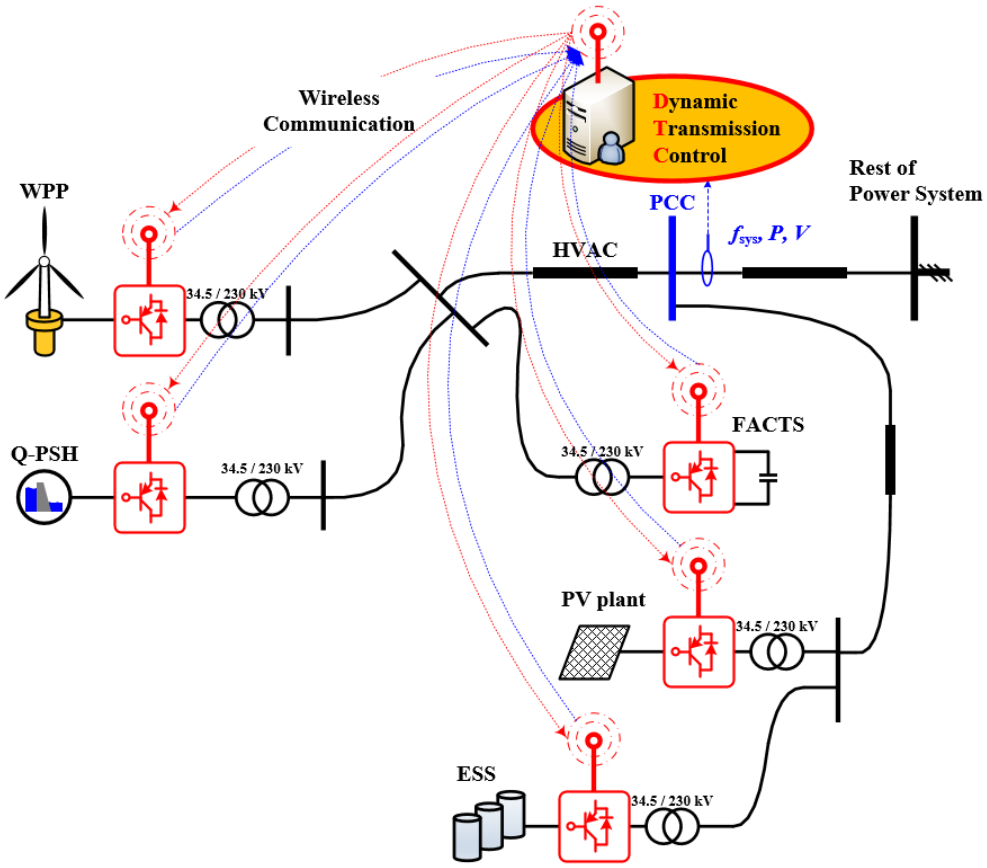

Figure 1. T/Q-PSH with dynamic transmission

The team chosen to complete the study was diverse, including Absaroka Energy, GE Renewable Energy, Grid Dynamics, Auburn University, U.S. Department of Energy (DOE), and the National Renewable Energy Laboratory (NREL). By choosing partners that are actively developing PSH projects, the team was able to leverage recent construction and installation bid proposals, marketization strategies, permitting/licensing/siting best practices, and technology performance and cost data. This approach allowed the team to validate the newly developed dynamic system modeling tools and refine the project design and levelized cost of energy (LCOE) estimates.

A summary of the primary tasks and associated tools and methods the team used to achieve the project objective are as follows:

1. Market Overview

A market study was performed to provide context for this research. The underlying work for the section comes from Absaroka Energy's due diligence efforts in developing their 400-megawatt (MW) Gordon Butte Advanced Pumped Storage Hydro Project in central Montana, which is the reference project for this study (Appendix B; hereafter termed "Reference Project"). The Gordon Butte work provided updated knowledge of the capital and development costs of T/Q-PSH and contributed lessons learned in siting, licensing, and equipment selection from the recent development efforts (Appendix C).

2. Grid Reliability and Stability Analysis

For this power system study, a vendor-neutral dynamic model of T/Q-PSH technologies was developed using GE's positive sequence load flow (PSLF) platform. These models were applied

for varying renewable energy penetration use cases to measure the dynamic benefits, specifically frequency response and output response in the Western Interconnection (WI). The study analyzed the ability of T/Q-PSH, coupled with dynamic transmission, to provide a more cost-effective solution for the power system and greater grid stability (Section 4).

3. Techno-Economic Analysis

A traditional LCOE analysis was completed for this project. Estimated capital and development costs were established by the project team using the Reference Project, strictly following DOE guidelines. A cost sensitivity analysis was also performed to determine which cost categories present the highest risk and to quantify the impact of that risk on LCOE (Section 5).

2 Market Overview

This section summarizes global trends in PSH and market conditions, as well as details on the selection of equipment and the study regions that the Reference Project would likely serve.

2.1 PSH Trends

Globally, there are 170 GW of pumped storage units in operation or under construction. Europe has experienced steady growth of PSH whereas China has undergone accelerated growth (Figure 2). In the past 10 years, China has commissioned 14 GW of PSH, all fixed speed except for one 600-MW variable-speed plant that is under construction. China typically locates their PSH facilities near large cities and can manage the grid with this configuration. In this same period, there has been 1 GW of ternary designs installed in Europe.[5]

In the United States, there are 40 PSH facilities in operation that provide more than 20 GW of capacity and energy storage—approximately 98% of the country's grid energy storage. Grid operators across the United States rely on PSH as an important source of clean, flexible capacity, ancillary services, and energy storage at a low dollar-per-kilowatt rate.

Growth of pumped storage in the United States mainly occurred from 1955 to 1995 as all fixed speed, and most were designed and built to pair with large, inflexible nuclear and coal-fired generation. The paired pumped storage unit was, and still is, a perfect solution for absorbing

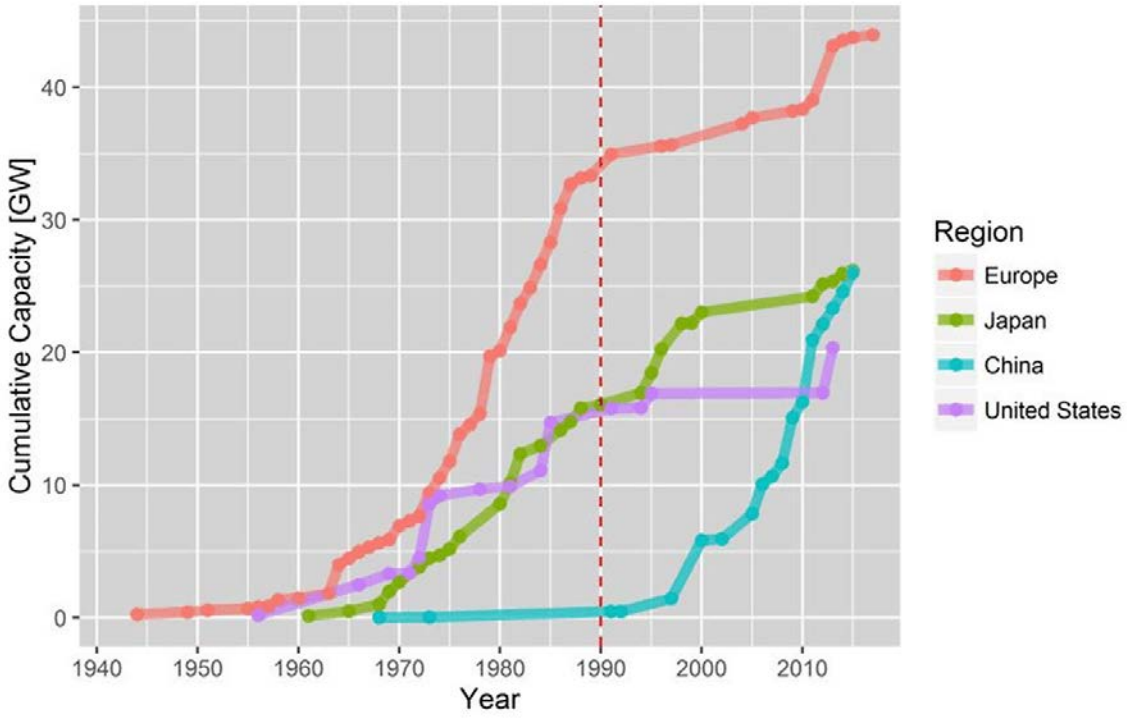

Figure 2. Global installed PSH

Source: Scottish Renewables (2016)

[5] See https://www.andritz.com/hydro-en/hydronews/hn-europe/pumped-storage-by-andritz

excess generation. As these first-generation units aged and rehabilitation was needed, and as new global markets emerged for PSH, the second generation focused on efficiency in the 2000s. Equipment manufacturers designed units with turbine and pump efficiencies greater than 90%. These efficiency gains offered operators competitive solutions to ultimately improve their bottom lines.

Today, we are in the third generation of PSH design, and with the advent of high renewable grids, the application of PSH has evolved from the diurnal time-shifting of large, often inflexible thermal energy generation (nuclear and large coal facilities) to the integration and firming of new VRE such as wind and solar generation. In the older paradigm, PSH technology was only required to change mode twice per 24 hours, from pumping to generating in the morning and generating to pumping at night.

As the grid moves to higher contributions of renewable energy, faster ramping assets that can cycle multiple times per day are required to manage the intra-hour fluctuations of the generation fleet. PSH is now competing with fast-ramping natural gas units (aeroderivative turbines, reciprocating internal combustion engines, and frame combustion turbines) and chemical battery technology to provide this flexible capacity. The contrasts between these different resources are notable, as summarized in Table 1.

Table 1. Market Drivers and Barriers of PSH, Natural Gas, and Batteries

Technology	Driver	Barrier
Natural Gas	• Historically provided peaking and ramping services	• Limitations with fast response for frequency and regulation control • CO_2 emissions as states work toward a carbon-free grid
Batteries	• Install quickly and at points near load centers or other optimal locations • Quickly evolving technology	• Expensive when assuming degradation due to heavy cycling requirements
PSH	• Proven technology that has successfully operated in utility systems around the world for decades • Performance characteristics and costs for individual projects are well known	• Capital intensive • Long lead times and requires a lengthy permitting process to become operational

Given recent experience with T/Q-PSH in Europe, grid operators in the United States and elsewhere are increasingly focusing their attention on T/Q-PSH as a proven, financeable technology that can offer utility-scale, long-duration, fast-acting energy storage capabilities and grid services. In addition, these facilities can also offer replacement grid inertia, helping to replace the spinning mass lost through coal and gas retirements. Therefore, T/Q-PSH is quickly emerging as a viable resource and is appears to be well-positioned for future deployment throughout the United States.

There are more than 16 GW of PSH projects that have received preliminary permits from the Federal Energy Regulatory Commission (FERC), and more than 8 GW pending preliminary FERC permits. In addition, three projects (including the Gordon Butte Reference Project) totaling nearly 2 GW have received FERC licenses. All three projects are in late-stage design. However, a T/Q-

PSH project has yet to be built in the United States. While T/Q-PSH represents one of the most effective, efficient, and robust long-term technologies available to meet the challenges facing the evolving U.S. grid, the technology involves significant engineering, construction, and financing challenges. Although it appears likely that many of the engineering and construction challenges may have been addressed given recent overseas deployments, financing challenges remain.

In the United States, PSH projects have traditionally been deployed through the utility model, which allowed for long-term valuation methodologies that bolster their ability to be cost-effective in incumbent markets. However, as power markets and the capital markets that support them have evolved, valuation methodologies have become more market-based and shorter-term. Valuations are often limited to a 30-year horizon, which does not adequately value the long-term nature of PSH technology. As this body of work demonstrates, this technology represents significant value to our energy system but does not fit into today's traditional valuation engines.

The demonstrable shift in the composition of the supply fleet and market operations has led to the development of an entire portfolio of new advanced products to support the grid. Volumes of product in this segment are low, but the risk implications associated with their underperformance are very high. This has led to a careful and measured adoption of these products to date. As each balancing authority across the country addresses these products, they will value different aspects of their performance uniquely based on their fleet makeup, load profile, and business model. This results in a lack of standardization, which complicates product definition and pricing methodologies.

To further advance the deployment of the next generation of PSH, knowing how these new technologies will operate with the anticipated future grid is of great interest for developers/financiers, utilities, balancing authorities, and grid operators. Developers and the like are relying on T/Q-PSH modeling to quantify the benefits of the technology to the future grid.

2.2 Regional Study Areas

When considering a PSH project, the developer must analyze numerous items, as categorized in Figure 3. Of first consideration is the potential markets that the PSH plant would serve, including details such as load curves, market type (regulated or deregulated), generation portfolio, grid stability, and renewable portfolio standards. Developers often model these markets for today's generation mix as well as for the anticipated markets based on offtakers' integrated resource plans and state renewable portfolio standards.

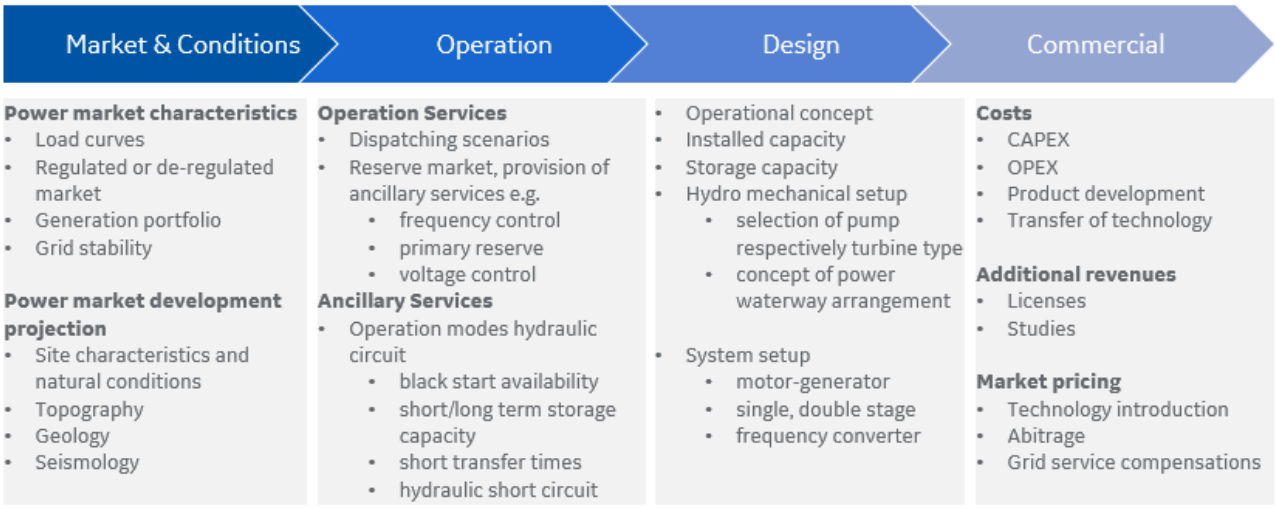

Figure 3. Main decision criteria for PSH technologies (from a developer's perspective)

Once the market has been well-defined, matching the equipment to serve this market requires additional detailed analysis. The four available PSH technologies come in different configurations and generate differently, which impacts costs and creates different flexibility profiles that result in different value/revenue streams depending on the market. In addition, flexibility and reactivity are very important considerations for the future market, and thus transition speeds and response times for each of the four equipment options also need to be considered. This equipment evaluation process, as noted, requires complete collaboration with the comprehensive project team, and at the end, the completed matrix shown in Table 2 was used to make the final equipment selection of Q-PSH for the Reference Project. The quaternary design was initially selected for the Reference Project.

Table 2. PSH Equipment Selectivity Matrix Completed for the Reference Project (Source: Absaroka Energy)

	Costs					Revenues					Main Interests	
400 MW PSH Configuration	Electrical & Mechanical	Submergence	Footprint	O&M	Refrences	Power	Efficiency	Arbitrage	Capacity	Ancillary Services	Flexibility	Reactivity
T-PSH (3 units)	-	+	-	-	-	+	-	+	+	+	+	+
C-PSH (3 units)	+	-	+	+	+	+					-	-
C-PSH (4 units)	+	-		+	+	+						-
Q-Pump + Pelton (3 + 3 units)	-		-	-	+	+	+	+	+	+	+	+
Q-Pump 2 stages + Francis (200MW)	-		-	-	+	+	+	+	+	+	+	+
Q-Pump 3 stages + Francis (200MW)	-	+	-	-	+	+	+	+	+	+	+	+
Q-Pump 2 stages + Francis (133MW)	-		-	-	+	+	+	+	+	+	+	+
Q-Pump 3 stages + Francis (133MW)	-	+	-	-	+	+	+	+	+	+	+	+
VS-PSH (3 units - all fully fed)		-	+	-		+	+	+		+	+	+
VS-PSH (3 units - 2 fully fed)		-	+	-		+	+	+		+	+	+
VS-PSH (3 units - 1 fully fed)	+	-	+			+		+		+	+	
VS-PSH (4 units - all fully fed)		-		-	+	+	+	+		+	+	+
VS-PSH (4 units - 2 fully fed)	+	-			-	+		+		+	+	
VS-PSH (2 STAGE 3 units - all fully fed)	-		+	-		+	+	+		+	+	+
VS-PSH (2 STAGE 3 units - 2 fully fed)			+		-	+		+		+	+	
VS-PSH (2 STAGE 4 units - all fully fed)	-			-	+	+	+	+		+	+	+
VS-PSH (2 STAGE 4 units - 2 fully fed)					-	+		+		+	+	

With the above in mind, Absaroka Energy chose the Gordon Butte site for the new pumped storage plant—a new utility-scale energy storage facility providing transmission system regulation

services, integration of renewable energy generation, flexible capacity, and ancillary services to maintain transmission reliability for electrical utilities in the northern Great Plains and Northwest. The project will be in the Western Interconnection and connect to the Colstrip twin 500-kilovolt (kV) transmission lines, which run from Colstrip, Montana (Figure 4), to load markets in Washington, Oregon, and Northern California.

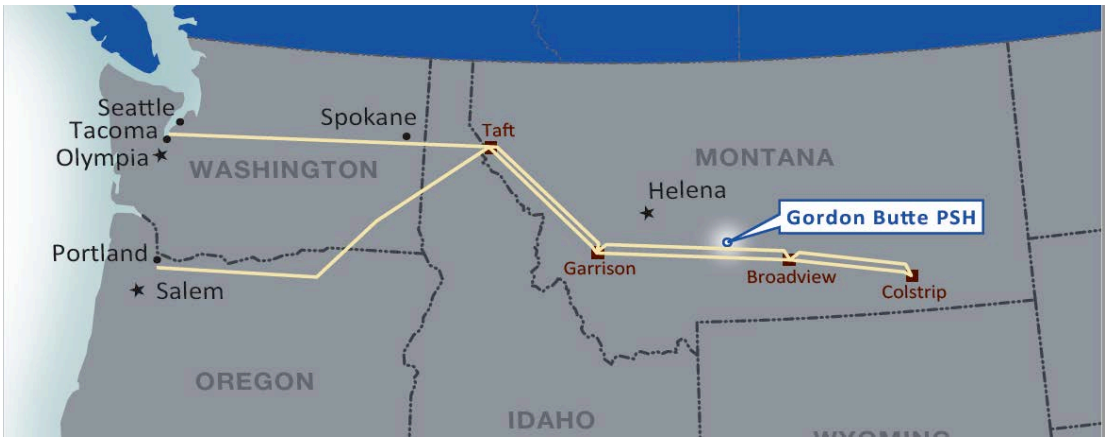

Figure 4. Reference project location

Source: Absaroka Energy

In this study, the team assessed the two potential service markets for the Gordon Butte project, the Northwest Power Pool (NWPP) and the area operated by the California Independent System Operator (CAISO). Both areas have high amounts of renewables and would benefit from the ability of T/Q-PSH to support variable generation.

2.2.1 Northwest Power Pool

Examining PSH in the Northwest Power Pool (Figure 5), Energy and Environmental Economics (E3) recently published a study titled *Resource Adequacy in the Pacific Northwest* (Ming et al. 2019). This study was sponsored by Puget Sound Energy, Avista Utilities, NorthWestern Energy, and the Public Generating Pool—a trade association representing 10 consumer-owned utilities in Washington and Oregon. Among the most salient findings of E3's comprehensive analysis of Pacific Northwest capacity issues was that, due to load growth and announced coal plant retirements, the region faces a potential 8-GW capacity deficit by 2030 unless new dispatchable capacity is constructed. Absent such construction, the regional loss of load probability will grow to 48% by that date (5% loss of load probability is the standard used by Western Electric Coordinating Council utilities).

The Northwest Power and Conservation Council is currently drafting its midterm assessment of its Seventh Power Plan and has also noted the Pacific Northwest faces resource adequacy issues absent new construction. The Council's Resource Adequacy study is anticipated to predict loss-of-load probability numbers of 30% and over, along the same trend line as E3's assessment. In discussions with regional utilities and regulatory commissions, there is disagreement about the modeling and estimates of the region's resource adequacy deficits, but many agree that resource adequacy is a concern going forward.

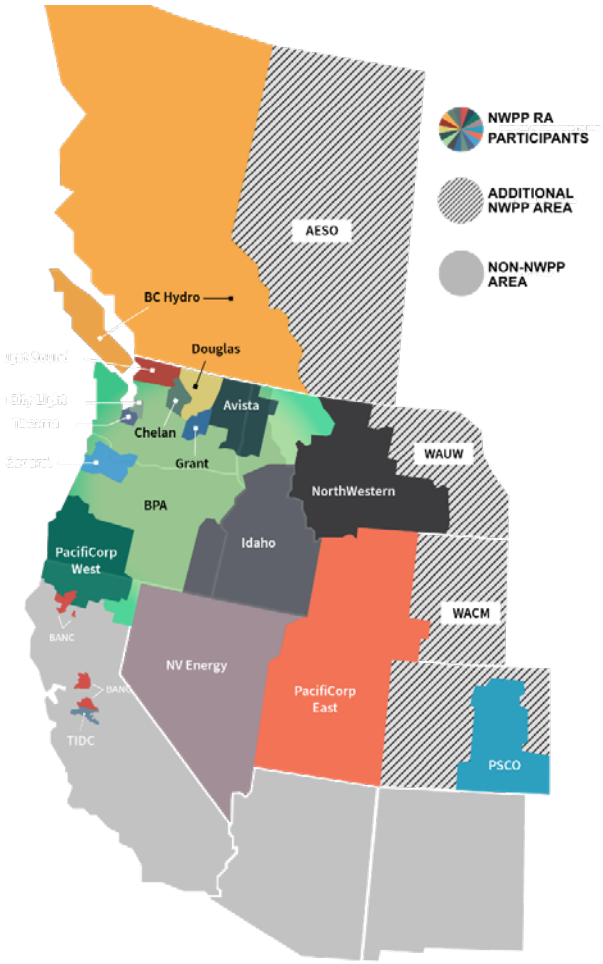

Figure 5. Northwest Power Pool territory

Illustration from NWPP Resource Assessment, Jan. 22, 2021

In addition to resource adequacy deficits, there is the upcoming retirement of Colstrip Units 3 and 4, which will add an additional 1.5 GW to the regional capacity deficit. In June 2019 Talen Energy, the operator of Colstrip Generation Station, announced the closure of the older Units 1 and 2 by December 2019, which have a total capacity of 614 MW. While nothing has been announced to date, the future of the newer and larger Units 3 and 4 (with a combined capacity of 1,500 MW) is being legislated in Washington and Oregon, where those states are taking aggressive measures to end coal-by-wire imports.

Recently, the Washington state legislature enacted mandates that their utilities achieve zero fossil fuels in their resource base by 2045. This was modeled after California's zero-carbon legislation passed in 2018. Its major near-term provisions include a directive that no Washington utility is supplied by coal by 2025. This provision will impact Puget Sound Energy, Avista, and PacifiCorp, all of whom own shares of Colstrip Generation Station Units 3 and 4, raising the likelihood that the plant will close in 2025—10 years early. Next, by 2030, all Washington utilities must be 80% carbon-free, in terms of the power resources used to supply their load. This provision will not only require substantial renewable energy acquisition by the utilities

over the next 10 years but will also require those utilities to offset any carbon emission associated with the use of their existing gas-fired resources with purchase of renewable energy credits or other approved noncarbon measures.

In 2016, Oregon passed the Clean Electricity and Coal Transition Act. This law transitions Oregon's largest utilities, Portland General Electric and Pacific Power, off coal-fired electricity by 2030. On a parallel path, the utilities are also required to generate 50% of their electricity from renewable generation. In 2019, a legislative effort to implement a statewide cap and trade program and reinvest the money from this program into clean energy and infrastructure, job creation, and environmental remediation, narrowly failed in the state's legislature.

As a result of these dynamics, energy storage technologies such as batteries and closed-loop PSH are the most likely new capacity resources for Pacific Northwest entities. There may be some limited carbon-free capacity from existing hydropower providers (e.g., Bonneville Power Administration, the Columbia River public utility districts, Seattle City Light, PowerEx), but it is likely to be limited in both quantity and duration. With only batteries and PSH available (in lieu of combustion turbines), and an 8-GW projected capacity deficit by 2030, capacity acquisitions will be different and significantly more challenging than during the past 20 years. In addition to renewable energy, battery and PSH resources are expected to be needed to help meet reliability needs and provide renewable resource firming requirements as the region approaches 2030.

2.2.2 California Independent System Operator

CAISO (Figure 6) has been an early adopter of the trends that are currently playing out in the NWPP. In September 2018, the State of California passed a bill requiring 60% of the state's electricity to come from renewables by 2030. In addition to this legislation is their Climate Strategy, which set the goal of reducing greenhouse gas emissions to 40% below 1990 levels by 2030. CAISO already struggles with issues of oversupply, curtailment, and adequate ramping with current variable renewable energy resources at 30% penetration.

According to CAISO daily net load curves, four distinct ramp periods occur each day. The steepest daily ramp is in the evening, when CAISO must dispatch resources to meet a ramp of 11,000 MW. CAISO's difficulty meeting system demands, illustrated by the daily net load curves (now commonly known as the "Duck Curve"), is due to their lack of sufficient flexible capacity. Presently, gas plants and electricity imports are used to meet ramping requirements, but these options face compliance issues with the mandates focused on clean electricity and climate change from the State of California.

Additionally, contractual-based imports that do not provide CAISO the ability to reduce and ramp down are forcing the curtailment of renewables. In 2018, CAISO curtailed 460,000 megawatt-hours (MWh) of renewables. This number is only projected to increase as more renewables enter the grid. As a result, CAISO is looking to increase their energy storage capacity to store renewable energy oversupply for use during hours of high demand. Energy storage is also being evaluated to reduce CAISO's reliance on gas plants and imports to meet daily ramping requirements.

As of August 2018, California's three largest investor-owned utilities procured or sought approval to procure almost 1.5 GW of energy storage. This is in response to an assembly bill that set a target of 1.3 GW of energy storage by 2020. In order to meet this goal and encourage energy storage growth, CAISO is working on an initiative called Energy Storage and Distributed Energy Resources. The goal of this initiative is to reduce barriers to energy storage resources, fully compensate storage for the services it provides, and increase participation in the wholesale market.

FERC issued Order 841 on February 15, 2018, in which it directed regional grid operators to remove barriers to the participation of energy storage resources in wholesale markets. Regional grid operators were asked to establish rules that open capacity, energy, and ancillary services markets to energy storage. In December 2018, CAISO filed revisions to Order 84 that outlined their plans for energy storage integration. According to the Energy Storage Association, CAISO's filings were the closest to compliance with FERC Order 841 when compared to other grid operators, and the organization commended CAISO for its efforts.

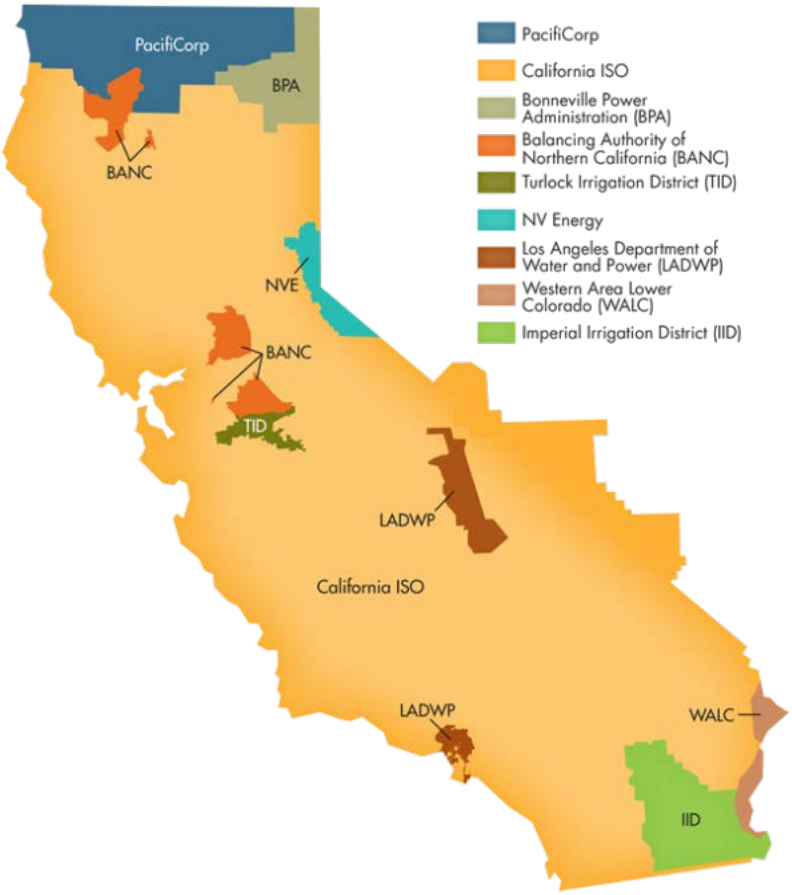

Figure 6. CAISO operating footprint.

Illustration from California Energy Storage Alliance

3 Technology Overview

Depending on the market site-specific conditions, the developer will need to decide whether a fixed-speed, variable-speed, ternary, or quaternary PSH configuration is the best market fit.

Each of these four configurations (Figure 7) provides a different grid solution and varying capital, operation, and maintenance costs. Both conventional and ternary are fixed-speed units, where the pump/turbine operates at a fixed synchronous speed for all modes of operation. The two differ in that for the ternary unit, an innovative hydraulic design allows ternary units to modulate their pumping output by recirculating flow and shifting it as needed. At the right side of Figure 7 are adjustable-speed designs (also known as variable speed). These designs use power electronics (typically variable frequency drives) to vary flow to meet grid needs. Finally, the new designs such as quaternary which combine aspects of both fixed- and variable-speed technologies (Q-PSH has a fixed-speed turbine with a ternary-like design, which is supplemented by a variable-speed pump).

Conventional Pumped Storage Hydropower (C-PSH):
C-PSH units are reversible pump-turbines that are typically composed of a Francis-type pump-turbine with spiral case and elbow-type draft tube (Figure 8). A synchronous motor/generator is located at the top of the pump-turbine, which is fed by wicket gates to allow for load variation (wicket gates control the water flow). In pumping mode, the pump starts dewatered, with the necessary blowdown (i.e., the time to remove water from the housing) adding to the time required to change from generating to pumping mode.

According to GE Renewable Energy (Hydro Division), turbines are historically operated at 50%–100% of rated power; however, from GE's analysis and industry experience, they note that the range is expanding to continuous operation from 0% to 100% of rated power in certain cases.

Pump operation is limited to a unique, fixed operating point, which is only a function of the head, thereby limiting C-PSH's ability to provide ancillary services while pumping.

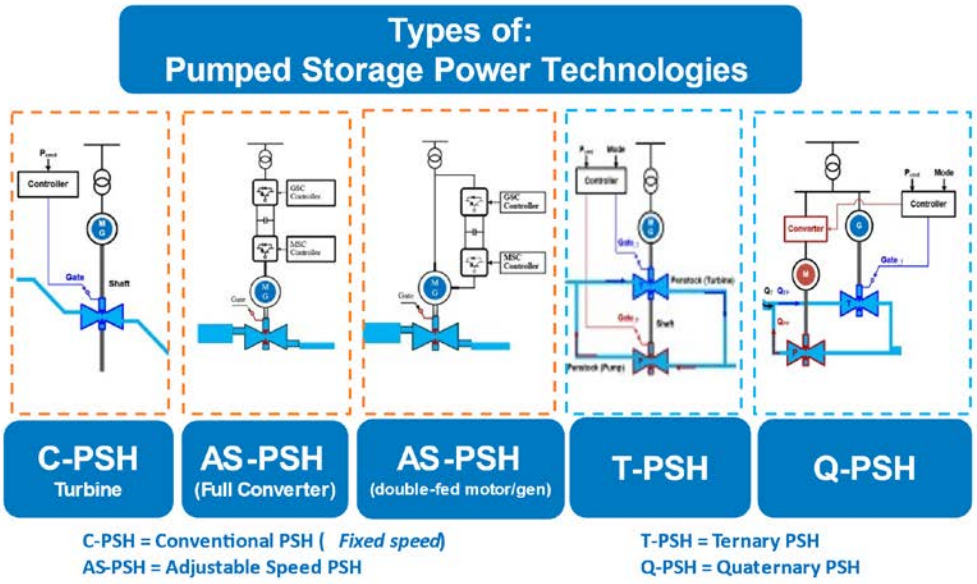

Figure 7. Overview of PSH technologies

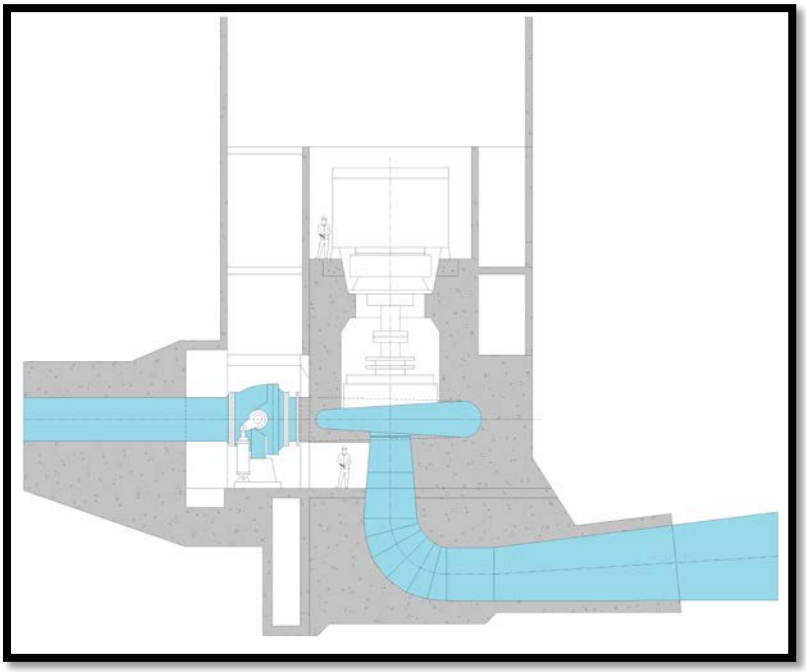

Figure 8. C-PSH typical section view

Illustration from GE

Adjustable-Speed Pumped Storage Hydropower (AS-PSH):
AS-PSH is based on the C-PSH design with variable-speed pumping capabilities. Variable-speed pumping is made possible with the use of power electronics that vary the AC frequency at the pump motor. Whether it has a doubly-fed excitation on the rotor, or a fully fed stator with salient poles rotor, it has the capability to vary the speed of the pump, resulting in the capability to vary the load absorbed by the pump. Generally, the continuous pump power absorption range will be in the 70%–100% range. In some cases, it could be as much as 60%–100%.

AS-PSH was proposed in the 1980s (Kerkman et al. 1980). The mathematical model for these systems—as well as model improvements for control and new application areas—has been reported thoroughly (Lung et al. 2007; Koritarov et al. 2013b; Muljadi et al. 2015). Argonne National Laboratory conducted a series of comprehensive studies to research the value of AS-PSH in the United States, and their reports provide a systematic summary of modeling and analysis (Koritarov et al. 2013a).

Ternary Pumped Storage Hydropower (T-PSH):
Different from C-PSH and AS-PSH, T-PSH is a nonreversible PSH technology. It has the same shaft rotational direction in all operational modes, and this characteristic helps the T-PSH technology to have shorter transition times than reversible technologies, such as C-PSH. This type of arrangement is more flexible than C-PSH or AS-PSH in that it can continuously vary its output over the whole ±100% range. It is composed of a pump (often multistage), a torque converter, a turbine (typically Francis or Pelton type), and a salient poles motor/generator (Figure 9). The motor/generator is operated in one speed direction; only the torque is inverted.

Because of the unique design, the T-PSH system operates such that the pump and the turbine have the same rotation direction. As a result, the T-PSH system does not require the reversal of the rotational direction of the shaft when changing the operating mode, and T-PSH units can switch operating mode more quickly compared to other PSH technologies. The hydraulic transition times, and thus their impacts, are significantly reduced. This differs from reversible PSH technologies like C-PSH and AS-PSH that must change rotational direction when changing from generating to pumping and vice versa. For these units to change operating mode, a significant amount of time is required for these high rotational mass (and high inertia) systems to slow to a stop before the rotation direction can be reversed.

Submergence needs are less stringent than for single-stage pumps, reducing excavation costs for sites that cannot host a cavern arrangement. The required net positive suction head for such multistage pumps is divided by the number of stages, so that a three-stage pump will require generally a smaller net positive suction head by a factor of three when compared to a single-stage reversible pump-turbine.

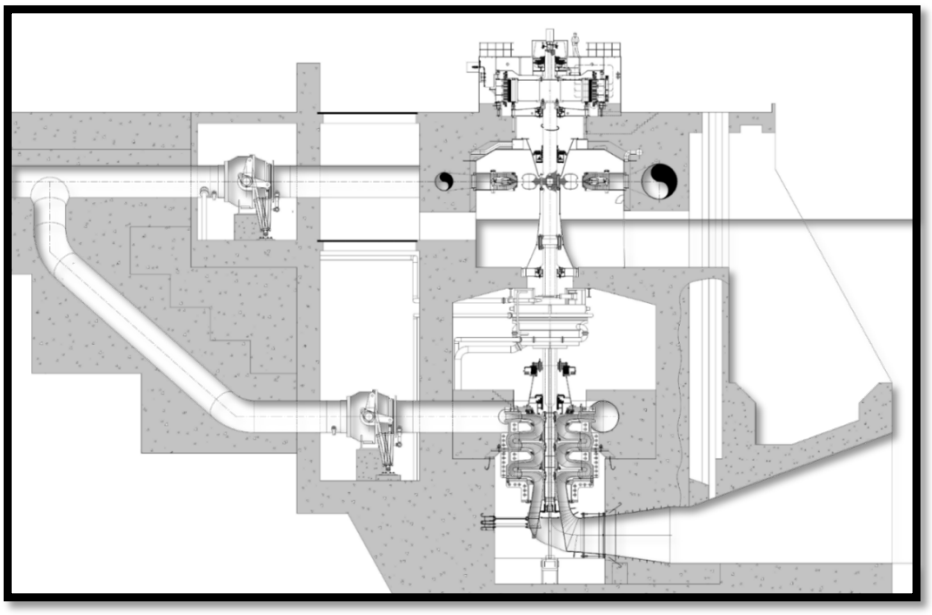

Figure 9. T-PSH typical section view of the turbine and pump housing

Illustration from GE

The ternary configuration was first described in La Houille Blanche (i.e., the International Water Journal) in early 1963 (Puyo 1963) and was used in Puente-Bibey underground pumped storage station in Spain (Pretro 1972); however, due to technical limitations at that time, the turbine and pump could only be operated separately. In 2009 a 525-MW T-PSH plant named Kops II was commissioned in Gaschurn, Austria. In the United States, the first planned T-PSH project is the Gordon Butte Reference Project (Koritarov et al., 2013c; Dong et al. 2018).

Quaternary Pumped Storage Hydropower (Q-PSH):
This type of arrangement is composed of separate pumping and generating units. Instead of having a torque converter between the pump and turbine like the T-PSH unit, the Q-PSH uses separate shafts (Figure 10). Operation of the pump is made possible electrically with fully fed power electronics, rather than mechanically with a torque converter. Unlike C-PSH, there is no need to compromise between pumping and generating capabilities because both the pump and turbine can be optimized for their specific functions.

Benefitting from the combination of adjustable-speed pump and conventional hydropower unit, Q-PSH has the capability to provide frequency regulation whether it is in generating mode, pumping mode or hydraulic short-circuit (HSC) mode whereas T-PSH can only respond in generating mode and HSC mode.

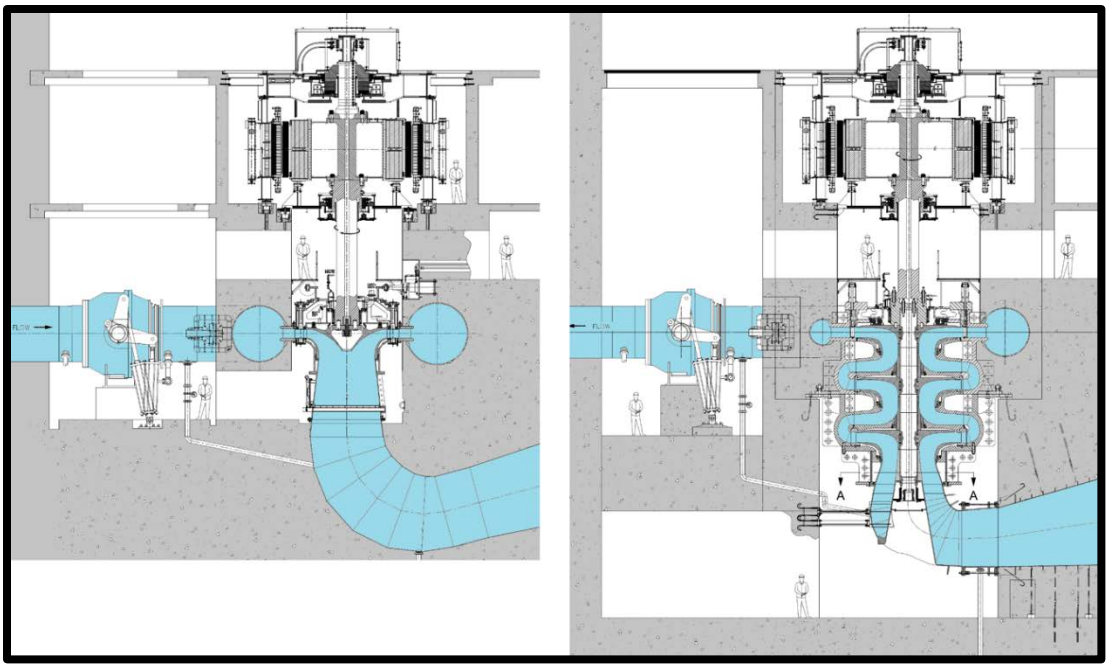

Fixed-Speed Turbine Adjustable-Speed Pump

Figure 10. Q-PSH typical section view

Illustration from GE

4 Grid Reliability and Stability Analysis

This section shares the analysis and findings of how T/Q-PSH technologies can contribute to improved grid reliability and system stability. Results for C-PSH, AS-PSH, and Q-PSH are also presented for comparison purposes. Note that project initially focused on the feasibility of T-PSH technology at the Gordon Butte Pumped Storage Project. During this project, the developers determined that Q-PSH had significant cost-reduction advantages. Therefore, the costs and performance models referenced in this analysis reflect the quaternary technology.

4.1 Methodology

For this work, the team used two primary approaches: GE's positive sequence load flow (PSLF) platform to characterize T-PSH's frequency response performance in both a test and an actual system, and a PSCAD-based approach to investigate how T-PSH could be used as a part of dynamic transmission control (DTC) system.

The PSLF test platform was used to investigate T-PSH's performance under a variety of frequency events and operating conditions and sensitivities:

- Operation mode tests: generating, pumping, and hydraulic short circuit
- Mode switching tests: pumping to generating and back again
- Sensitivity studies (shared penstock and gate valve velocity effects).

Performance was evaluated for a small, 10-bus test system that helped establish benchmarks for T-PSH performance and for the WI, which demonstrated how T-PSH could help improve frequency response in an actual system (i.e., system stability).

The PSCAD test platform was used to investigate how T-PSH could be used as a part of a wide-area FACTS-based DTC system. For this work, the following control scenarios were investigated:

- Congestion control
- Constant power control
- Voltage control.

The section closes with a summary of T-PSH's frequency support capabilities for both the small test system and the WI.

4.2 Analysis and Modeling

4.2.1 Preliminary Analysis of Capability of Different Types of PSH

To accurately study the values and benefits of different types of PSH in the time scales from seconds to minutes, there is a need for new models that can capture the dynamics of T-PSH and Q-PSH as well as their advanced control performance. During this study, dynamic models for T-PSH and Q-PSH were developed, as discussed in Section 4.2.2. The models are described and documented in more detail in Appendix D.

To arrest frequency drops following the sudden loss of generation, frequency response and control from the synchronous generators are important. Frequency response and control include inertia response, primary frequency response, secondary frequency response, and tertiary control. This study focuses on inertia response and primary frequency response.

The standard ternary unit can provide inertia response in both pumping and generating mode. Because the T-PSH is evolved from C-PSH, the synchronous machine can provide the physical inertia at any time. T-PSH can provide primary frequency control not only in the generating mode but also in the hydraulic short-circuit mode.

The quaternary set is a type of hydropower plant configuration. In this configuration, the turbine and the pump are mechanically independent hydraulic machines: they have their own shaft line with their own speed and separate electric machines, separate intake, and out-take, and control/regulation systems. Benefitting from the combination of adjustable-speed pump and conventional hydropower unit, Q-PSH has the capability to provide frequency regulation whether it is in generating mode, pumping mode or HSC mode whereas the ternary PSH (T-PSH) as another type of advanced-PSH technology can only respond in generating mode and HSC mode.

The AS-PSH could be an application of the doubly-fed induction machine with AC/DC and DC/AC converter or it could be connected to the grid through a full-size converter (Type 4). There is no physical inertia for the Type 4 AS-PSH, since the hydro turbine and generator have been fully decoupled with grid through converters. While the advanced control make it possible to change rotor and pump/turbine mechanical speed to provide synthetic inertia or primary frequency response by detecting the frequency changes.

The capability comparisons of different types of PSH providing frequency response are summarized in Figure 62.

4.2.2 T-PSH Modeling

In earlier ternary modeling work performed by Argonne National Lab (Koritarov et al. 2014), a T-PSH model was developed for the Siemens PSS/E platform for the purpose of characterizing T-PSH's behavior while generating and pumping. The investigation here expands on these earlier efforts to examine transients associated with the unique characteristics of T-PSH: rapid mode switching and hydraulic short-circuit operation, penstock-sharing, and gate valve operation. The motivation for the work was that these characteristics are believed to be increasingly important to grid operation as the amount of variable generation increases, something that is occurring in numerous areas throughout the United States. To do this work, a new dynamic model with increased fidelity was required, and detailed information regarding the model's development, structure, and use is provided in Appendix D.

The following sections present the results of the work described in the methodology section, and the first set of tests demonstrate T-PSH's dynamic response while operating in the generating, pumping, and hydraulic short-circuit modes.

4.3 T-PSH Benchmark Simulation

In this section, a small, benchmarking test system (Dong et al. 2019; Dong 2019) is described and the results are presented for how T-PSH performs in this system during both underfrequency and overfrequency conditions for various operating modes and during mode switching. The stability effects of the ternary technology's shared penstock and gate value on system stability are also investigated.

4.3.1 Test System: 10-Bus System

A small, 10-bus test system was used for initial T-PSH benchmark simulation. In this system, there are three different types of generators placed on separate buses (shown in Figure 11). The PSH unit under test was placed on Bus 19, a gas turbine was placed on Bus 20 and a small C-PSH unit was placed on Bus 15. The capacities of test T-PSH units are shown in Table 3. To highlight the influence and performance of test T-PSH units operated in the system, the capacity of the test PSH unit exceeds the actual size of a normal PSH unit by a factor of approximately three. In addition, in some of the test scenarios, the governor and exciter in the gas turbine were disabled to restrict the response of the gas turbine during the frequency event in the system to better help illustrate the contribution of the test unit to the system. Note that in the test system, the swing bus assignment varied by case and that two different loads used: 1,000 MW (No. 1), and 100 MW (No. 2), both placed on Bus 11. The No. 2 load was used for applying frequency events to the system. More detailed dynamic models of the 10-bus system for each operation mode studies are shown in Appendix D.

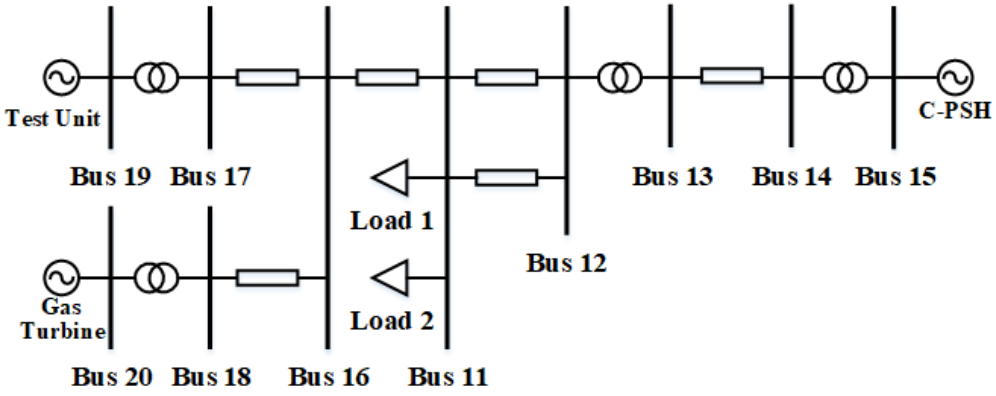

Figure 11. Circuit diagram of 10-bus system

Table 3. Details of System Components

	Generating Mode Case	Pumping Mode Case	HSC Mode Case
Bus 15 C-PSH	GENSAL IEEET1 HYGOV 28.9MW		
Bus 19 T-PSH	GENSAL IEEET1 EPCTRB		
	1,176.0 MW	1,276.0 MW	1,276.0 MW
Bus 20 Gas Turbine	GENROU	GENROU EXAC1 GAST	GENROU
	200.0 MW	2,400.0 MW	2,400.0 MW
Bus 11 Load	No.1 1,000.0 MW, No.2 100.0 MW		
Measurements	IMETR VMETR FMETR		
Swing Bus	Bus 19	Bus 20	

4.3.2 Operation Mode Test

Three operational modes of T-PSH were validated in the 10-bus system, and the frequency responses of each operation mode were tested via induced frequency events. The swing bus was set as Bus 19 for the generating mode case, whereas Bus 20 was the swing bus in two other

simulation cases. Meanwhile, in the generating mode case and HSC mode case, the gas turbine was operated without a governor or exciter to make it not respond to the frequency event. Thus, it helps to highlight the response of T-PSH. In contrast, in the pumping mode case, the gas turbine unit was configured to utilize its governor and exciter to respond to the frequency event to keep system balance, as there is no frequency support from T-PSH in the pumping mode.

4.3.3 Generating Mode

In the generating mode case, the test T-PSH was the main generator in the system and supplied 83.7% of the generating capacity. The test T-PSH unit was the main response unit for the frequency event whereas the gas turbine was configured to not respond to the frequency event. The valve velocity was configured to 1/20 p.u./s, which means the injector needed 20 seconds to open from minimum to maximum (same in opposite action) when responding to load changes. At the beginning of the simulation the T-PSH, operating in the generating mode, supplied 900 MW (0.765 p.u.) power to the system (as shown in Figure 12). At 10 seconds, Load 2, with its rated power as 100 MW, was connected to create an underfrequency event and then tripped at 50 seconds to create an over frequency event. When frequency events occur, the frequency deviation is not zero. In each case, the turbine's governor modulated the gate valve in response to the frequency events and helped return the system to balance by providing frequency regulation when a system contingency occurred.

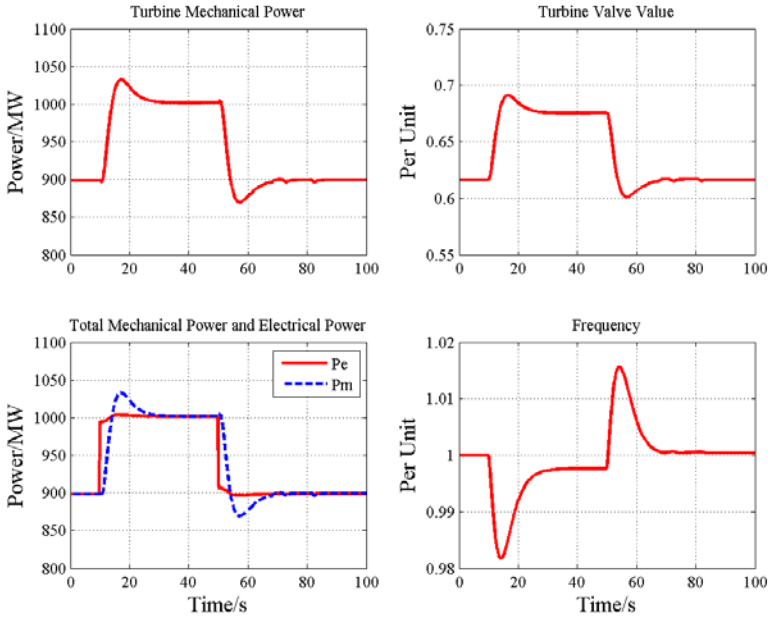

Figure 12. Dynamic responses of T-PSH in generating mode

4.3.4 Pumping Mode

In the pumping mode case, the T-PSH was operated as an inductive load, which absorbed 500 MW (-0.392 p.u.) of power from the system at the beginning. As in the generating mode case, the valve velocity limit was set as 1/20 p.u./s, and only the larger load (1,000 MW) was connected to the system. The 100-MW frequency events were applied at 10 seconds and 50 seconds, respectively, by connecting and tripping Load 2. After the frequency events, the T-PSH did not respond to the frequency events, owing to its fixed pump output, as shown in Figure 13. Note that the pump is fixed speed, and, consequently, there is not governor associated with pumping. The turbine

governor was also disabled in this simulation so the T-PSH operating in pumping mode did not respond to any frequency events in the system. The small variances in the mechanical power output after the frequency events were caused by the frequency fluctuations. These fluctuations, although they cannot affect the gate value, slightly impacted the frictional resistance on the shaft, which caused the variances in the mechanical power output in the turbine part and the pump part. This case illustrates that the T-PSH in pumping mode cannot respond to frequency events, which means that the T-PSH unit cannot provide power regulation while operating in pumping mode.

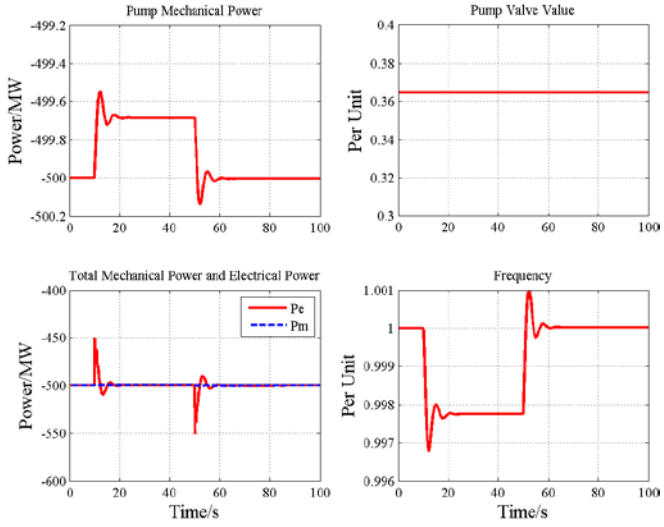

Figure 13. Dynamic responses of T-PSH in pumping mode

4.3.5 Hydraulic Short-Circuit Mode

In the last validation case, the HSC mode case, the T-PSH was set in the HSC mode, absorbing 500 MW (-0.392 p.u.) power from the system for the initial condition. The valve velocity limit was kept the same as the previous cases (1/20 p.u./s), and only the 1,000-MW load was connected in the system. At 10 seconds, the 100-MW Load 2 was added to the system to apply an underfrequency event, and it was tripped at 70 seconds to apply an overfrequency event. Because the T-PSH in HSC mode is a combination of turbine and pump, after each frequency event, the turbine's governor adjusted the valve (and modulated the power output) to help the system recover from the frequency deviation. At the same time, the pumping power remained constant, although there was a small variance in the mechanical power output caused by the frequency fluctuation after the system frequency event as discussed above. This case, as shown in Figure 14, illustrates how the turbine part gives the T-PSH system frequency regulation ability in HSC mode. Compared with the pure pumping mode, T-PSH in the HSC mode can provide power adjustments to help stabilize a system after a frequency event.

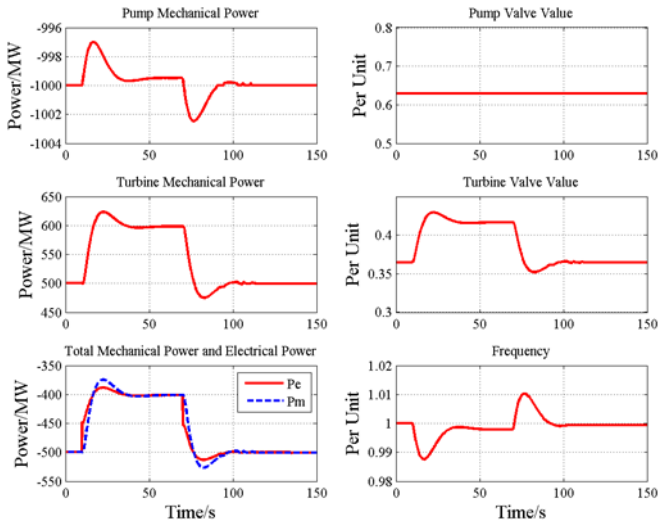

Figure 14. Dynamic responses of T-PSH in HSC mode

4.3.6 Mode Switch Test

The nonreversible nature of the T-PSH technology means that there is no need to wait for the pump/turbine to spin down before switching modes, and a comparison of how this affects transition times is shown in Figure 15 and Table 4. Comparison of Transition Times. T-PSH technology can switch its three operation modes in less than 1 minute, whereas the other two reversible PSH technologies need about 6 minutes to change from generating mode to pumping mode, and about 3.5 minutes to switch from pumping mode to generating mode.

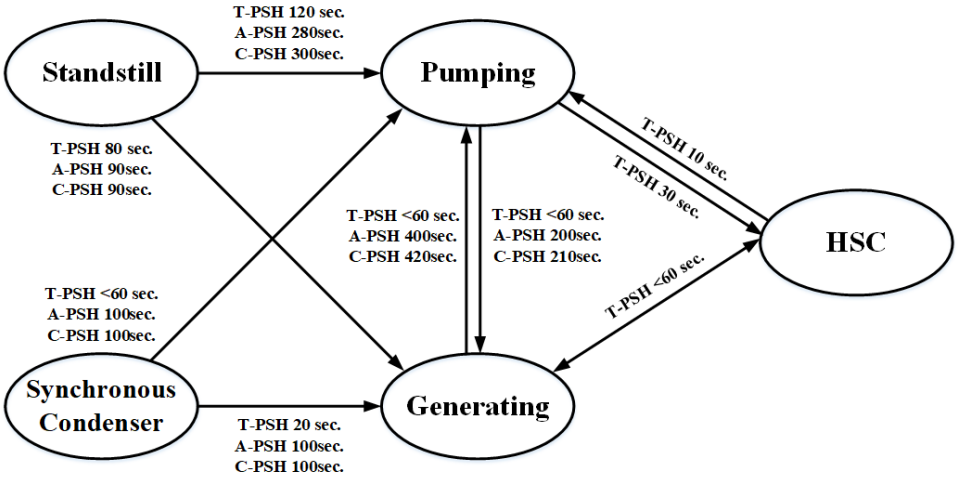

Figure 15. Transition time between operation modes

Illustration from GE Renewable Energy

Table 4. Comparison of Transition Times

Type	A	B	C	D	E	F
C-PSH	210s	420s	90s	300s	100s	100s
AS-PSH	200s	400s	90s	280s	100s	100s
T-PSH	<60s	<60s	80s	120s	20s	<60s

A is pumping to generating, B is generating to pumping, C is standstill to generating, D is standstill to pumping, E is synchronous condenser to generating, and F is synchronous condenser to pumping.

4.3.7 Test Results

Three operation modes are switched clockwise, according to the sequence shown in Figure 15 (from generating mode, to pumping mode, then to HSC mode, and finally back to generating mode). The different transition times from actual operation, according to operation data shown in Figure 16, for each switching event were set as 25 seconds, 30 seconds, and 60 seconds separately, which means the valve velocity was 0.25 p.u./s, 1/30 p.u./s, and 1/60 p.u./s, respectively. In this case, Bus 20 was assigned as the swing bus where the gas turbine was located. To help the system remain steady during T-PSH operation mode switching, the governor model and exciter model were enabled in the gas turbine system to help regulate grid frequency. At the beginning of the simulation, the T-PSH was operated in the generating mode with 500 MW (-0.392 p.u.) power output. Mode-switching events were applied at 10 seconds, 30 seconds, and 150 seconds sequentially, as shown in Figure 16.

Summary of Results:

- The operation mode switching ability of T-PSH was verified.
- The design of the user-defined governor model allowed the T-PSH system to do the switching during the simulation case.
- The different transition times used in this case demonstrate that the user-defined governor model can capture the transition between different operation modes and modify the valve velocity limit.

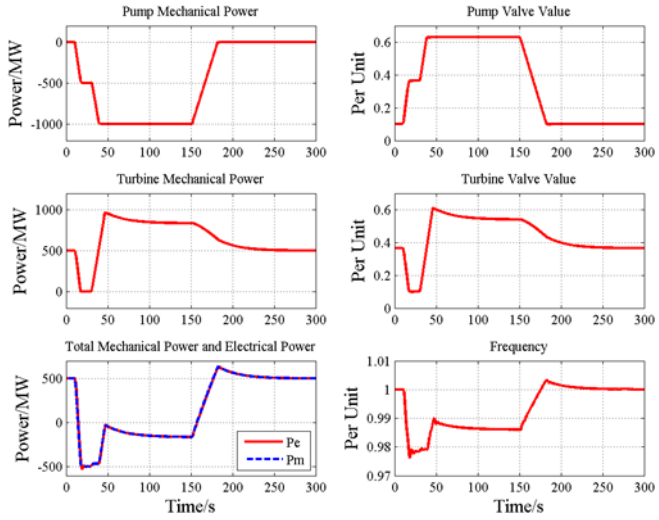

Figure 16. Dynamic responses of T-PSH in operation mode switching

4.3.8 Impact of Shared Penstock

In the previous simulations, the effects of a shared penstock were not included in studies. As mentioned above, the ability to use a shared penstock is an important advantage of T-PSH technology, and this section is focused on investigating the impact of various transition times and penstock configurations on system performance. Several comparison cases are presented.

Parallel penstocks between the upper reservoir and lower reservoir typically do not exist because of the high excavation cost. Usually, there is one main penstock to connect T-PSH unit chambers and reservoirs. Near the T-PSH chambers, the main penstock is divided into two sub-penstocks to connect it to the turbine and pump parts of the unit. The water flow of these two sub-penstocks will be in different directions during HSC operation, and because of this, simplified parallel penstock models cannot be used in the T-PSH simulation. Two sensitivity study cases that illustrate the influence of the shared penstock in T-PSH operation are presented below.

Case Study of the Effect of Shared Penstock on Frequency Response:
The T-PSH unit in HSC mode with the shared-penstock model was operated with 500 MW (0.392 p.u.) at the beginning and tested under a system frequency event in the three-generator system. A 100-MW overfrequency event was applied at 1 second by tripping Load 2 on Bus 11. The gas generator was operated with an exciter and governor to help keep the system stable after the frequency event. The baseline for this study is a nonshared case whose T_{w_pt} and T_{w_tp} were set equal to zero, which is the same as the cases tested in the small system. Three shared-penstock cases with different water time constants were investigated to simulate different length-to-cross-sectional-area ratios for the penstocks.

Results (refer to Figure 17 and Figure 18):

- Shared-penstock modeling does not have a significant effect on the frequency response during the system frequency event.
- Different lengths in cross-sectional area ratios in the penstocks do not significantly affect the frequency response performance of T-PSH; the difference in frequency at the maximum point among the four cases was less than 0.005 Hz.
- For the purposes of modeling, the effects of the shared penstock on frequency can be ignored.

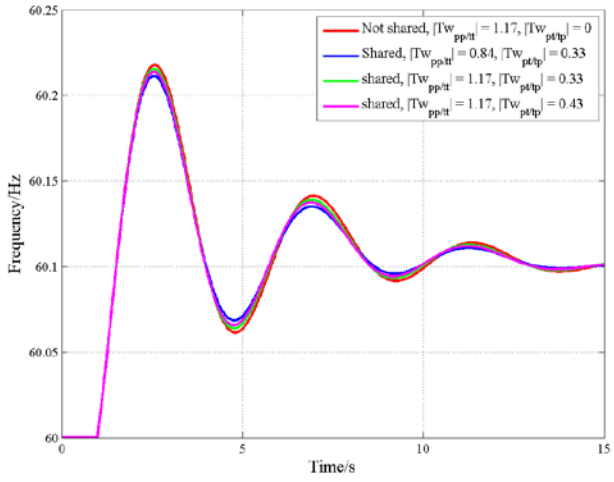

Figure 17. Frequency responses of T-PSH in HSC mode under different penstock conditions

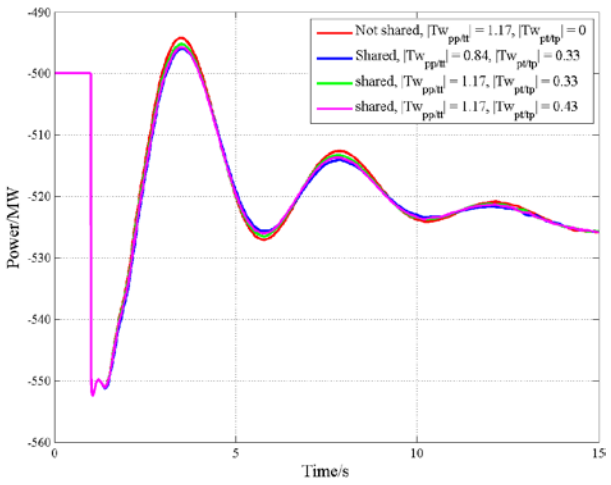

Figure 18. Electrical power outputs of T-PSH in HSC mode under different penstock conditions

Case Study of Operation Mode Switching for Units With a Shared Penstock:
The shared-penstock influence on operation mode switching is studied in this section by using the same simulation parameters as the last section. The mode switching event was applied at 1 second to switch the T-PSH from HSC mode to pumping mode. The T-PSH unit has the same output, 500 MW (-0.392 p.u.), before and after switching.

Results (refer to Figure 19 and Figure 20):

- All PSH technologies, with or without a shared penstock, have a significant oscillation in the response. The shared-penstock cases all have a significant overshoot in the response compared with the nonshared case.
- The interaction constants, T_{w_pt} and T_{w_tp}, produced a larger overshoot into the system compared with the nonshared case (baseline).
- The larger main water constants, T_{w_tt} and T_{w_pp}, in the two shared-penstock cases, yielded more significant oscillation in the response. Larger main water constants mean larger length to cross-sectional area ratio in penstock parameters, which indicates the penstock has the longer length or the smaller cross-section area.
- Another set of coefficients, T_{w_pt} and T_{w_tp}, result in smaller overshoot when they are smaller. The overshoot after the operation mode switching was positively related to the interaction constants, T_{w_pt} and T_{w_tp}, and main water constants T_{w_tt} and T_{w_pp}.
- Above all, an appropriate set of penstock parameters should be considered when designing the T-PSH unit, because the water interactions in shared penstock affect the output performance during the operation mode switching.

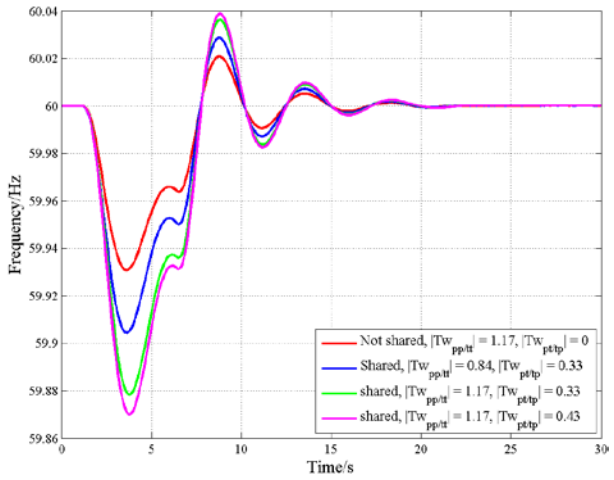

Figure 19. Frequency responses of T-PSH in mode switching under different penstock conditions

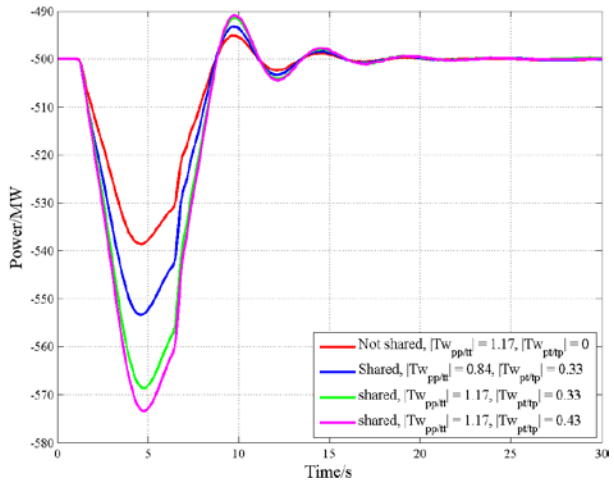

Figure 20. Electrical power outputs of T-PSH in mode switching under different penstock conditions

4.3.9 Impact of Valve Velocity

In the T-PSH modeling, the transition time is quantified as gate valve velocity. In daily operation, the gate valve in the T-PSH unit requires 30–60 seconds to open from minimum to maximum (same time in closing). The largest transition time of the T-PSH unit is about 60 seconds during operation mode switching. The time spent adjusting the valve delays changes in water flow, which leads to a delay of mechanical power output changes. The transition time affects the performance of T-PSH response in daily operation. Several sensitivity study cases for T-PSH in different operation scenarios are studied in the small test system used in the previous chapter to illustrate the impact of the transition time.

Case Study of the Effect of Valve Velocity in the Generating Mode:

In daily operation, the T-PSH unit adjusts its output power according to the operation plan and the power system status. Therefore, effective valve modulation is essential; the speed of the valve adjustment directly affects the rate of change in the power output. In this sensitivity study, the test

T-PSH with 400-MW capacity was operated in generating mode and pumping mode separately. Bus 20 was assigned as the swing bus where the gas turbine unit was operated with governor and exciter models in two cases. In each case, there are four types of gate valve velocity. The first one used a deflector to cut the mechanical torque off the shaft immediately, which is always used in system protection. In this operation, the gate valve, or injector, is not operated. The other three groups use the injector to adjust water flow at different velocities. One has no velocity limit, which means the gate valve can adjust the value as quickly as possible. The other two have velocities of 1/30 p.u./s, and 1/60 p.u./s (30 and 60 seconds from minimum to maximum), respectively.

In the generating case, the T-PSH was operated at a maximum of 400 MW initially and then set to zero output at 1 second to simulate the system terminates power generation. At 100 seconds, it was returned to the maximum to repower the system.

Results:

- The response results of different gate valve velocities shown in Figure 21 indicate that there is still a delay in the no-velocity-limit case, which is an inherent characteristic of the injector.
- In the frequency response and electrical power results shown in Figure 22 and Figure 23, respectively, significant overshoot and longtime oscillation occurred in the deflector case and the no-velocity-limit case.
- In contrast, in the 1/30 p.u./s, and 1/60 p.u./s cases, there was not any obvious overshoot and oscillation after the power output adjustment.

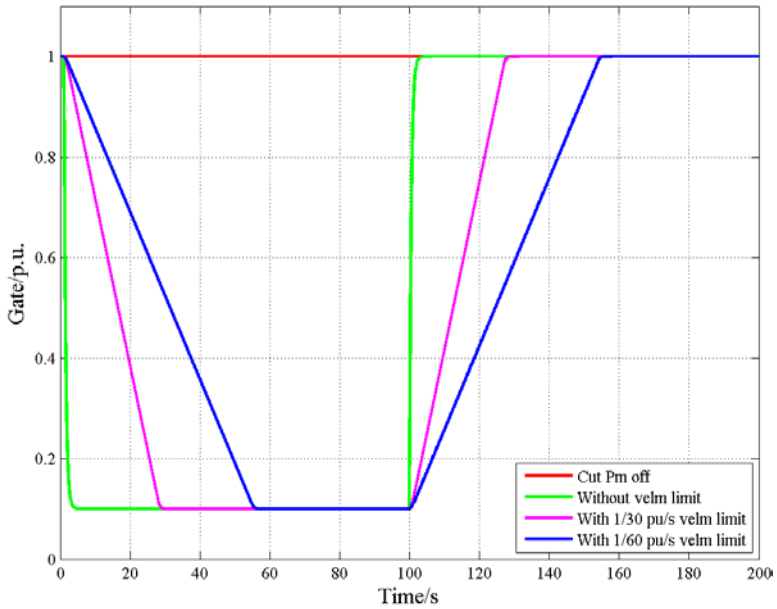

Figure 21. Gate valves of T-PSH in the adjustment of general generating with different valve velocities

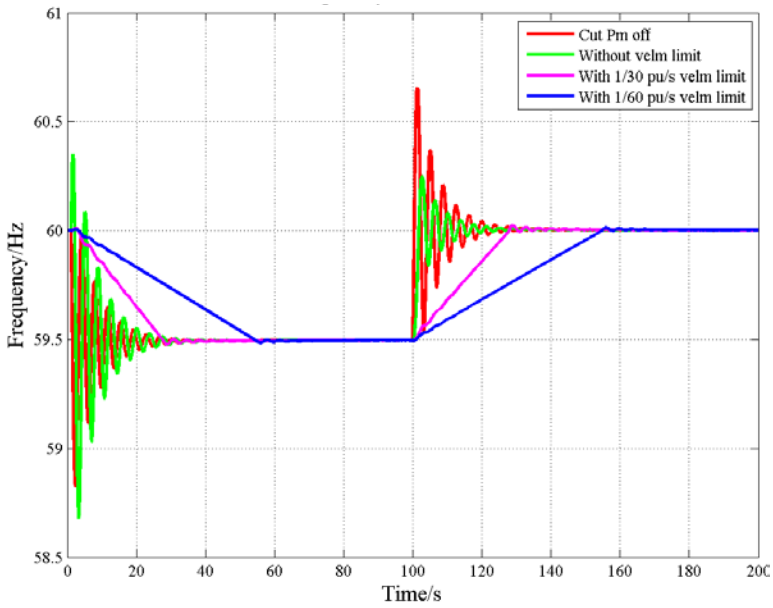

Figure 22. Frequency responses of T-PSH in adjustment of general generating with different valve velocities

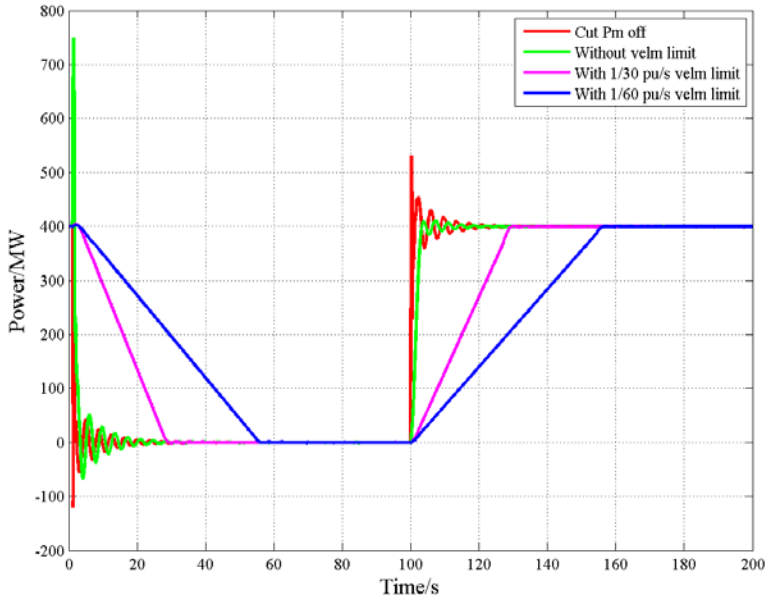

Figure 23. Electrical power outputs of T-PSH in adjustment of general generating with different valve velocities

Case Study of the Effect of Valve Velocity in the Pumping Mode:

In the pumping case, the T-PSH was operated at -400 MW (-0.313 p.u.) at the beginning, which is the maximum pumping output. At 1 second, the unit is adjusted to zero output to simulate no excess energy generation in the system. After that, the T-PSH was returned to maximum pumping output at 100 seconds. The velocity groups and other system parameters were the same as the generating case. The results obtained were similar to the previous case, as shown in Figure 24, Figure 25, and Figure 26.

Results:

- Again, a near-zero transition time caused significant oscillation in the system after output adjustment. Conversely, larger transition times effectively minimize the effect of the adjustment.

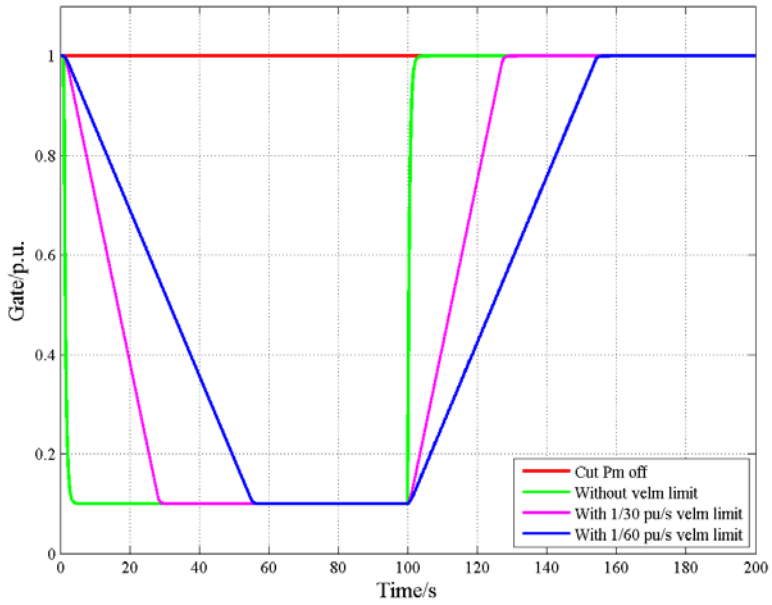

Figure 24. Gate valves of T-PSH in adjustment of general pumping with different valve velocities

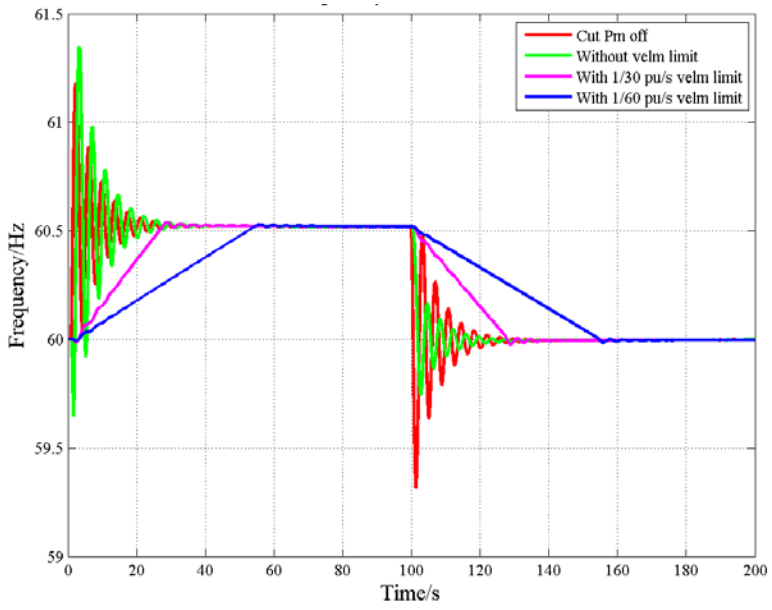

Figure 25. Frequency responses of T-PSH in adjustment of general pumping with different valve velocities

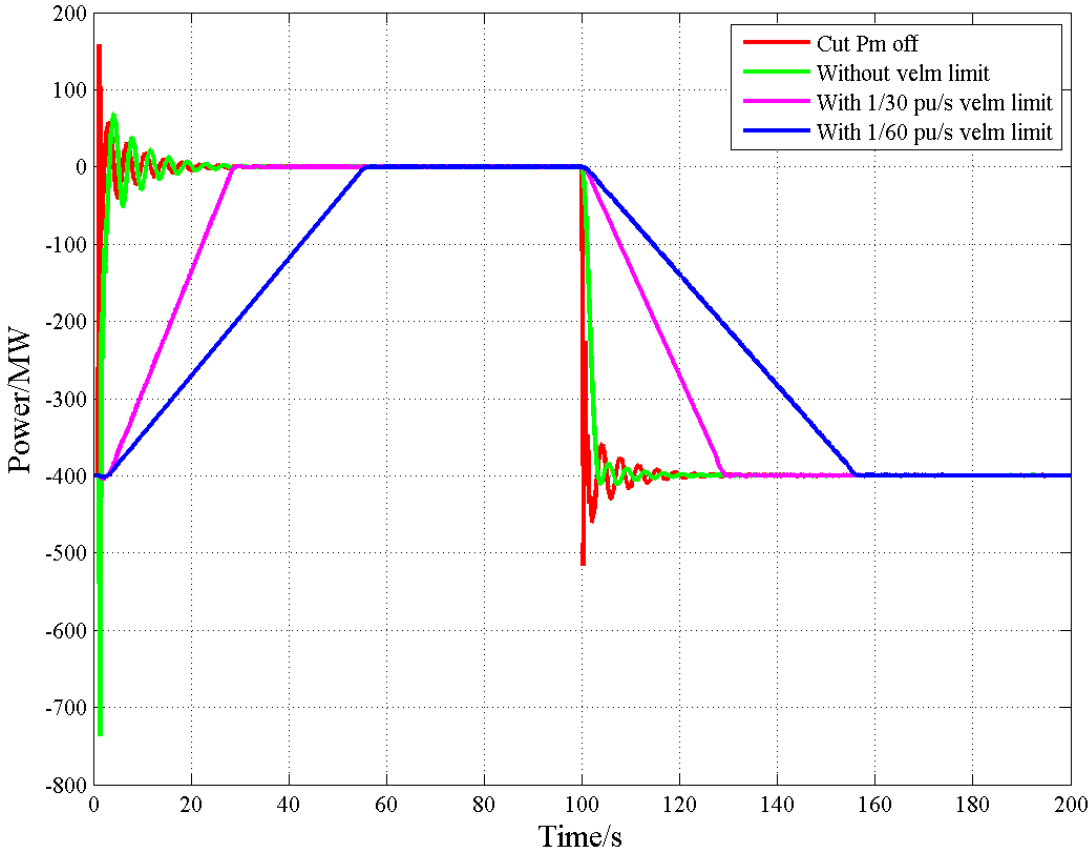

Figure 26. Electrical power outputs of T-PSH in adjustment of general pumping with different valve velocities

Based on these results in the daily output adjustment, a suitable transition time should be utilized for the T-PSH unit to minimize any adverse impacts on the system. The study found that system inertia prevents quick adjustments, which can cause significantly deleterious effects on the system. It is worth mentioning that the protective cutoff action does cause a significant influence on the system, even though it is used to protect the T-PSH unit.

Case Study of the Effect of Valve Velocity on Frequency Response:

After clarifying the influence of valve velocity in the daily adjustment, the next issue studied is the effect on the frequency response of T-PSH after a frequency event. Recalling that the pump part cannot respond to the event, this sensitivity study is based on T-PSH's response in the generating mode. In addition, the frequency response of T-PSH after the frequency event is mainly provided by the gate valve adjustment, which is controlled by the governor. For this experiment, the gas turbine was set with the governor and exciter models disabled so that the turbine would not respond to system frequency events. The swing bus, in this case, was Bus 19, where the T-PSH is.

In the beginning, both loads on the Bus 11—with a total of 1,100 MW—were connected to the system, and the T-PSH unit provided most of the power (about 1 GW) to the system. At 1 second, a 100-MW overfrequency event is applied in the system by tripping Load 2.

Results:

- The response results of the T-PSH, shown in Figure 27 and Figure 28, with 1/30 p.u./s coincided with the results without a velocity limit. This means the valve speed at 1/30 p.u./s was short enough to respond to this frequency event, and 30 seconds was shorter than the inherent response time of the test T-PSH unit.
- When compared with results of 1/30 p.u./s and 1/60 p.u./s, there was a significant delay in the 1/60 p.u./s case. This indicates that a valve velocity longer than the T-PSH unit inherent response time will cause an obvious delay in response after a frequency event.
- Similarly, this valve velocity effect is also applicable in the HSC mode, owing to only the turbine part responding to the frequency event in this mode.

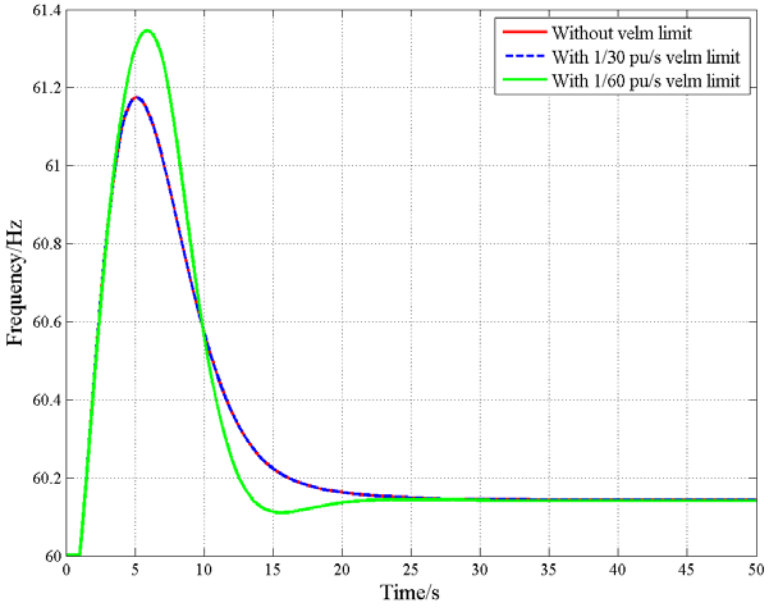

Figure 27. Frequency responses of T-PSH after an overfrequency event under different valve velocities

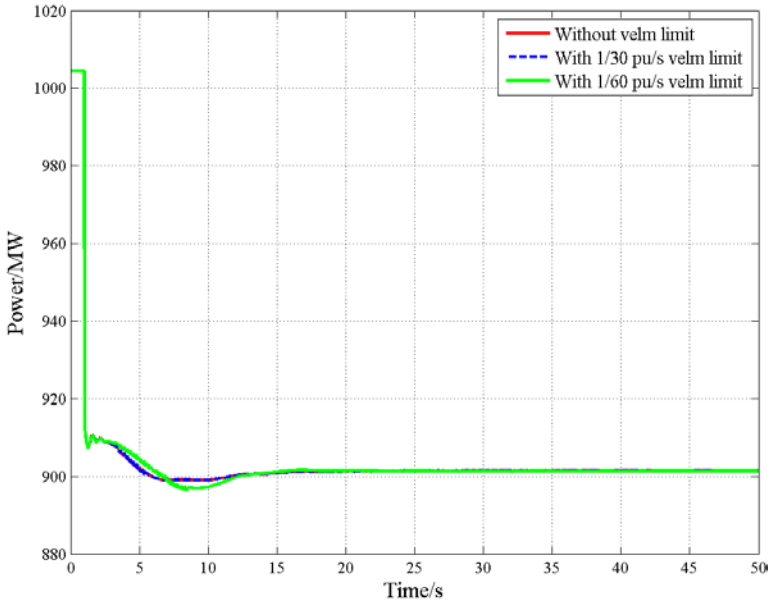

Figure 28. Electrical power outputs of T-PSH after an overfrequency event under different valve velocities

Case Study of the Effect of Valve Velocity in Operation Mode Switching:

In this sensitivity study, a comparison case was set up to show the effect of valve velocity on operation mode switching. To make the system stable, the swing bus was changed to the gas turbine's bus (Bus 20), and the gas generator's governor and exciter models were enabled. The test groups were the same groups in the general operation study. Also included in the results is the deflector case (denoted as "cut Pm off" in Figures 29 and 30), simulated to demonstrate performance at the theoretical limit (i.e., if valve movement were instantaneous). Usually, this operation mode should use the injector and clutch to switch. The simulation began with the T-PSH operating in generating mode with an output of 500 MW. At 1 second, the operation mode switched from generating to pumping. After the operation mode switching, the T-PSH absorbed 500 MW (-0.425 p.u.) from the system.

Results:

- As shown in Figure 29 and Figure 30, there are some significant delays in 1/30 p.u./s and 1/60 p.u./s cases. Although a substantial delay existed in these two cases, especially in the 1/60 p.u./s case, the oscillation was much smaller compared with the no-velocity-limit and the deflector cases.
- When looking at the deflector case and the no-velocity-limit case, they both responded quickly but caused oscillation in the system. There was a small delay in the no-velocity-limit case, compared with the deflector case, due to the inherent delay in the gate valve.
- Therefore, the selection of valve velocity should consider both the response speed and the impact on the system.

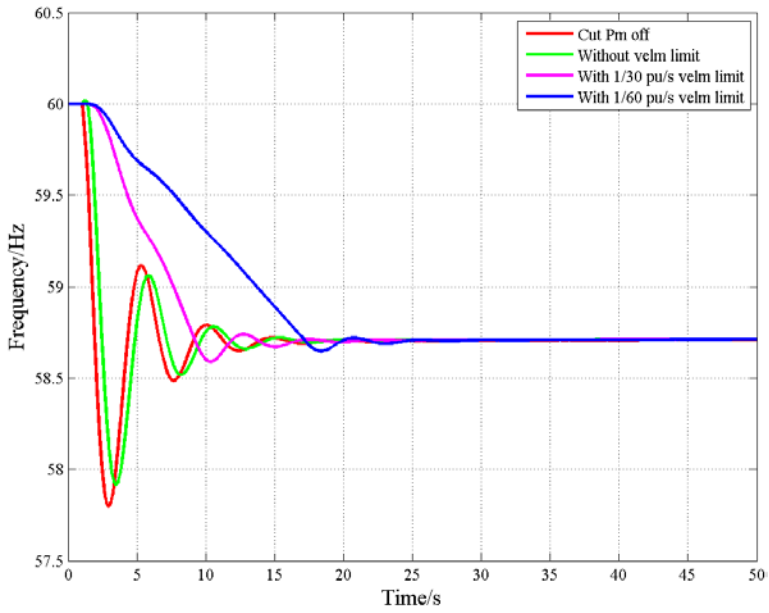

Figure 29. Frequency responses of T-PSH in operation mode switching with different valve velocities

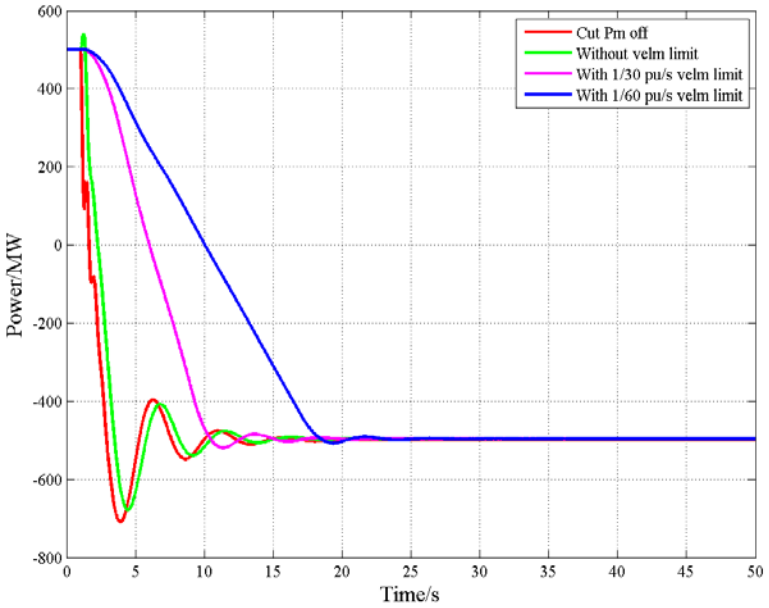

Figure 30. Electrical power outputs of T-PSH in operation mode switching with different valve velocities

4.3.10 Comparison of T-PSH and C-PSH During an Underfrequency Event

After studying the characteristics of T-PSH in several cases, a comparison case between T-PSH and C-PSH was designed to better understand HSC mode. Because a significant difference between T-PSH and C-PSH is the additional HSC mode, this section focuses on the difference between T-PSH in HSC mode and C-PSH in pumping mode. In two simulations, the test unit was set to the T-PSH unit and C-PSH unit with the same parameters. In the beginning, both test units were operated as absorbing 500 MW (-0.392 p.u.) of power from the system. The 2,400-MW gas

turbine on the swing bus (Bus 20) with the governor model and exciter model helped keep the system stable during the frequency event. In the beginning, only Load 1 (1,000 MW) was connected. An underfrequency event was applied at 1 second by connecting Load 2 (100 MW) into the system.

Results:

- As mentioned before, the T-PSH in the HSC mode can respond to the frequency event, as shown in Figure 31 and Figure 32. After the frequency event, the governor in the turbine part adjusted the gate valve reference to increase the mechanical power output, as shown in Figure 33.
- The output of the pump part remained the same. This power regulation increased system frequency by 68.49 mHz at steady state and by 11.16 mHz at the frequency nadir, compared with the pumping case.
- In the T-PSH case, frequency regulation is provided by the gas turbine and T-PSH unit, although the contribution of the T-PSH is limited, owing to its limited capacity. On the contrary, the C-PSH in pumping mode cannot provide any support during the frequency event.

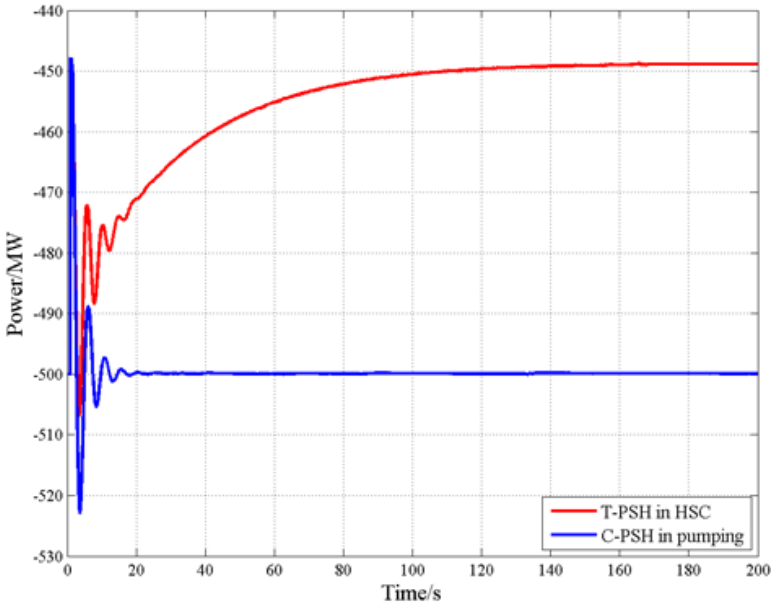

Figure 31. Electrical power outputs of T-PSH and C-PSH

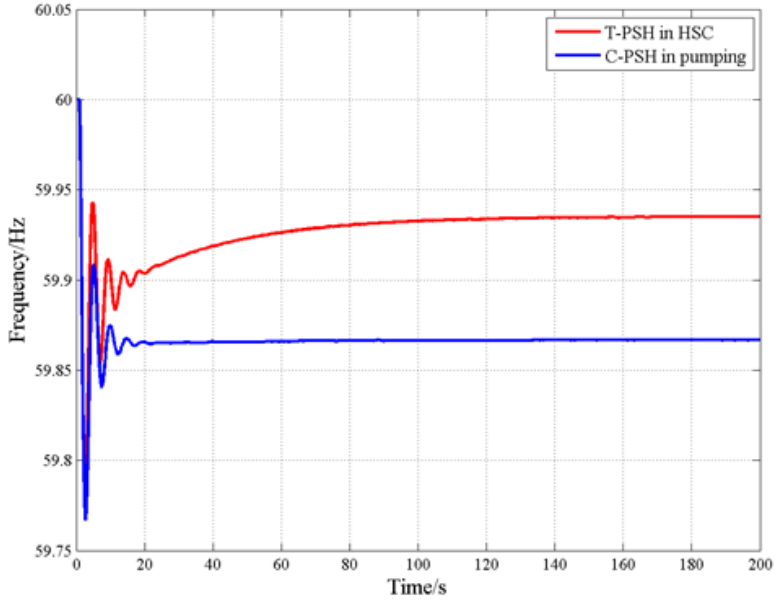

Figure 32. Frequency responses of T-PSH and C-PSH

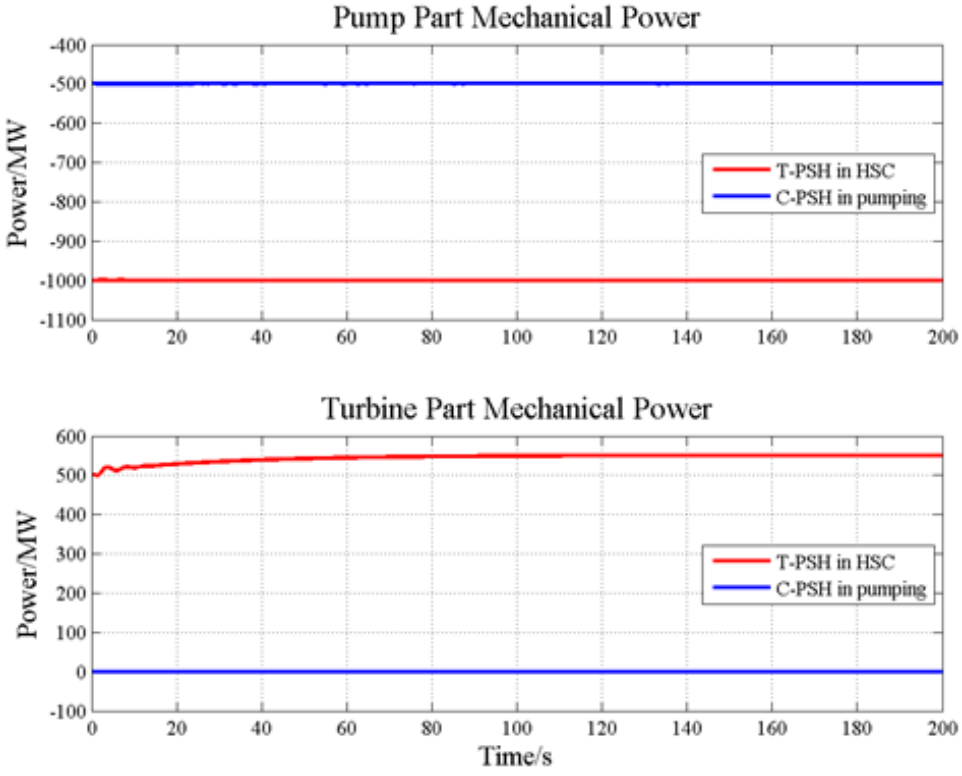

Figure 33. Mechanical power outputs of T-PSH and C-PSH

4.3.11 Comparison of Frequency Response Across PSH Technology Types

In the small test system comparison case, the same 10-bus system is used as in previous validation cases. All test PSH units are placed on Bus 19 in each simulation case. In these cases, the C-PSH unit, AS-PSH unit, and one case of Q-PSH, are operated in pumping mode. The T-PSH unit and

one case of Q-PSH are operated in HSC mode. As shown in Figure 35, the reference power of all PSH units is set to absorb 500 MW of power from the system. The swing bus (Bus 20) is the gas turbine, and only Load 1 (1,000 MW) is connected to the system. At 1 second, Load 2 (100 MW) is connected to the system, the demand surpasses the supply, and the grid frequency drops (Figure 34).

Results:

- As shown in Figure 34, C-PSH working in pumping mode only shows its frequency response in the initial response period and cannot respond to this frequency event in the primary frequency response period.
- All contributions to system frequency regulation come from the gas turbine. On the contrary, all other advanced PSH units provide better frequency response after the underfrequency event.
- In the initial frequency response period, all advanced PSH contribute to frequency support. Compared with the T-PSH, all other advanced-PSH technologies have much higher frequency nadir as a result of their fast response from power electronics and their initial frequency controller.
- Q-PSH operating in HSC mode can provide more power back to the system than other cases, benefiting from contributions from both the pump and the turbine.
- The Q-PSH operating in pumping mode is similar to AS-PSH operating in pumping mode with the same frequency response at steady state. Since there is not any power electronic device in T-PSH, the frequency regulation provided by the T-PSH is slower than that provided by the AS-PSH and Q-PSH technologies.
- The frequency support provided by the advanced PSH technologies improve both frequency nadir and steady-state frequency after the system contingency.

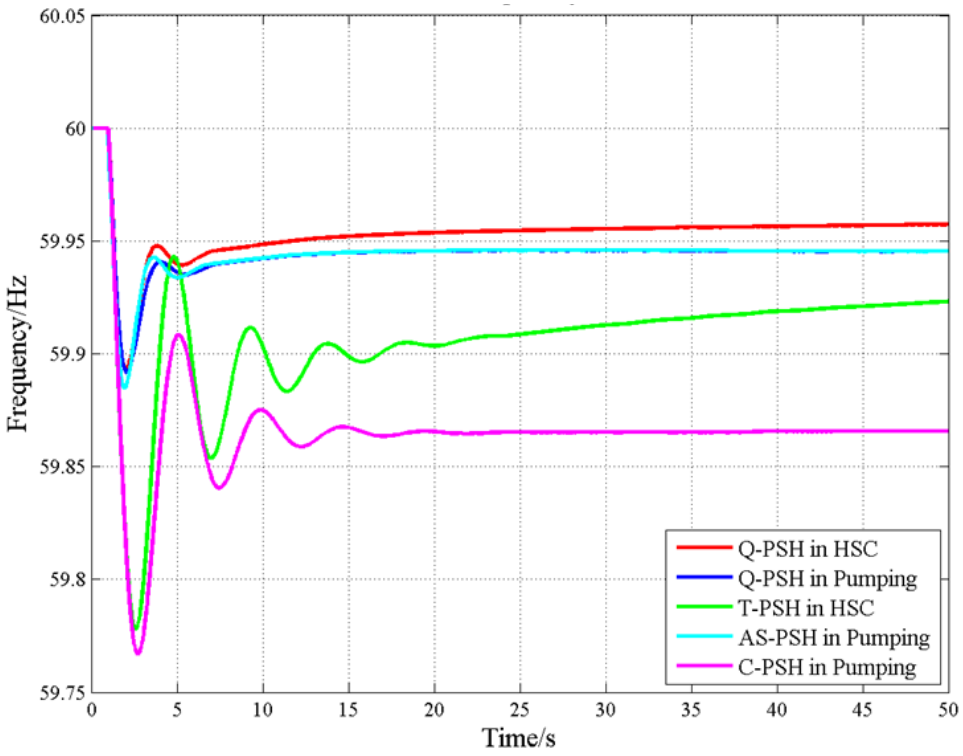

Figure 34. Frequency responses of advanced PSH technologies

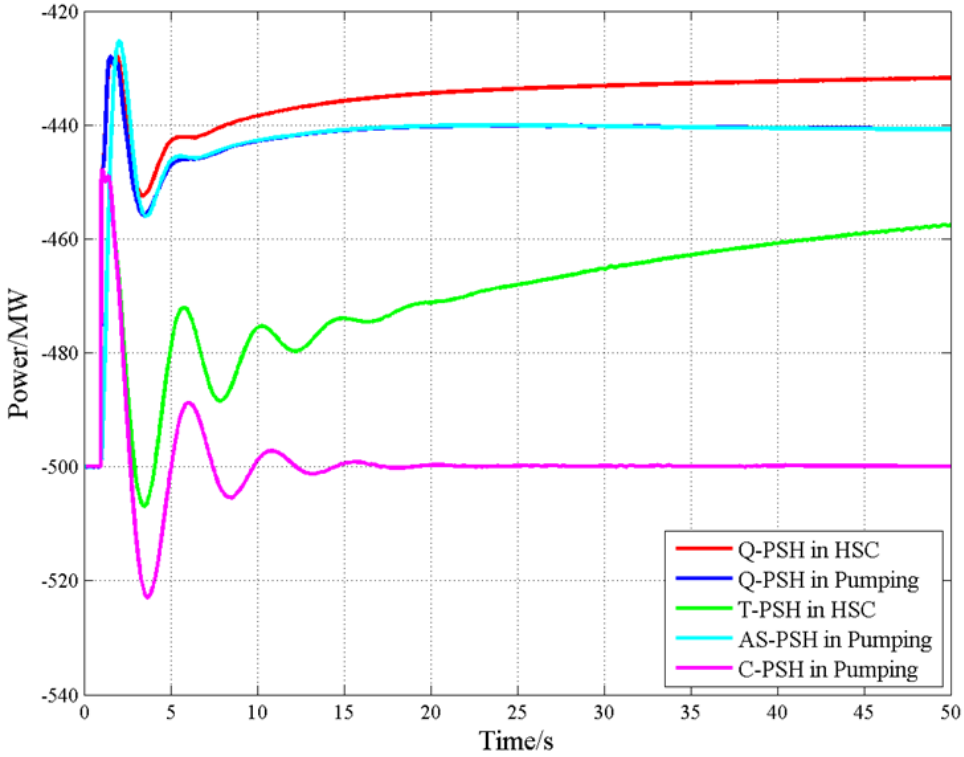

Figure 35. Electrical power outputs of advanced PSH technologies

4.4 The Capabilities of T-PSH in Wide-Area Stability and Control

The stability of power systems is influenced by many factors, and T-PSH can contribute in a variety of ways. Power system characteristics contribute to power system stability; for example, many power plants are remote generations (e.g., wind plants or photovoltaic [PV] plants at a distance). Remote generation power plants present a weak transmission to the grid (large line reactance, series/parallel compensation). The generator type can also influence its characteristics (synchronous generator or inverter-based resources). Similarly, the load characteristics (PQ or PV bus; or simple ZIP load model) also influence power systems.

T-PSH can be helpful in compensating for remote generation; as an example, large wind power plants (WPP) that are far from the load center may impact grid frequency and voltage due to the fluctuating power output and voltage drop across the weak grid. By using T-PSH to smooth power fluctuations and limit the ramp rates of the remote variable renewable energy plants, the power system will be kept stable.

Another important aspect of power system stability is the operating conditions; for example, what is the power transfer level at a certain time of the day (e.g., wind generation occurs at night, while PV generation occurs during the day). Nighttime transmission congestions will likely be caused by wind generation, while during the day it is likely caused by PV generation. T-PSH can be used to store the excess energy generated by the WPP during the night or by PV during the day, helping to reduce line congestion.

In performing the wide-area stability and reliability study, the team performed the power flow and transient dynamics studies on GE's PSLF analysis platform. The investigation focused on demonstrating how the fast response of T-PSH can be used to maintain stability and improve the reliability of power systems.

4.4.1 Introduction of Western Interconnection Validation Studies

This section is dedicated to studying the performance of T-PSH in a much larger and more realistic setting, the WI. The WI is the second largest of three major interconnected power grid systems in the United States, with a total generating capacity of 179 GW. The system covers 12 states, two Canadian provinces, and a small area in Mexico, as shown in Figure 36.

Figure 36. Geographic scope of the Western Interconnection

Illustration from Schlag et al. (2015)

4.4.2 Comparison of C-PSH and T-PSH Performance in California

As the results in the small system (10-bus) experiments showed, T-PSH has a significant advantage over C-PSH in that it can provide the frequency regulation in HSC mode, even when pumping water. To verify this advantage in a real system, a comparison case between T-PSH and C-PSH was developed based on the 2022 Light Spring (LSP) foundation (Appendix G). In the study's model, five C-PSH units, all located California, were replaced by T-PSH units (DOE Global Energy Storage Database Undated[a–e]). The locations and details of the units are given in Figure 37 and Table 5.

Figure 37. Geographic location of five C-PSH units

Illustration from Google Maps with additions by Jin Tan, NREL

Table 5. Details of Five Replaced C-PSH Units

Name	Units	Total Capacity	Online Power
Castaic	6	1,500 MW	-894 MW
Helms	3	1,287 MW	-930 MW
Hyatt	6	714 MW	-469 MW
San Luis	8	424 MW	-53 MW
Big Creek	1	222 MW	-207 MW
Reference Project	3	400 MW	-315 MW
Total	27	4,547 MW	-2,868 MW

4.4.3 The Role of Fast Mode Switching in Wide-Area Frequency Control Response

In addition to the ability of T-PSH to contribute to frequency response while pumping in HSC mode, its ability to quickly change operating modes can be helpful for maintaining system stability. This section summarizes T-PSH operation in HSC mode compared with operation in conventional pumping mode.

A comparison simulation among operation mode switching, HSC mode, and conventional pumping mode of the T-PSH was conducted. For the experiment, the 2022 LSP model was used. In this scenario, five PSH units (Castaic, Helms, Hyatt, San Luis, and Big Creek) were replaced

by same-size T-PSH units, and then the response of these plants to an N-2 contingency at the Palo Verde Nuclear Generating Station was modeled. The units were operated in pumping mode at the beginning of the simulation, and the same largest N-2 contingency was applied at 10 seconds to create a generation loss contingency (i.e., two of the units at Palo Verde tripped). To quantify the effects of the frequency event and get the value of the generation loss, the rate of change of frequency (ROCOF) measurement expressed below was employed:

$$\Delta P = 2\sum_{i=1}^{n} H_i \frac{df_{coi}}{dt} \qquad (1)$$

where ΔP is the power change in the system, H_i is the system inertia in i^{th} area, and f_{coi} is the center of inertia frequency. A new block for this measurement was designed and added to the T-PSH system, shown in Figure 38.

Figure 38 introduces the entire process of detection and implementation for the operation mode switching and graphically depicts the location of the T-PSH plants under study as well as that of the nuclear units that trip. To simplify the design, the T-PSH units were preselected according to the N-2 contingency. Here, the preselected T-PSH units were the Castaic and Hyatt PSH plants.

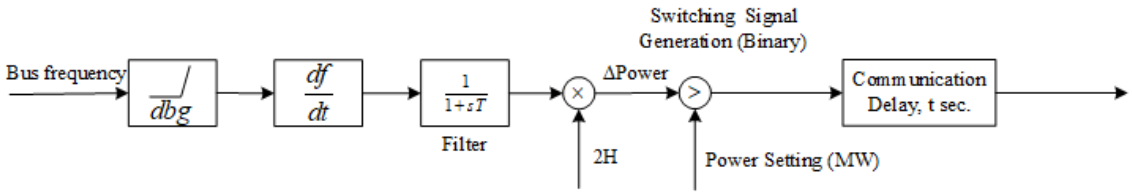

Figure 38. Block diagram of ROCOF measurement

Illustration by Jin Tan, NREL

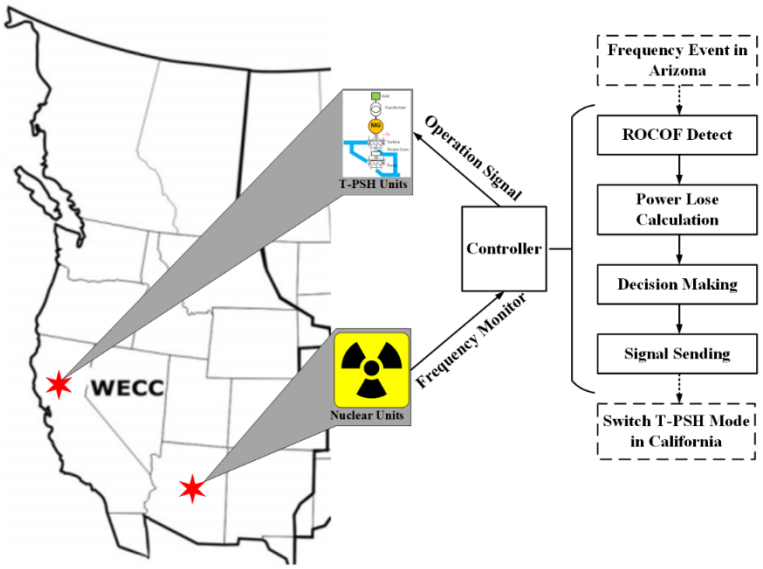

Figure 39. Schematic diagram of T-PSH operation mode switching application

Note that the sampling interval for the ROCOF calculation was 0.1 second, and the error in generation loss estimation was less than 2.51%, which is considered acceptable for the mode switching studies. When the measurement block generates the trigger signal, the preselected T-PSH units will be switched from pumping to generating. Also, a delay of 0.5 seconds was added to the switching trigger signal to simulate the actual inherent delay in the frequency event detection and signal communication, as shown in the bottom plot of Figure 41. The measurements of ROCOF and generation loss estimation for the frequency event are shown in Figure 40. and Figure 41.

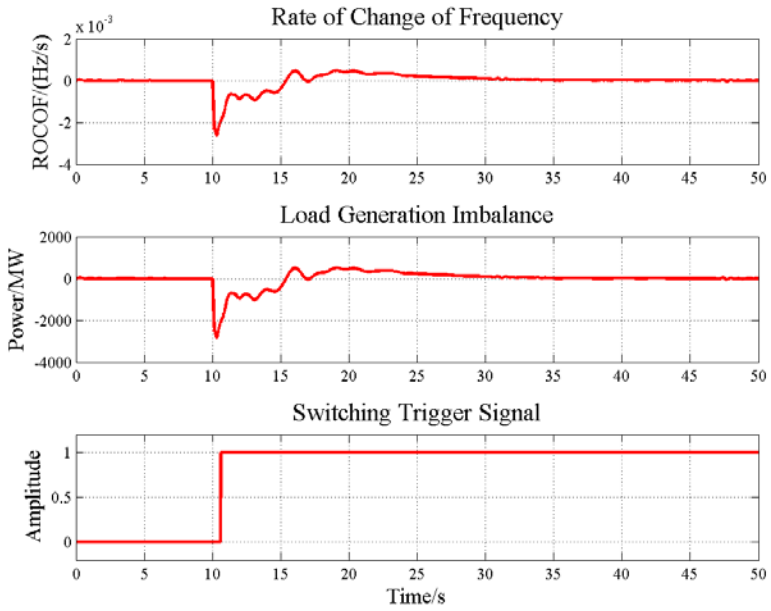

Figure 40. Measurements in the ROCOF block, HSC mode

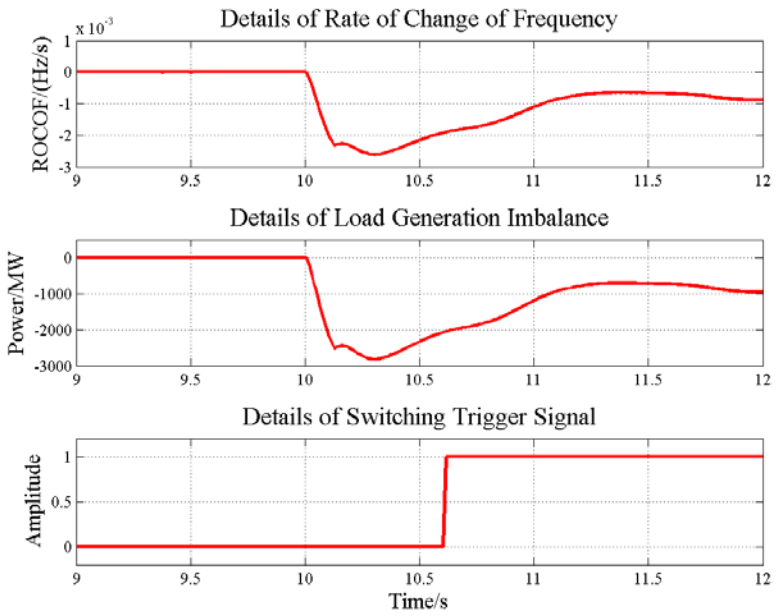

Figure 41. Details of measurements in the ROCOF block, conventional pumping mode

When the T-PSH units received the switching trigger signal, the Castaic and Hyatt units were switched from pumping mode to generation mode with 20 seconds of transition time. Meanwhile, the other three T-PSH units were kept in conventional pumping mode. Figure 42 illustrates that the switched T-PSH units can do the quick mode switching and provide a larger proportion of power back to the grid in about 10 seconds where the name "ROCOF" in the legend refers to the ROCOF-based wide-area control method. After this, the governor in the turbine continues to adjust the electrical power output.

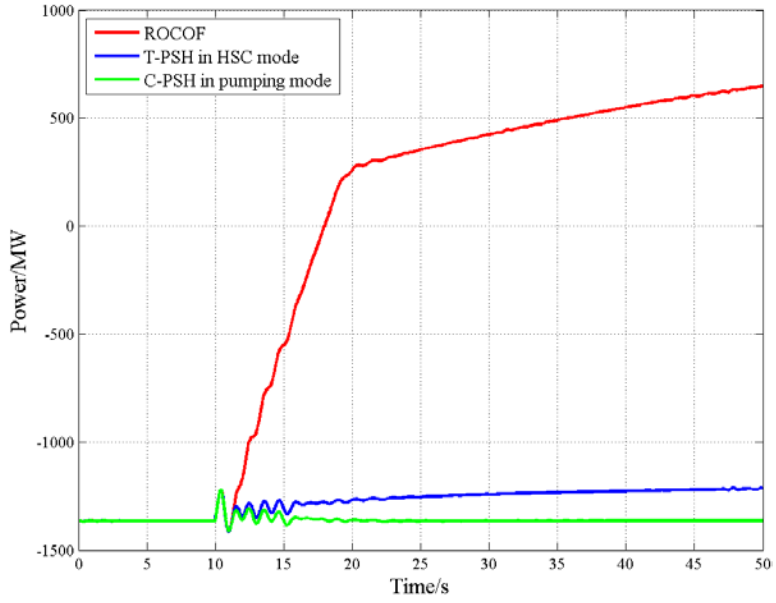

Figure 42. Electrical power output of switched T-PSH units

Results:

- The frequency response and electrical power, shown respectively in Figure 43 and Figure 44, illustrate that the operation-mode-switched T-PSH units improve the system frequency response significantly by feeding a large amount of power back to the system. The switching application brings the settling frequency to 59.95 Hz, which directly solves the problem of triggering underfrequency load-shedding and greatly reduces the need for subsequent frequency regulation.

The frequency improvement and additional injection power given by two switched T-PSH units is compared with the HSC mode case and conventional pumping case in Table 6.

- Combining these results, the operation mode switching application can significantly improve the performance of the system after the contingency.
- The natural inertia of the T-PSH can assist in stabilizing the system. Because of this, operation mode switching is a preferable solution to deal with the contingencies under 60% high renewable contribution levels.
- The wide range of power injection provided by switching operation mode gives T-PSH the potential to participate in wide-area control.

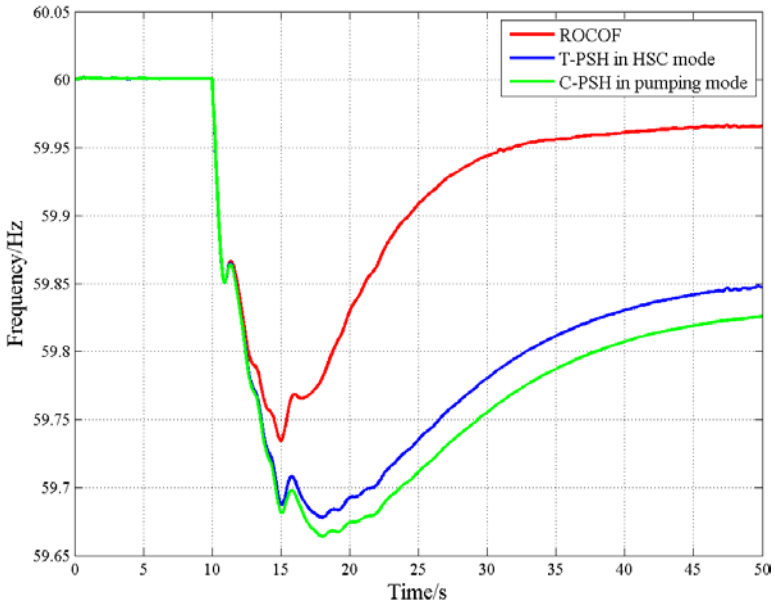

Figure 43. Frequency response of T-PSH units in operation mode switching

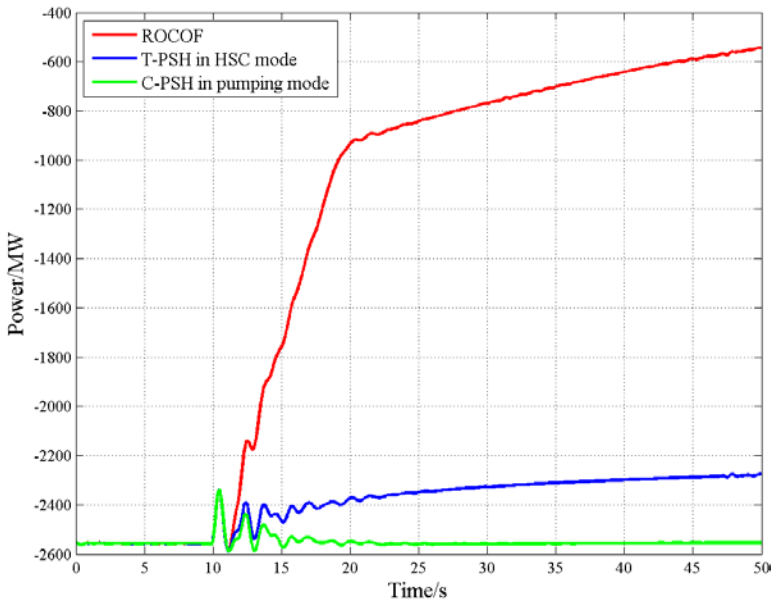

Figure 44. Total electrical power output of T-PSH units in operation mode switching
Note: The name "ROCOF" in the legend refers to the ROCOF-based wide-area control method

Table 6. Details of Improvement by T-PSH in Operation Mode Switching

Metrics	Compared with HSC	Compared with Pumping
Frequency Nadir	59.40 mHz	70.50 mHz
Settling Frequency	119.22 mHz	140.12 mHz
Extra Power	1727.5 MW	2,010.5 MW

4.4.4 AS-PSH Frequency Response Under Increasing Renewables Penetration

Building on the LSP test case described above, Figure 45 compares C-PSH, T-PSH, and Q-PSH performance within the WI system. The modeling results demonstrate that under high renewable energy contribution, both Q-PSH and T-PSH provide faster and greater frequency support than C-PSH.

The generation mix along with the approach for configuring these high-renewables, low-system-load test cases can be found in Appendix G.

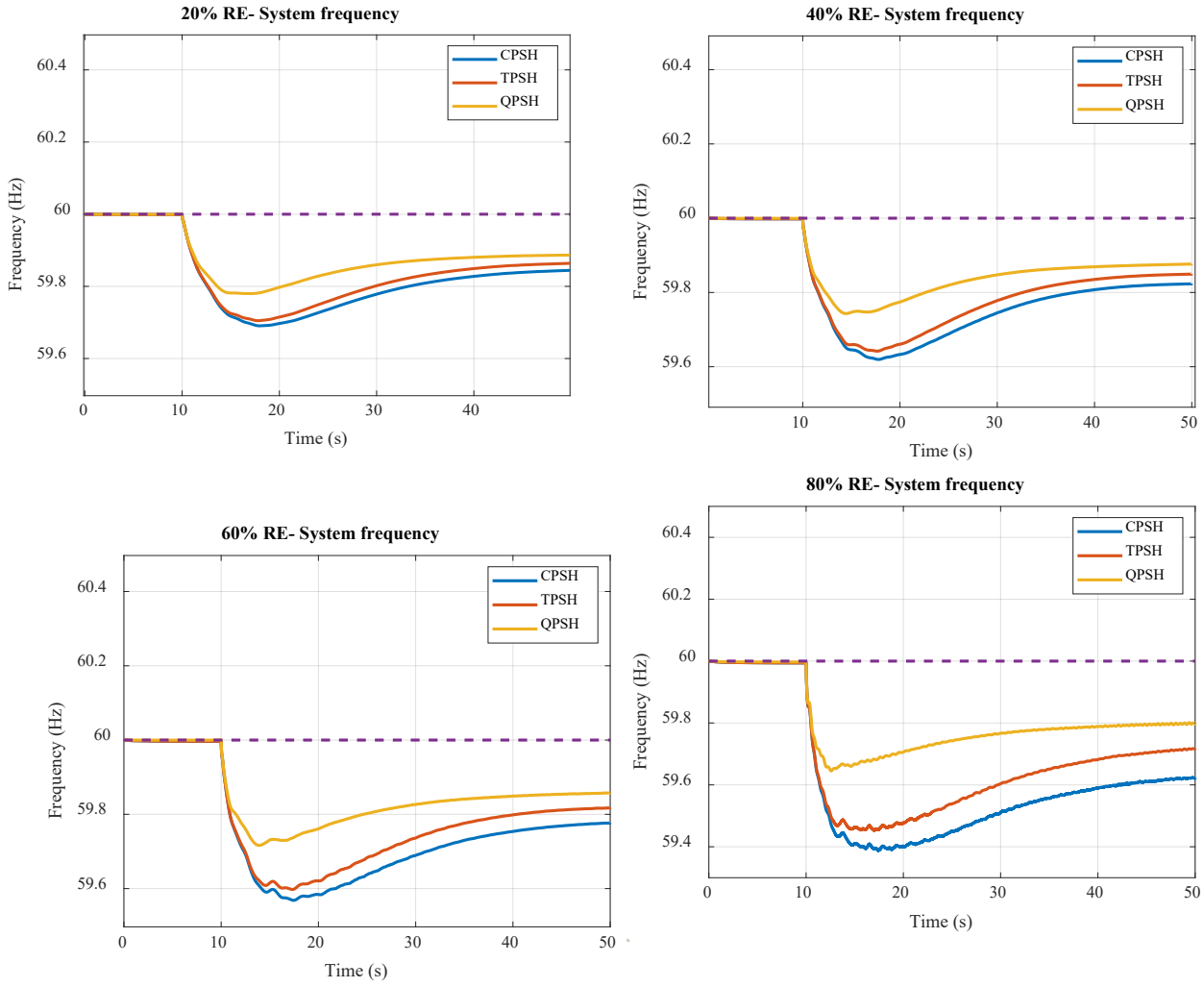

Figure 45. Frequency responses of advanced PSH technologies in WI

4.5 Dynamic Transmission Control

Synchrophasor-based control combined with the FACTS equipment can be used to create a DTC system that leverages the capabilities of T-PSH in the context of wide-area monitoring, protection, and grid control, as shown in Figure 46. The transient system stability margin can be tracked in real time, and the trajectory of stable operation can be forecasted and used to guide the operation of the T-PSH even under constrained transmission. The benefits of T-PSH pump/turbine technology are greatly expanded when leveraged with FACTS devices and the thousands of existing synchrophasors presently installed on strategic buses in the U.S. power system network.

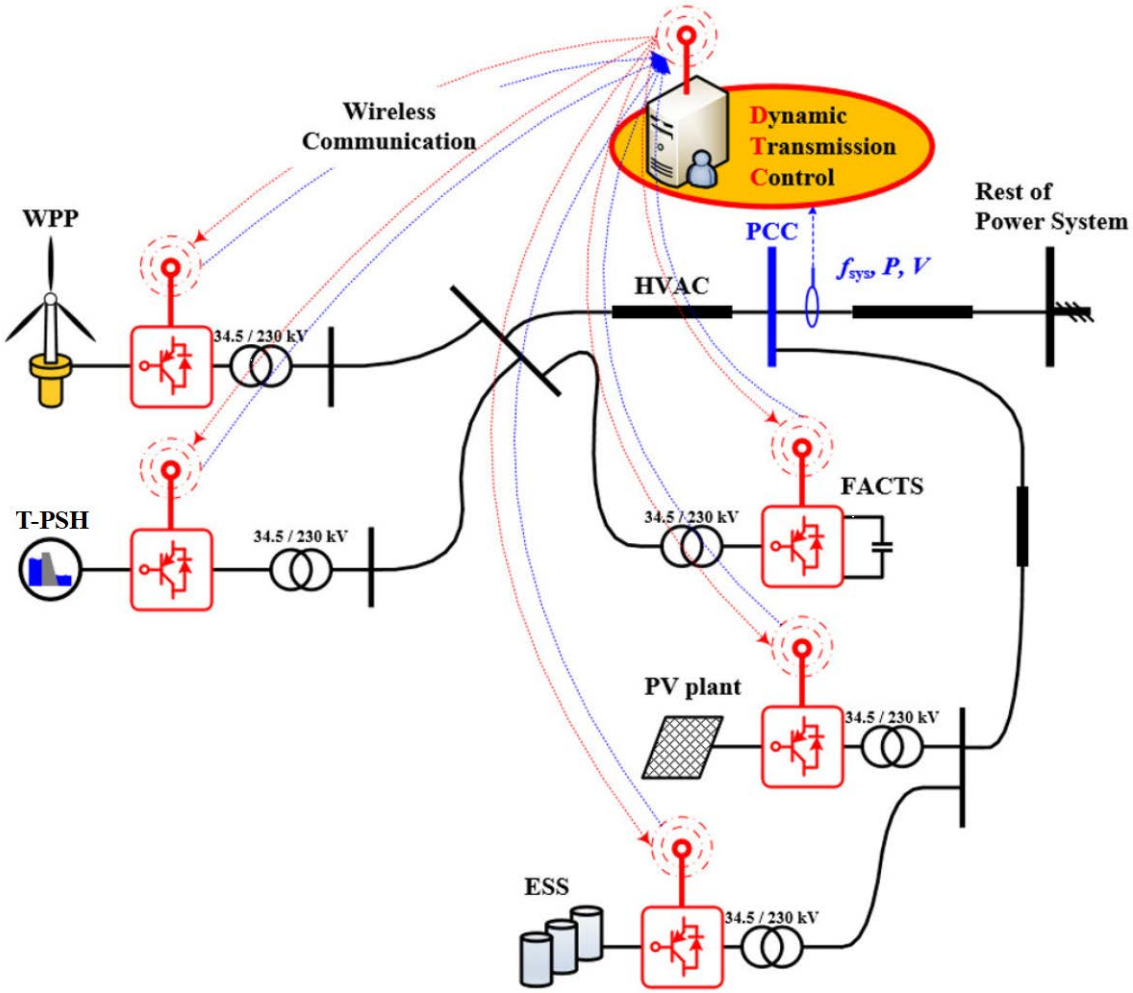

Figure 46. Overview of a DTC application in a power system

To investigate the value of T-PSH as a part of a wide-area control strategies that can provide flexible control functions, the team developed the DTC shown in Figure 47. The DTC acquires real-time data from the transmission system and generation and storage units and makes control decisions based on the information gathered to mitigate dynamic variability of electrical variables over the transmission system.

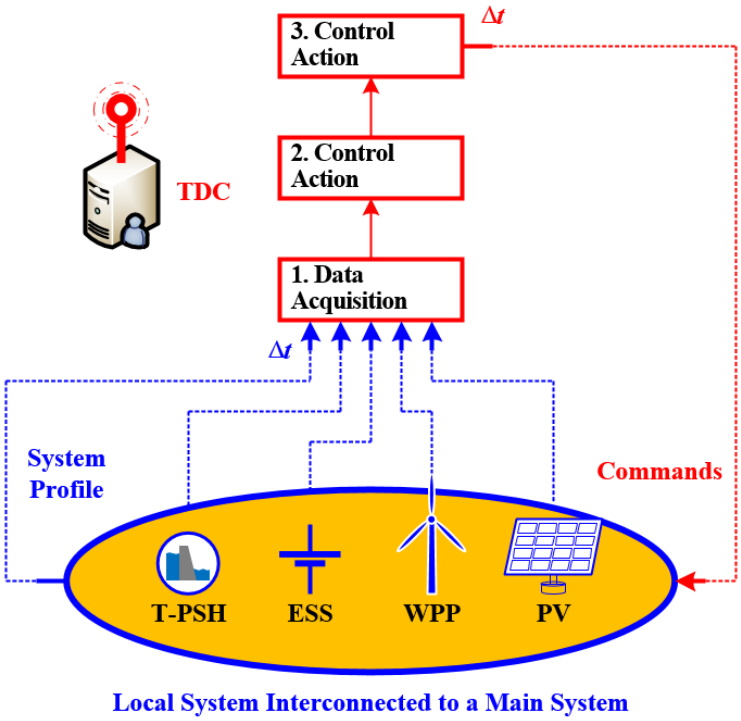

Figure 47. Overview of DTC application in a power system

4.5.1 Case Studies—Dynamic Transmission Control

The objective of the case studies in this section are to investigate the role that T-PSH can play in wide-area control, where control coordination among T-PSH, renewable generation, and static synchronous compensation (STATCOM) is used to reinforce grid stability. Thus, the profile of the main system or interconnection area where the units are integrated would remain stable, and the renewable generation would continue efficient operation through the control coordination by providing flexible control functions. To achieve these, the control coordination—DTC—provides three control functions: congestion relief, constant power, and voltage control. Figure 48 shows the control functions of the DTC. The functions are described as follows:

Congestion Control:

This control scheme aims to relieve transmission congestion associated with variable renewable generation while avoiding variable generation curtailment. To do this, the congestion relief function in the DTC monitors the active power in the transmission system and then modulates the active power accordingly at the T-PSH plant.

Constant Power Control:

This function aims to make best use of the capacity of the transmission system under variable generation conditions. To do this, the constant power function in the DTC monitors the active power into the transmission system and uses the T-PSH plant to provide firming.

Voltage Control Function:

This function aims to mitigate voltage issues relating to active power variation caused by variable generation. To do this, the voltage control function in the DTC monitors the voltage at the point of common coupling and commands a STATCOM to provide reactive power.

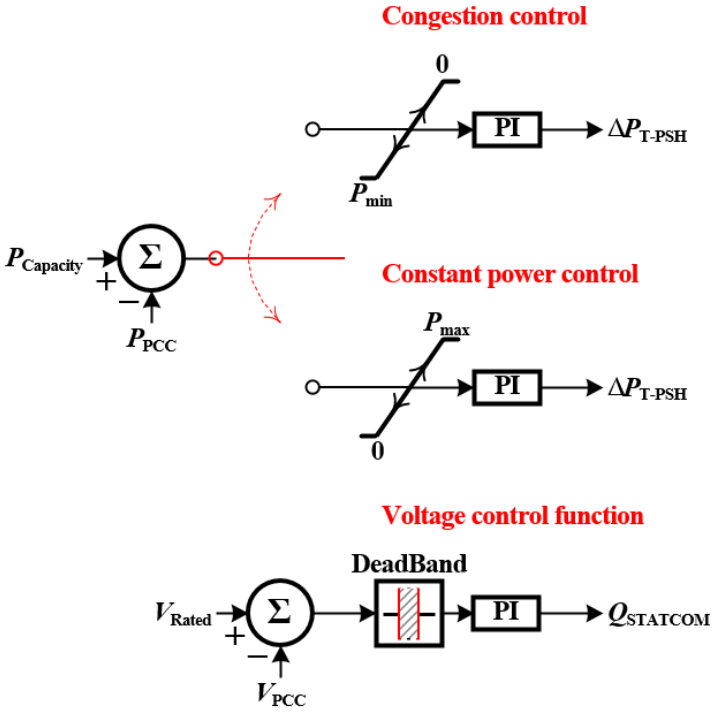

Figure 48. Control functions in the DTC

To test the performance of the functions in the DTC, the test system shown in Figure 49. was used. The test system consists of a 400-MW T-PSH, 200-MW WPP, 100-MVAr STATCOM, and two synchronous generators. The power transfer capacity of the transmission system is set to 400 MVA.

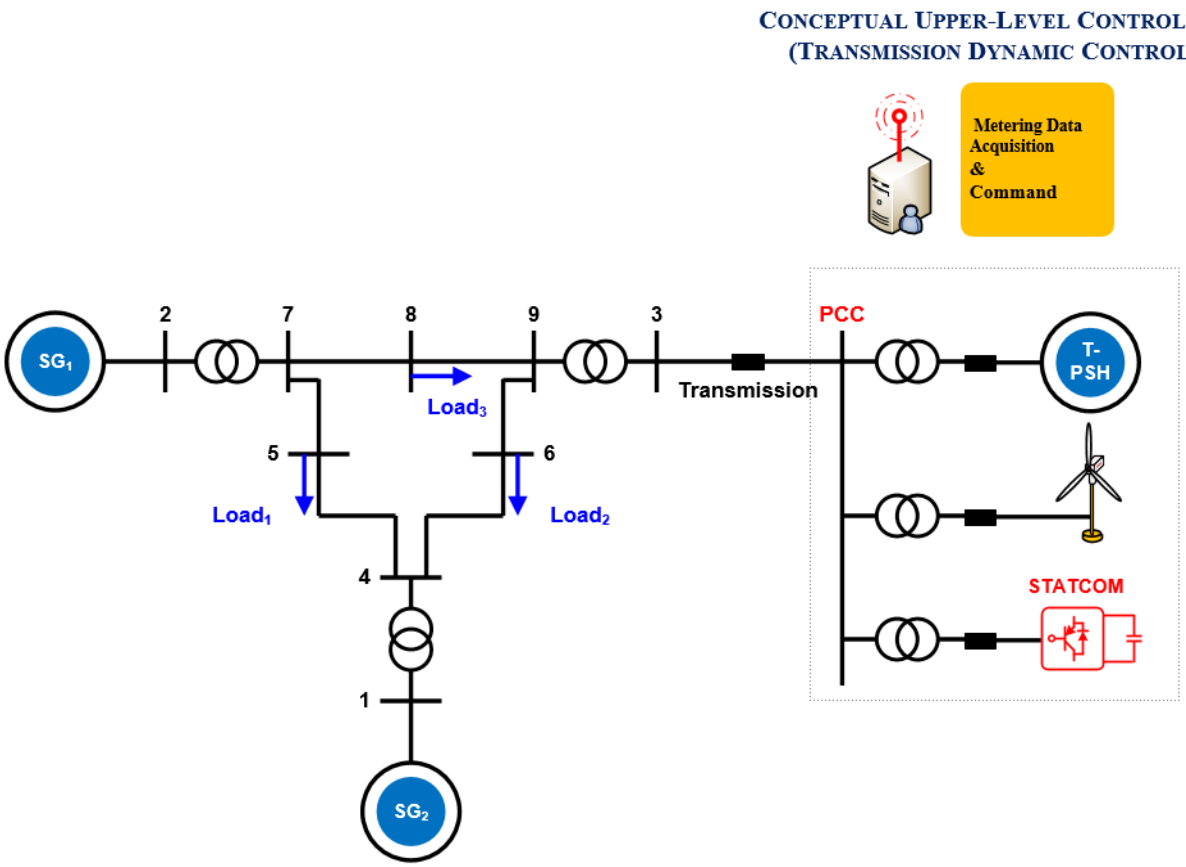

Figure 49. The test system

4.5.2 Case 1: Congestion Control

To test the performance of the DTC's congestion control, the WPP in the test system ramps up from 110 MW to 200 MW while the transmission system is delivering 360 MW. Thus, the transmission system exceeds its transfer capacity by 50 MW and risks curtailment. In addition, the congestion control is compared with the wind power curtailment scheme and no control scenarios.

Figure 50, Figure 51, Figure 52, and Figure 53 show the results for Case 1. As the WPP ramps up, the active power from the WPP exceeds its transfer capacity of the transmission system for approximately 66 seconds for all schemes (Figure 50). In response, the wind power is curtailed, and congestion control schemes correct the active power under the capacity, 400 MVA, with time. To achieve this, the wind power curtailment scheme limits the active power production from the WPP by utilizing pitch control, as shown in Figure 51. The congestion control scheme does not regulate the WPP; instead, it regulates the production from the T-PSH to correct the active power into the power control center (PCC) under its capacity limit, as shown in Figure 52.

Results:

- The congestion control scheme of the DTC is able to lessen WPP curtailment by reducing the output power from the T-PSH, as shown in Figure 53, saving the energy stored in the T-PSH's upper reservoir for later use.

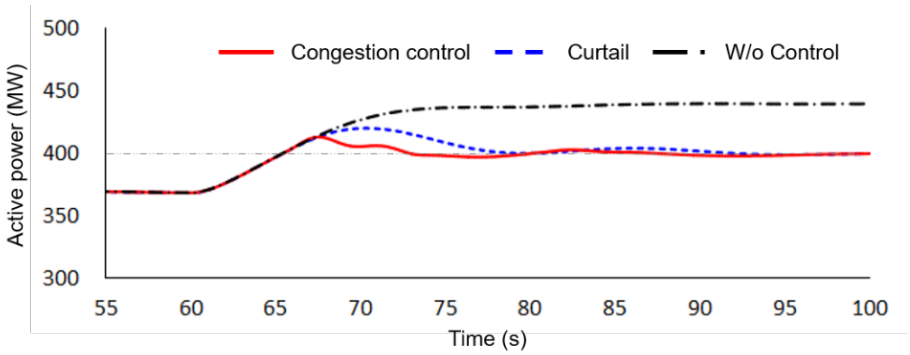

Figure 50. Results for Case 1 active power into the power control center

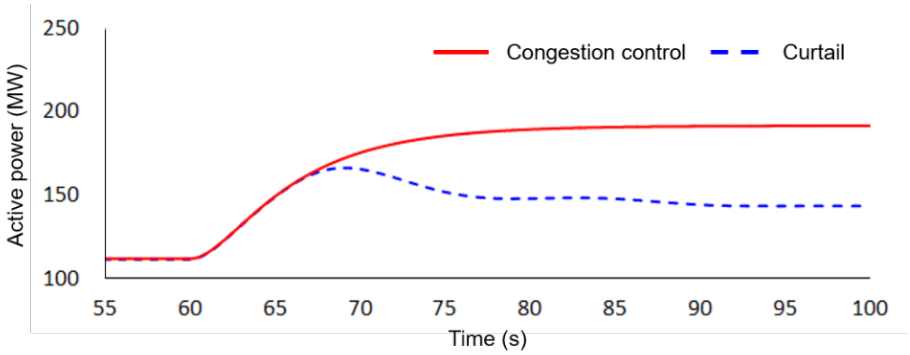

Figure 51. Results for Case 1 active power from the wind power plant

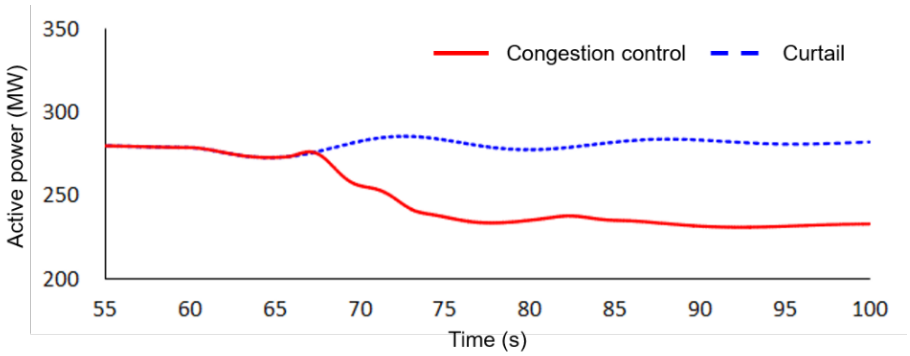

Figure 52. Results for Case 1 active power from the T-PSH

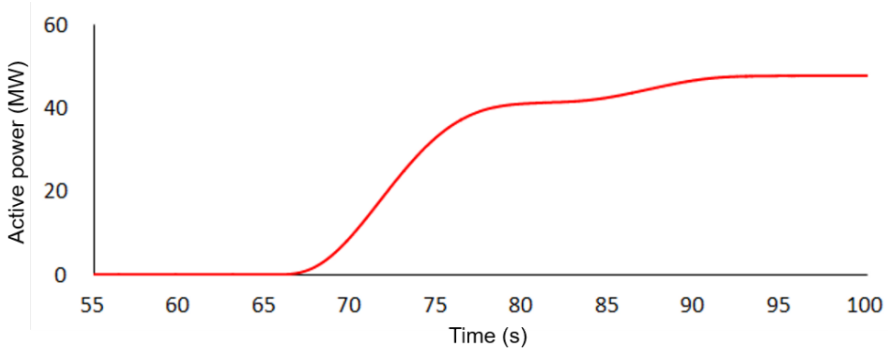

Figure 53. Results for Case 1 curtailed power from the wind power plant

4.5.3 Case 2: Constant Power Control

To test the performance of the constant power control, the WPP in the test system ramps down from 150 MW to 100 MW while the transmission system is delivering 400 MW. Thus, the transmission system experiences a sudden active power reduction by 50 MW.

Figure 54, Figure 55, and Figure 56 show the results for Case 2. As the WPP ramps down from 150 MW to 100 MW (Figure 54), the active power being transferred through the transmission system starts to decrease (Figure 55).

Results:

- The constant power control scheme stabilizes the system by increasing the power from the T-PSH (Figure 56) thereby compensating for the loss of power form the WPP.

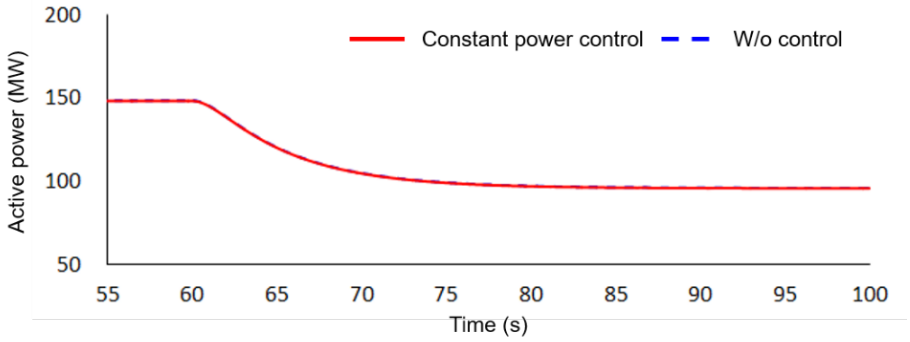

Figure 54. Results for Case 2 active power from the WPP

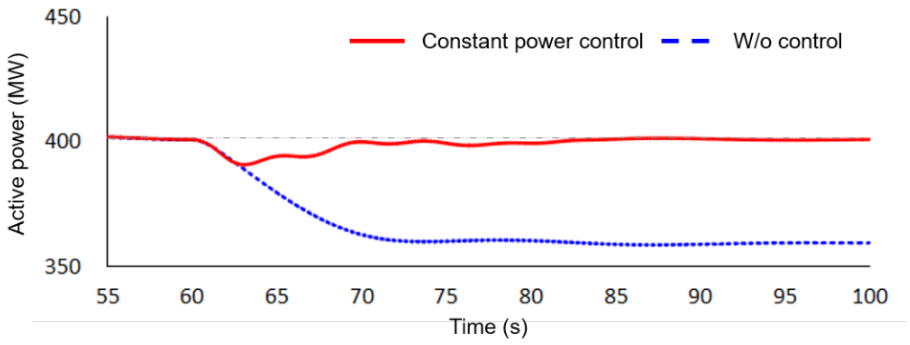

Figure 55. Results for Case 2 active power into the PCC

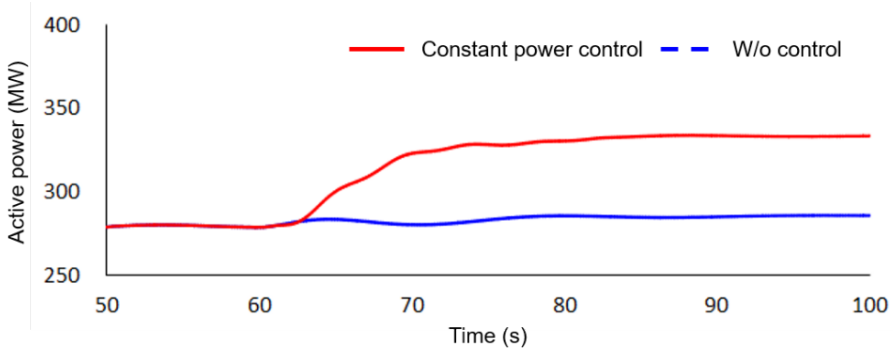

Figure 56. Results for Case 2 active power from the T-PSH

4.5.4 Case 3: Voltage Control

To test the performance of the DTC's voltage control capabilities of the STATCOM, the same scenario with Case 1 was simulated for Case 3. In this case, the ramp-up from the WPP causes an overvoltage condition at the PCC, and the STATCOM is deployed to mitigate the overvoltage. The voltage control of the STATCOM is compared with no STATCOM.

Figure 57, Figure 58, and Figure 59 show the results for Case 3. As the WPP ramps up, the voltage at the PCC and the WPP increases (Figure 57 and Figure 58).

Results:

- The STATCOM helps to prevent the overvoltage at the PCC once the voltage exceeds its control deadband, 1.05 p.u., by injecting lagging reactive power into the transmission system (Figure 59).

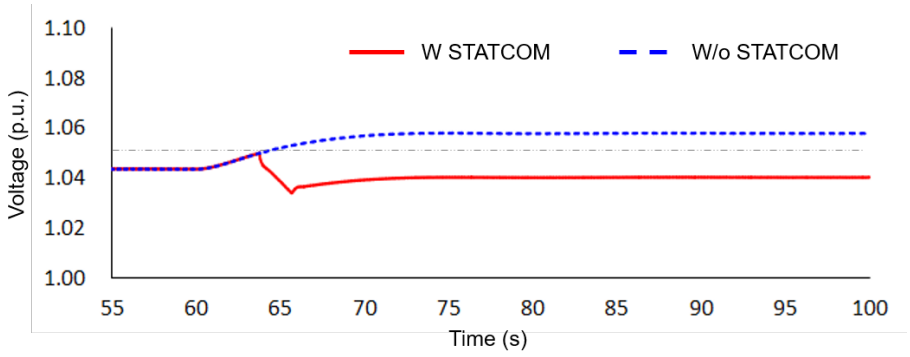

Figure 57. Results for Case 3 voltage at the PCC

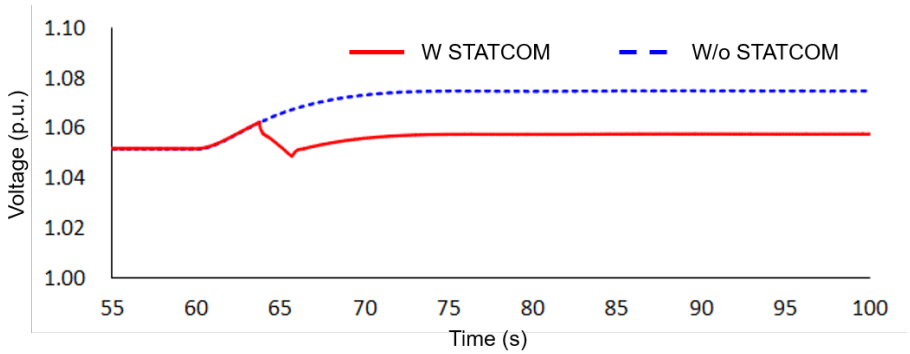

Figure 58. Results for Case 3 voltage at the WPP

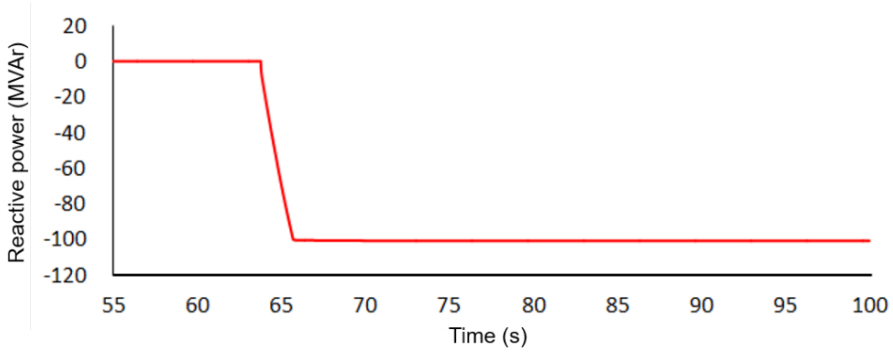

Figure 59. Results for Case 3 reactive power from the STATCOM

5 Techno-Economic Analysis

This section describes the methodology used to analyze the economic feasibility of T/Q-PSH, including LCOE estimates for the Reference Project.

5.1 Methodology

One method of evaluating the economic feasibility of PSH technology is the LCOE approach. This metric enables a wide variety of technologies to be compared using a set of standard assumptions. To simplify the analysis, it is common practice to lump all equipment, construction, development, and any other costs before production as Year 0 costs that are referred to as capital expenditures (CapEx). Capex is spread over a number of years, and one must take caution in comparing projects with significant variance in construction time, financing, and so on. For simplicity, this analysis assumes overnight pricing on all CapEx categories. Operational expenditures (OpEx) are considered as an average annual cost in years 1–*n* of the project. It is important to note that hydropower projects, including PSH, typically operate well past their economic life, and LCOE does not capture the entire project life. Given that hydropower projects, including PSH, are one of the few technologies that can secure 50-year loans, this analysis assumes a 50-year economic life. This varies from many other technologies that may only be able to secure 20-year financing. To capture the economic life, interest, inflation, and other financial parameters, the team used the simple, but effective, fixed charge rate (FCR) method of calculating LCOE. With these three inputs (CapEx, OpEx, and FCR), the annual cost to operate the PSH facility can be approximated. Dividing this annual cost value by the average annual energy production provides the LCOE for a given project, as shown in the following equation:

$$\text{LCOE} = \frac{(\text{CapEx} \times \text{FCR}) + \text{OpEx}}{\text{AEP}}$$

Where:

- **CapEx** represents all capital expenditures associated with the planning, design, manufacturing, deployment, and project management of a project. These are assumed as overnight capital costs.
- **FCR**, fixed charge rate, is the annual return, represented as a fraction of installed capital costs, needed to meet investor revenue requirements.
- **OpEx**, operational expenditures, includes all routine maintenance, operations, and monitoring activity (i.e., non-depreciable). In the case of storage technologies, this includes any electricity that is purchased for storage. For PSH technologies, this includes the electricity required to pump to the upper reservoir.
- **AEP**, annual energy production, describes the average annual energy generated (after accounting for device or array availability) and delivered to the point of AC grid interconnection (i.e., the measurable basis for power purchase contracts).

Capital and Development Costs:

Estimated capital and developments costs () were established by the project team at Absaroka Energy, strictly following DOE guidelines. As such, the capital costs and project development costs are assumed to be overnight costs. It should be noted that many of these costs are site-specific and are based on quotes that have been provided for Absaroka for their Gordon Butte project.

This project initially focused on the feasibility of T-PSH technology at the Gordon Butte Pumped Storage Project. During this project, the developers determined that Q-PSH had significant cost-reduction advantages. Therefore, the costs and performance models referenced in this analysis reflect the quaternary technology.

A summary of the capital and development costs were provided by the developer that estimated baseline capital and development costs at $3,175/kW. After this analysis was completed, the Reference Project received revised equipment and installation bids that improved the baseline capital and development costs to approximately $2,500/kW. The report will use the more conservative costs first reported.

Operating Parameters and Financial Assumptions:
Certain assumptions were made to approximate the LCOE of a project and to better understand the potential impact of technology variances. To ensure this project was comparable with other PSH projects, the following operating parameters and financial assumptions were made (Table 7).

Table 7. Operating Parameters for Baseline Project

Category	Baseline
Plant Rating (MW)	400
Storage Duration (Hours)	12
System Design Life (Years)	50
Real Discount Rate (%)	5.5
Fixed Charge Rate (%)	5.9

Annual Operating Expenses:
The annual operating expenses for PSH projects are primarily driven by the cost of pumping, similar to a fuel cost associated with fossil fuel or biomass-derived power plants. Note that storage technologies can operate based on market conditions in both pumping and generating mode; therefore, pumping costs are likely to vary. For the sake of this analysis, NREL estimated the pumping cost based on an average pumping rate of $0.025/kWh. Conversations with Absaroka have confirmed that this rate is a realistic yet conservative estimate. To understand the impact of this assumption, a sensitivity analysis has been performed on this assumption (Section 5.3). A summary of the operating expenses, assuming the pumping rate of $0.025/kWh, is presented in Table 8.

Table 8. Summary of Baseline Operations and Maintenance

Category	Baseline ($/kW/yr)
Operating Cost	**$73**
Environmental, Health & Safety	$1
Annual Leases/Fees/Cost of Doing Business	$19
Insurance	$17
Operations, Management, and General Administration	$8
Pumping Electricity Cost[6] ($/kWh)	$28
Maintenance	**$11**
Total Operating Expenses	**$84**

Annual Energy Production:

Annual energy production for storage technologies is heavily dependent on market conditions rather than physics like traditional renewable technologies (e.g., wind turbines can only produce energy when the wind is blowing). However, there are physical limits based on capacity, ability to ramp up and ramp down, and availability of excess power on the grid. For the baseline analysis, energy production was estimated using a price-taker model. The price-taker model approximates pumping costs and generation revenue based on historic data in that market. The initial analysis estimated an annual production of approximately 587 GWh while purchasing approximately 722 GWh for pumping. These production numbers produce a relatively low plant utilization (approximately 37%). It should be noted that, even with the low plant utilization, the LCOE for the current scenario is still competitive with traditional storage technologies.

5.2 LCOE Estimates

Combining the capital costs, development costs, and operational costs with the anticipated energy production, the Q-PSH Reference Project will be able to sell electricity at an average rate of $0.185/kWh; however, as previously described, this is heavily dependent on the level of plant utilization. Figure 60 illustrates how LCOE changes as a function of capacity factor, defined as the ratio of generation to nameplate capacity of the turbine (i.e., 50% capacity factor represents 100% utilization for a 1:1 pumping to generation ratio). The plot also highlights the approximate range for LCOE that is stated in the 2017 Lazard Levelized Cost of Storage report for lithium-ion technologies. Lastly, the LCOE is plotted for three different pumping-to-generation ratios ranging from 1 to1.5, with 1.25 representing the ratio that was used in the price-taker model.

[6] The cost of pumping is determined by the overall plant utilization and the assumption for electricity rates. Electricity rates for this project have been assumed at $0.025/kWh.

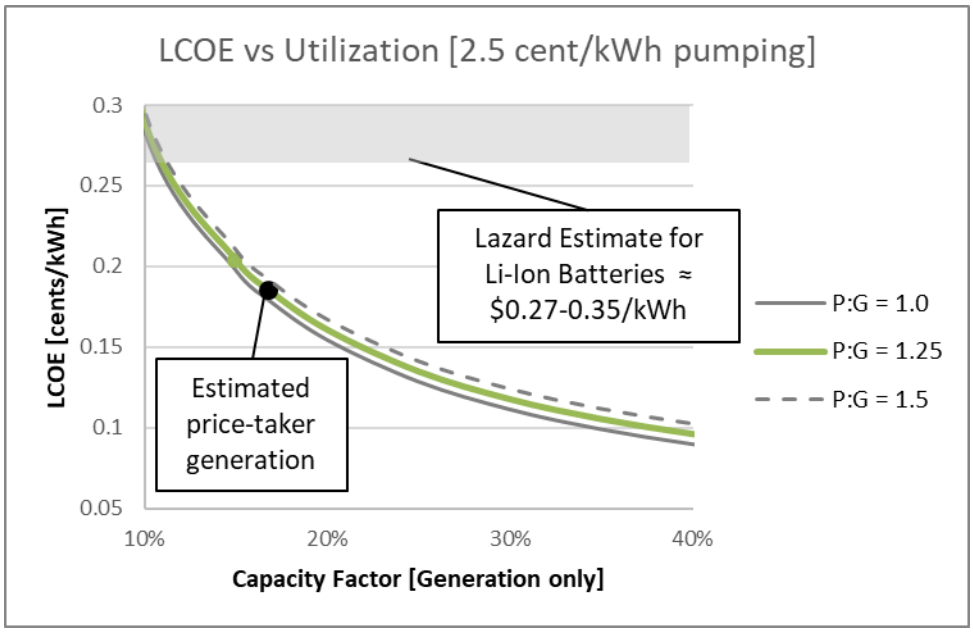

Figure 60. LCOE vs. utilization of Gordon Butte project

Illustration by Absaroka Energy

The cost estimates provided by Absaroka, along with the generation and pumping estimates, show that the Q-PSH technology proposed at this location is approximately 40% less expensive than a traditional lithium-ion battery system of similar nameplate capacity and energy storage capability, with significant opportunities for additional revenue generation either through capacity or through the ancillary benefits that are provided from a Q-PSH project.

5.3 Sensitivity Analysis

The LCOE analysis presented in this report only considers the cost and revenue associated with building and operating a Q-PSH facility at the Gordon Butte location for the purposes of energy time shifting (e.g., energy arbitrage) and does not consider additional revenue streams for this facility. This choice was made to help ensure that the LCOE presented can be easily compared with other storage technologies. To fully understand the economic viability, a more detailed cost and revenue model should be developed to capture the variability in market conditions. But the LCOE presented previously suggests that Q-PSH technology is a viable alternative when compared to traditional storage technologies. Additionally, if the plant utilization increases, the LCOE will be reduced even further.

A straight-line cost sensitivity was performed to determine which cost categories present the highest risk and to quantify the impact of that risk on LCOE. As anticipated, the three highest-cost categories for the Q-PSH technology are the costs associated with civil works, electromechanical equipment, and pumping costs. In this scenario, civil works are by far the largest contributor to risk, with a $0.027/kWh variance with a +/-20% sensitivity, and electromechanical another +/- $0.17/kWh. Due to the status of the Gordan Butte project, these costs are not likely to vary significantly as they are based on years of development and project quotes. Figure 61 visualizes the sensitivity for the Level 2 cost categories, except for operating costs, which are described at a Level 3 so that pumping costs can be visualized.

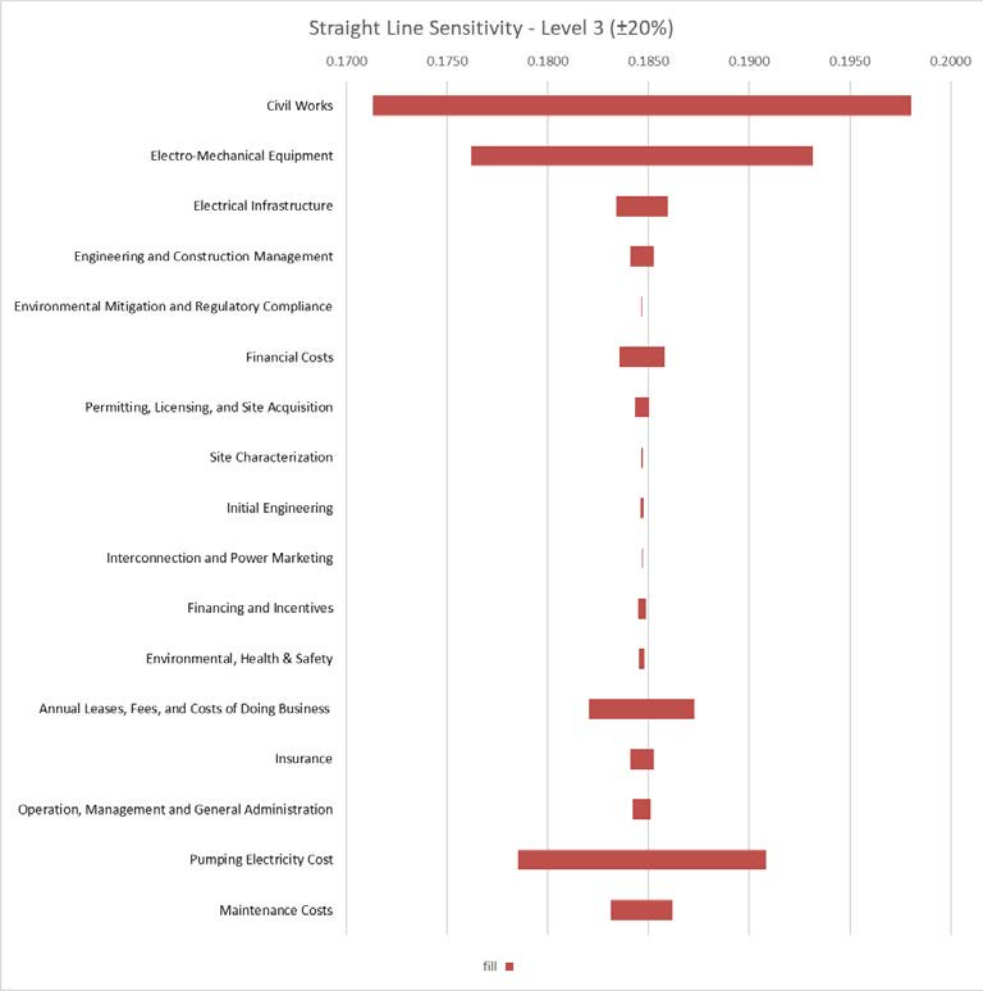

Figure 61. LCOE sensitivity to Level 2 cost categories

Illustration from Absaroka Energy

It should be noted that, as the plant utilization is increased, the pumping costs become the largest driver (this occurs at approximately 35% capacity factor, or 78% of overall plant utilization). Because the LCOE is significantly reduced at these higher utilizations, the absolute impact of cost variance is reduced. At a capacity factor of 35%, the LCOE is reduced from $0.185/kWh to approximately $0.104/kWh (before adjusting for any potential increase in per unit of energy pumping costs). At this utilization level, even if the assumed pumping costs are increased from $0.025/kWh to $0.05/kWh, the LCOE only increases to approximately $0.135/kWh, still highly competitive with other storage technologies.

6 Conclusions

This work provided an overview of ternary and quaternary pumped storage hydropower (i.e., T/Q-PSH) technologies and investigated how they performed in grid reliability and stability analysis (dynamic modeling) settings. The main findings of the report are:

1. Q-PSH, when operating in hydraulic short-circuit (HSC) mode, can provide better frequency support (faster response and more power to the system) than any of the other PSH technologies investigated in this work. It offered the inertia of a C-PSH unit combined with the fast mode switching ability of T-PSH and the fast response associated with the power electronics of an AS-PSH unit—leveraging the best of each.
2. In underfrequency event simulations at high penetrations of renewables (80% renewable energy), the Q-PSH unit (operating in HSC mode) provided frequency support like that of a C-PSH unit twice its size.
3. T/Q-PSH shows promise when configured as part of a DTC system and can provide congestion, power, and voltage control. In the power control demonstration, T-PSH the grid recover from an unexpected 50 MW wind-down ramp event in approximately 10 seconds. The response time of Q-PSH would be even faster.
4. Cost estimates show that the T/Q-PSH technology proposed for the Reference Project is approximately 40% less expensive than a traditional lithium-ion battery system of similar nameplate capacity and energy storage capability (400 MW/5,000 MWh).

Figure 62 provides a summary of how the capabilities across the various types of PSH compare.

Pumping Mode of different PSH technologies						
Service Types		C-PSH	AS-PSH DFIG	AS-PSH Full Conv.	T-PSH	Q-PSH
Ancillary Services	Inertial Response	🟢	🟡	🟡	🟢	🟢
	Primary Frequency Response	🔴	🟡	🟡	🟢	🟢
	Frequency Regulation	🔴	🟡	🟡	🟢	🟢
	Load Following	🔴	🟢	🟢	🟢	🟢
	Spinning Reserve	🔴	🟢	🟢	🟢	🟢
Others	Start-up (s)	300	280	40	120	120
	Pump-Generating (s)	190	190	190	25	30
	Synchronous Condenser-Generating (s)	100	100	100	20	30
	Pumping range (%)	100%	60%–100%	60%–100%	0%–100%	0%–100%

🔴 Incapable 🟡 Capable with ancillary control 🟢 Capable

Figure 62. PSH technology capability comparison (in pumping mode)

References

70 FR 47093. F. O. No, 661-A, "Interconnection for Wind Energy," Docket No, RM05-4-001, December 2005.

Clark, K., R. Walling, and N. Miller. 2011. "Solar photovoltaic (PV) plant models in PSLF." in *2011 IEEE Power and Energy Society General Meeting.* https://doi.org/10.1109/PES.2011.6039117.

Clark, K., N. W. Miller, and J. J. Sanchez-Gasca. 2010. *Modeling of GE wind turbine-generators for grid studies*. Schenectady, NY: GE Energy. Available at https://www.researchgate.net/publication/267218696_Modeling_of_GE_Wind_Turbine-Generators_for_Grid_Studies_Prepared_by.

Choo, Yin Chin, Kashem Muttaqi, and M. Negnevitsky. 2008. "Modelling of hydraulic governor-turbine for control stabilisation." *ANZIAM Journal* 49: 681–698. https://doi.org/10.21914/anziamj.v49i0.333.

Concorda, G. 2012. *PSLF User's Manual, ver 18*. Schenectady NY.

del Toro García, Xavier, Pedro Roncero-Sánchez, Alfonso Parreño, and Vicente Feliu. 2010. "Ultracapacitor-based storage: Modelling, power conversion and energy considerations." in *2010 IEEE International Symposium on Industrial Electronics*. https://doi.org/10.1109/ISIE.2010.5637966.

DOE Global Energy Storage Database. Undated(a). "Castaic Pumped Storage Plant." Sandia National Laboratories. https://sandia.gov/ess-ssl/gesdb/public/projects.html#76.

DOE Global Energy Storage Database. Undated(b). "San Luis (William R. Gianelli) Pumped Storage Hydroelectric Powerplant." Sandia National Laboratories. https://sandia.gov/ess-ssl/gesdb/public/projects.html#50.

DOE Global Energy Storage Database. Undated(c). "Helms Pumped Hydro Storage Project." Sandia National Laboratories. https://sandia.gov/ess-ssl/gesdb/public/projects.html#1029.

DOE Global Energy Storage Database. Undated(d). "Edward Hyatt (Oroville) Power Plant." Sandia National Laboratories. https://sandia.gov/ess-ssl/gesdb/public/projects.html#44.

DOE Global Energy Storage Database. Undated(e). "Big Creek (John S. Eastwood) Pumped Storage." Sandia National Laboratories. https://sandia.gov/ess-ssl/gesdb/public/projects.html#175.

Dong, Z., R. Nelms, E. Muljadi, J. Tan, V. Gevorgian, and M. Jacobson. 2018. "Development of Dynamic Model of a Ternary Pumped Storage Hydropower Plant." in *2018 13th IEEE Conference on Industrial Electronics and Applications (ICIEA)*, May 31–June 2, 2018, Wuhan, China. https://doi.org/10.1109/ICIEA.2018.8397796.

Dong, Zerui. 2019. "Dynamic Model Development and System Study of Ternary Pumped Storage Hydropower." PhD diss., Auburn University. https://etd.auburn.edu/bitstream/handle/10415/6632/Final%20Version_4_clean.pdf?sequence=2&isAllowed=y.

Dong, Zerui, Jin Tan, Antoine St-Hilaire, Eduard Muljadi, David Corbus, Robert Nelms, and Mark Jacobson. 2019. "Modeling and Simulation of Ternary Pumped Storage Hydropower for Power System Studies." *IET Generation, Transmission & Distribution*. https://digital-library.theiet.org/content/journals/10.1049/iet-gtd.2018.5749.

E. C. GE Energy Applications and Systems Engineering, AWS Truewind. 2009 "Technical Requirements for Wind Generation Interconnection and Integration—New England Wind Integration Study." 2009.

FACTS Terms & Definitions Task Force. 1997. "Proposed terms and definitions for flexible AC transmission system (FACTS)." *IEEE Transactions on Power Delivery* 12(4): 1848–1853. https://doi.org/10.1109/61.634216.

Girdhar, Paresh, and Octo Moniz. 2011. *Practical Centrifugal Pumps*. Elsevier.

Hacobian, B., and H. Yee. 1978. "Pump Modelling for Power System Stability Studies." *Electric Energy Conference 1978: Australian Electrical Research; Preprints of Papers*, p. 239.

Hingorani, Narain, and Laszlo Gyugyi. 1999. *Understanding FACTS: Concepts and Technology of Flexible AC Transmission Systems*. Wiley-IEEE Press.

IEEE Committee. 1968. "Computer representation of excitation systems." *IEEE Transactions on Power Apparatus and Systems* PAS-87(6): 1460–1464. https://doi.org/10.1109/TPAS.1968.292114.

IEEE Committee. 1981. "Excitation System Models for Power System Stability Studies." *IEEE Transactions on Power Apparatus and Systems* PAS-100, no. 2 (February 1981): 494-509. https://doi.org/10.1109/TPAS.1981.316906.

Joshi, K. 2019. *Flexible A.C. Transmission System (FACTS) Devices with Energy Storage Systems*.

Kerkman, R.J., T. Lipo, W. Newman, and J. Thirkell. 1980. "An inquiry into adjustable speed operation of a pumped hydro plant part 1-machine design and performance." *IEEE Transactions on Power Apparatus and Systems* PAS-99(5): 1828–1837. https://doi.org/10.1109/TPAS.1980.319773.

Kim, J., V. Gevorgian, Y. Luo, M. Mohanpurkar, V. Koritarov, R. Hovsapian, et al. 2019. "Supercapacitor to Provide Ancillary Services with Control Coordination." *IEEE Transactions on Industry Applications* 55(5): 5119–5127. https://doi.org/10.1109/TIA.2019.2924859.

Kim, Jinho, Eduard Muljadi, Vahan Gevorgian, Manish Mohanpurkar, Yusheng Luo, Rob Hovsapian, Vladimir Kortarov. 2019. "Capability-coordinated frequency control scheme of a virtual power plant with renewable energy sources." *IET Generation, Transmission & Distribution* 13(16): 3642–3648. https://doi.org/10.1049/iet-gtd.2018.5828.

Knuppel, Thyge, Jorgen Nygard Nielsen, Kim Hoj Jensen, Andrew Dixon, and Jacob Østergaard. 2011. "Power Oscillation Damping Controller for Wind Power Plant Utilizing Wind Turbine Inertia as Energy Storage." in *2011 IEEE Power and Energy Society General Meeting*. https://doi.org/10.1109/PES.2011.6038908.

Koritarov, Vladimir, James Feltes, Yuriy Kazachkov, Bo Gong, Peter Donalek, and Vahan Gevorgian. 2013a. *Testing Dynamic Simulation Models for Different Types of Advanced Pumped Storage Hydro Units.* Argonne, IL: Argonne National Laboratory. ANL/DIS-13/08. https://ceeesa.es.anl.gov/projects/psh/ANL_DIS-13_08_Testing_Dynamic_PSH_Models.pdf.

Koritarov, Vladimir, Leah Guzowski, James Feltes, Yuriy Kazachkov, Bo Gong, Bruno Trouille, and Peter Donalek. 2013b. *Modeling Adjustable Speed Pumped Storage Hydro Units Employing Doubly-Fed Induction Machines*. Argonne, IL: Argonne National Laboratory. ANL/DIS-13/06. https://ceeesa.es.anl.gov/projects/psh/ANL_DIS-13_06_Modeling_AS_PSH.pdf.

Koritarov, Vladimir, Leah Guzowski, James Feltes, Yuriy Kazachkov, Bo Gong, Bruno Trouille, Peter Donalek, and Vahan Gevorgian. 2013c. *Modeling Ternary Pumped Storage Units*. Argonne, IL: Argonne National Laboratory. ANL/DIS-13/07. https://ceeesa.es.anl.gov/projects/psh/ANL_DIS-13_07_Modeling_Ternary_Units.pdf.

Koritarov, Vladimir, Leah Guzowski, James Feltes, Yuriy Kazachkov, Baldwin Lam, Carlos Grande-Moran, Gary Thomann, Larry Eng, Bruno Trouille, and Peter Donalek. 2013d. *Review of Existing Hydroelectric Turbine-Governor Simulation Models*. Argonne, IL: Argonne National Laboratory. ANL/DIS-13/05. https://ceeesa.es.anl.gov/projects/psh/ANL_DIS-13_05_Review_of_Existing_Hydro_and_PSH_Models.pdf.

Koritarov, V, T. D. Veselka, J. Gasper, B. M. Bethke, A. Botterud, J. Wang, et al. 2014. *Modeling and analysis of value of advanced pumped storage hydropower in the United States*. Argonne, IL: Argonne National Laboratory. ANL/DIS-14/7. https://publications.anl.gov/anlpubs/2014/07/105786.pdf.

Kundur, P, N. J. Balu, and M. G. Lauby. 1994. *Power System Stability and Control*. New York: McGraw-Hill.

Lasher, W. 2010. "Summary of Significant Wind-Plant Requirements in ERCOT." Washington, D.C.: North American Electric Reliability Corporation.

Liang, Jiaqi, and R. G. Harley. 2010. "Pumped storage hydro-plant models for system transient and long-term dynamic studies." in *IEEE PES General Meeting*. https://doi.org/10.1109/PES.2010.5589330.

Liu, Yong, Shutang You, Jin Tan, Yingchen Zhang, and Yilu Liu. 2018. "Frequency response assessment and enhancement of the US power grids toward extra-high photovoltaic generation penetrations—An industry perspective." *IEEE Transactions on Power Systems* 33(3): 3438–3449. https://doi.org/10.1109/TPWRS.2018.2799744.

Lung, Jen-Kuang, Ying Lu, Wen-Lung Hung, and Wen-Shiow Kao. 2007. "Modeling and dynamic simulations of doubly fed adjustable-speed pumped storage units," *IEEE Transactions on Energy Conversion* 22(2): 250–258. https://doi.org/10.1109/TEC.2006.875481.

MacDowell, Jason, Kara Clark, Nicholas Miller, and Juan Sanchez-Gasca. 2011. "Validation of GE wind plant models for system planning simulations." in *2011 IEEE Power and Energy Society General Meeting*. https://doi.org/10.1109/PES.2011.6039485.

Miller, Nicholas, Miaolel Shao, Robert D'aquila, Siobodan Pajic, and Kara Clark. 2015. "Frequency Response of the U.S. Eastern Interconnection Under Conditions of High Wind and Solar Generation." in *2015 Seventh Annual IEEE Green Technologies Conference*. https://doi.org/10.1109/GREENTECH.2015.31.

Ming, Zach, Arne Olson, Huai Jiang, Manohar Mogadali, and Nick Schlag. 2019. *Resource Adequacy in the Pacific Northwest*. San Francisco, CA: Energy and Environmental Economics, Inc. https://www.ethree.com/wp-content/uploads/2019/03/E3_Resource_Adequacy_in_the_Pacific-Northwest_March_2019.pdf.

Morren, J., S. W. De Haan, W. L. Kling, and J. Ferreira. 2006. "Wind turbines emulating inertia and supporting primary frequency control." *IEEE Transactions on Power Systems* 21(1): 433–434. https://doi.org/10.1109/TPWRS.2005.861956.

Morren, J., J. Pierik, and S. W. De Haan. 2006. "Inertial response of variable speed wind turbines." *Electric Power Systems Research* 76(11): 980–987. https://doi.org/10.1016/j.epsr.2005.12.002.

Muljadi, E., M. Singh, V. Gevorgian, M. Mohanpurkar, R. Hovsapian, and V. Koritarov. 2015. *Dynamic modeling of adjustable-speed pumped storage hydropower plant: Preprint.* Golden, CO: National Renewable Energy Laboratory. NREL/CP-5D00-63587. https://www.nrel.gov/docs/fy15osti/63587.pdf.

N. A. E. R. Corporation. 2012. "2012 Special Assessment: Interconnection Requirements for Variable Generation."

Nanaware, R.A., S. Sawant, and B. Jadhav. 2013. "Modeling of Hydraulic Turbine and Governor for Dynamic Studies of HPP." in *IJCA Proceedings on International Conference on Recent Trends in Information Technology and Computer Science*, pp. 6–11. https://pdfs.semanticscholar.org/40dd/931830a27418227bb41a382f9216af528cf0.pdf.

Pretro, G. A. 1972. "Main types of machine building arrangement on present day pumped storage stations." *Hydrotechnical Construction* 6: 328–335. https://doi.org/10.1007/BF02377541.

Puyo, A. 1963. "Hydraulic turbine development during the last few years." *La Houille Blanche* 1: 3–41. https://doi.org/10.1051/lhb/1963001.

Sangal, S., A. Garg, and D. Kumar. 2013. "Review of Optimal Selection of Turbines for Hydroelectric Projects." *International Journal of Emerging Technology and Advanced Engineering*. 3(3): 424–430. Available at https://www.researchgate.net/publication/292726939_Review_of_Optimal_Selection_of_Turbines_for_Hydroelectric_Projects.

Schlag, Nick, Arne Olson, Elaine Hart, Ana Mileva, Ryan Jones, Carlo Brancucci Martinez-Anido, Bri-Mathias Hodge, Greg Brinkman, Anthony Florita, and David Biagioni. 2015. *Western Interconnection Flexibility Assessment—Final Report*. Golden, CO: National Renewable Energy Laboratory. https://www.ethree.com/wp-content/uploads/2017/02/WECC_Flexibility_Assessment_Report_2016-01-11-1.pdf.

Tan, Jin, Yingchen Zhang, Santosh Veda, Tarek Elgindy, and Yilu Liu. 2017. "Developing high PV penetration cases for frequency response study of U.S. Western Interconnection." in *2017 Ninth Annual IEEE Green Technologies Conference (GreenTech)*. https://doi.org/10.1109/GreenTech.2017.51.

Tan, Jin, Yingchen Zhang, Shutang You, Yong Liu, and Yilu Liu. 2018. "Frequency Response Study of U.S. Western Interconnection under Extra-High Photovoltaic Generation Penetrations." In *2018 IEEE Power & Energy Society General Meeting (PESGM)*. https://doi.org/10.1109/PESGM.2018.8586163.

U.S. Department of Energy. 2016. *Hydropower Vision: A New Chapter for America's First Renewable Electricity Source*. DOE/GO-102016-486. https://www.energy.gov/sites/default/files/2018/02/f49/Hydropower-Vision-021518.pdf.

U. S. F. E. R. Commission. 2005. "Standard Interconnection Agreement for Wind Energy, Docket No. RM05-4-001."

Volk, Michael. 2013. *Pump Characteristics and Applications*. CRC Press.

Zavadil, R., N. Miller, A. Ellis, and E. Muljadi. 2005. "Making connections [wind generation facilities]." *IEEE Power and Energy Magazine* 3(6): 26–37. https://doi.org/10.1109/MPAE.2005.1524618.

Additional Reading

Bodini, Nicola, Dino Zardi, and Julie K. Lundquist. “Three-Dimensional Structure of Wind Turbine Wakes as Measured by Scanning Lidar.” Atmospheric Measurement Techniques 10 (August 2017): 2881–2896. https://doi.org/10.5194/amt-10-2881-2017.

Dong, Zerui, Eduard Muljadi, Robert Nelms, and Mark Jacobson. 2019. “Impacts of Ternary-Pumped Storage Hydropower on U.S. Western Interconnection with Extremely High Renewable Contributions.” Presented at the 2018 IEEE Power & Energy Society General Meeting (PESGM), Atlanta, GA, 2019.

Torrealba , Ramírez and Pedro Javier. "The Benefits of Pumped Storage Hydro to the UK." Scottish Renewables(August 2016): https://www.researchgate.net/publication/312098425_The_Benefits_of_Pumped_Storage_Hydro_to_the_UK.

Zhu, Lei, Jacob Holden, Eric Wood, and Jeffrey Gender. “Green Routing Fuel Saving Opportunity Assessment: A Case Study Using Large-Scale Real-World Travel Data.” Paper presented at the 2017 IEEE Intelligent Vehicles Symposium (IV), Los Angeles, California, June 11-14.) https://doi.org/10.1109/IVS.2017.7995882.

Appendix A. Publications Generated from this Project

1. Dong, Z. R. Nelms, Eduard Muljadi, Jin Tan, Vahan Gevorgian, Mark Jacobson. 2018. "Development of Dynamic Model of a Ternary Pumped Storage Hydropower Plant." *Proceedings of the 2018 13th IEEE Conference on Industrial Electronics and Applications (ICIEA)*, 31 May - 2 June 2018, Wuhan, China: pp. 656–661. Piscataway, NJ: Institute of Electrical and Electronics Engineers (IEEE). https://doi.org/10.1109/ICIEA.2018.8397796 ***This paper was selected as the Best Paper Award***
2. Corbus, Dave, Mark Jacobson, Jin Tan, Erol Chartan, Greg Stark, Scott Jenne, Eduard Muljadi, Zerui Dong, Matt Pevarnik, Martin Racine, Carl Borgquist, Rhett Hurless, Eli Bailey, Chris Hodge. 2018. *Transforming the U.S. Market with a New Application of Ternary-Type Pumped Storage Hydropower Technology: Preprint.* Golden, CO: National Renewable Energy Laboratory. NREL/CP-5D00-71522. https://www.nrel.gov/docs/fy18osti/71522.pdf. *(Collaborator – Lead Author: David Corbus, National Renewable Energy Laboratory – NREL, Golden, Colorado)*
3. Dong, Z., R. Nelms, E. Muljadi, J. Tan, M. Jacobson. 2019. "Implementation of a Ternary Pumped Storage Hydropower System on Extremely High Renewable Penetrated U.S. Western Interconnection," poster presented at the 2019 DistribuTech Conference, Feb. 5-7. 2019, New Orleans, LA
4. Dong, Z., J. Tan, E. Muljadi, R. Nelms, M. Jacobson. 2019. "Impacts of Ternary-Pumped Storage Hydropower on U.S. Western Interconnection with Extremely High Renewable Penetrations" in *2019 IEEE Power and Energy Society General Meeting (PESGM)*. https://doi.org/10.1109/PESGM40551.2019.8973787.
5. Dong, Zerui, Jin Tan, Antoine St-Hilaire, Eduard Muljadi, David Corbus, Robert Nelms, Mark Jacobson. "Modeling and Simulation of Ternary Pumped Storage Hydropower for Power System Studies." *IET Generation, Transmission, & Distribution*. 13(19): https://doi.org/10.1049/iet-gtd.2018.5749.
6. Dong, Zerui, Jin Tan, Eduard Muljadi, Robert Nelms, Mark Jacobson. "Modeling of Quaternary Pumped Storage Hydropower (Q-PSH) for Power System Studies," to be submitted to an IEEE publication.
7. Tan, Jin. 2019. "Impacts of Ternary-Pumped Storage Hydropower on Frequency Response of WECC" Panel Session, present at IEEE Power and Energy Society General Meeting (PESGM), Atlanta, 2019.
   Soumyadeep, Nag, Zerui Dong, Jin Tan, etc. "Impacts of Quaternary-Pumped Storage Hydropower on Frequency Response of Western Interconnection" (to be submitted to ISGT

Appendix B. Gordon Butte Reference Project

GB Energy Park, LLC—a single-purpose subsidiary of Absaroka Energy Development Group, LLC (Absaroka)—is developing the Gordon Butte Closed Loop Pumped Storage Hydro Project, FERC Project No. P-13642.

Gordon Butte PSH will be a new utility-scale energy storage facility providing transmission system regulation services, integration of renewable energy generation, flexible capacity, and ancillary services to maintain transmission reliability for electrical utilities in the northern Great Plains and Northwest. The project will interconnect into the Colstrip twin 500-kV transmission lines, which run from Colstrip, Montana (Figure B-1), to load markets in Washington, Oregon, and Northern California.

Figure B-1. Gordon Butte PSH location

Illustration from Absaroka Energy

Gordon Butte is a prominent landform rising over 1,000 feet above the Musselshell River Valley near Martinsdale, Meagher County, Montana. As currently designed, two new reservoirs will be constructed, one at the top and one at the base of the butte, resulting in an estimated 1,020 feet of head. The upper and lower reservoirs will be equally sized at approximately 4,070 acre-feet in volume and connected by an 18-foot diameter penstock (Figure B-2) Assuming a starting condition of 4,000 acre-feet in the upper reservoir, the stored water volume will permit the project to generate electricity at maximum generating discharge for an estimated 8.5 hours.

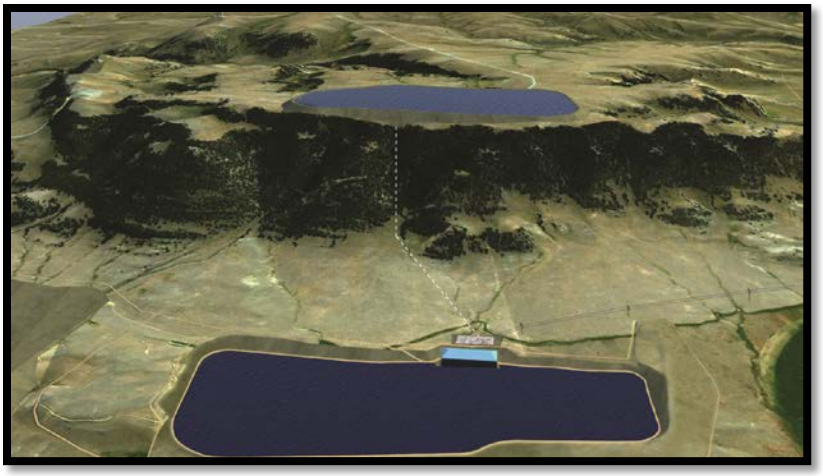

Figure B-2. Gordon Butte PSH overview

Illustration from Absaroka Energy

The powerhouse adjacent to the lower reservoir will contain advanced PSH configuration of equipment (ternary or quaternary design). This configuration will consist of three-unit pairs. Each pair will include a pump and a turbine with a dedicated 134-MW motor and a 134-MW generator, respectively, for an installed capacity of 400 MW. In addition, the powerhouse design will have a hydraulic short circuit connecting the turbine and the pump, utilizing the lower reservoir. The quaternary design was selected for the Reference Project. This configuration was selected as the ideal equipment technology for this specific site, providing fast-ramping and flexible operational capability with minimal construction and installation costs.

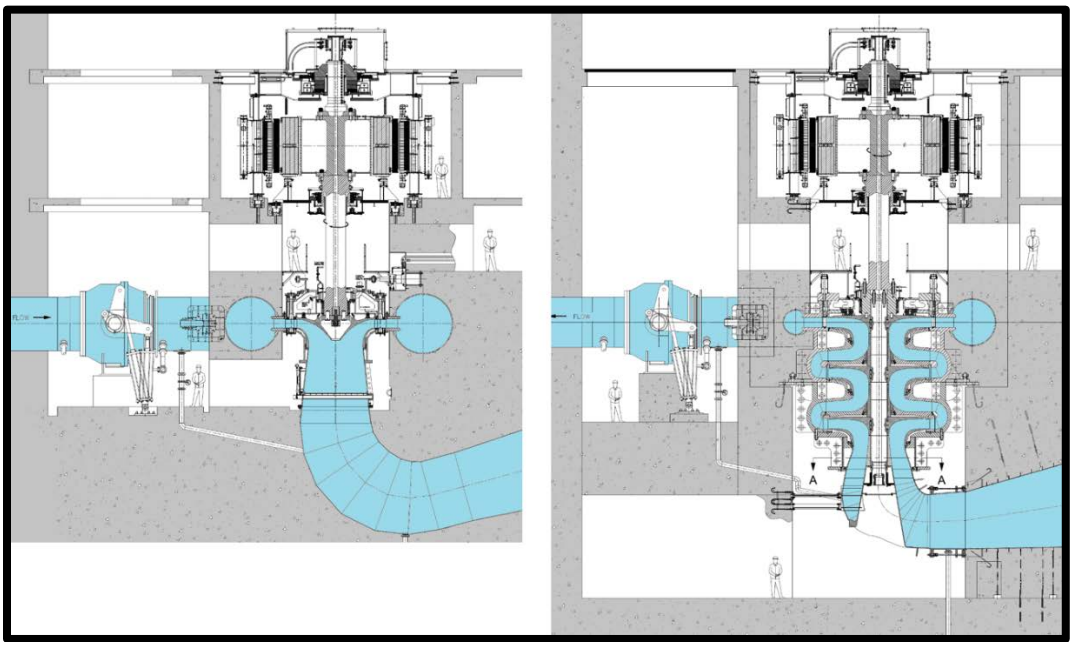

Figure B-3. Francis turbine and 3 stage pump

Illustration from GE

Appendix C. Project Development Best Practices

C.1 New PSH Site Selection

It has been decades since the last PSH facility was built in the United States. The development and deployment of a PSH facility is a lengthy, difficult, and complex process New PSH projects are increasingly focusing on siting closed loop configurations to minimize environmental impacts, conserve water consumption, and shorten development timelines.

There are countless decisions and considerations that go into designing a PSH facility, but site selection is likely the most important. Successful development of a PSH project requires developers to evaluate the proposed project site in all of the following categories:

Topology

One of the first, and possibly most crucial, considerations when evaluating sites for a PSH project is the topology of the location, as it dictates the feasibility, size/capacity/output, layout, and design of the facility. As a basic requirement, the site must have some amount of vertical height difference (or head) between the proposed sites of the lower and upper reservoirs. The required amount of head depends on the desired power output of the system and the allowable water flow rate through the system. In other words, to achieve a given power output the facility must achieve a specific head and flow rate. This dynamic is expressed in general mathematic terms below.

- $P_{th} = \rho\ q\ g\ h$

where

- P_{th} = power theoretically available (W)
- ρ = density (kg/m^3) (~ 1000 kg/m^3 for water)
- q = water flow (m^3/s)
- g = *acceleration of gravity* (9.81 m/s^2)
- h = falling height, head (m)

If this head is decreased (e.g., a location with a smaller vertical height difference), then the flow rate must be increased to maintain the same output, and vice versa.

It is often unreasonable to simply increase the flow rate to overcome a project site with a small vertical displacement, because the penstock and pumping and generating equipment must be enlarged to support the increased flow rate, and the equipment and piping may become too costly. Also, an increased flow rate means that the generation or storage duration of the system will be decreased, as the reservoirs will drain and fill at a faster rate (the storage/generation duration of the facility will be discussed in the Land section). As a result, it is desirable to choose a project site with a larger height difference, since this is typically a more cost-effective method of achieving a power output than increasing the flow rate.

When analyzing the head, flow, and power output of a project, it is also important to consider the design of the turbines to be used. A given turbine is well-suited to a limited range of applications, and each design has specific abilities and characteristics that will ultimately dictate the operation of the facility (i.e., the flexibility and response time). Due to the interrelated nature of head, flow,

power output, and turbine design, it is imperative to carefully evaluate these simultaneously for the site. This is often done using a chart similar to the one seen in Figure C-1.

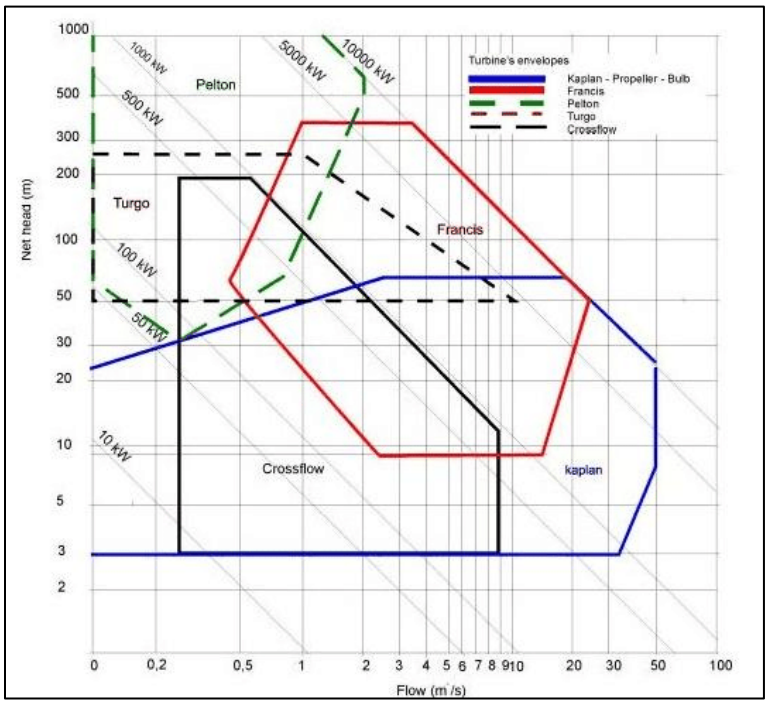

Figure C-1. Turbine selection chart showing relationship between head, flow rate, power output, and turbine design.

Illustration from Sangal, Garg, and Kumar (2013)

After evaluating the head, flow, power, and turbine design for a site, the horizontal distance between the reservoirs must also be considered. It is desirable to simply minimize the horizontal displacement between the reservoirs, as this will reduce the overall length of the penstock (reducing material and construction costs) and associated energy losses.

Simply put, when comparing the topology of multiple potential sites, it is ideal to select one with a greater vertical displacement and lesser horizontal displacement between the reservoirs.

Geology

Another important consideration during site selection is the geological makeup of the location. A large amount of excavation (depending on the size of the facility and topology of the land) is typically required for the reservoirs, powerhouse, penstock, and various other project features. As such, the geologic formations in the area should be examined; this can have a considerable effect on the cost of excavation, and, consequently, the feasibility of the project. Locations with geologic factors that greatly increase the difficulty of excavation can escalate the civil construction costs, affecting the overall marketability of the project.

Also of significance is the seismology of the area, stability of the rock formations, and the consequential constructability of the project features. Care should be taken to identify a site with minimal seismic activity, stable rock formations for construction, and is distant from any fault lines. This will help to ensure the project features can be safely and affordably constructed.

Land

There are several other important characteristics regarding land that must be evaluated—namely, the amount of land required and the composition of land ownership. The amount of land required is largely dependent on the desired output and storage/generation duration of the facility. PSH projects with higher outputs and longer storage/generation durations will require more land area. It is typical to first consider the desired operational duration of the facility that will dictate the required volume of the reservoirs. Once the necessary volume of the reservoirs is known, a project site of interest can be examined to determine if it provides enough room for the construction of the lower and upper reservoirs without excessive excavation (which greatly increases cost). It is also ideal to select a site where the lower and upper reservoir sites are relatively large and flat or contain natural features that can be incorporated into reservoir design and layout.

Land ownership of a project site is also a critical factor. Preference should be given to sites with few landowners, as this typically eases and speeds up obtaining rights to the land. It is also desirable to select project sites with private landowners, as this avoids complications and additional processes associated with construction on public lands. Having few and private landowners is an immensely important, and often overlooked, consideration that enables project developers to more easily interact with the affected parties, understand and alleviate concerns, and, ultimately, promotes the successful development and deployment of a PSH facility.

Water

Availability and obtainability of water are two of the most critical considerations when siting PSH. Closed-loop PSH projects require water to initially fill the lower reservoir and typically a smaller annual amount to replace what is lost to evaporation or seepage. Due to the relatively large volume of water required for the initial fill, importing from a distant source in inadvisable. A site should be selected that has direct access to a sufficiently large creek or river or has adequate groundwater to support the withdrawal of large amounts of water. In addition to simply locating a project site with access to water, it is also important to verify the source can truly provide the needed water and that the legal rights can be obtained.

When considering water availability at a project site, it is crucial to first examine the historic flow rates of running bodies of water and the size of underground aquifers to determine if the water supply is able to provide enough water. Part of this investigation often involves looking at the amount and location of irrigation or other diversions by existing water users in the area. It is important to determine how much (if any) excess water is available and who the existing water users are that may be affected by withdrawal of water for the facility.

After confirming that the location can physically supply the necessary water and that existing water users will not be significantly impacted, the next and equally important step is to determine the means of obtaining the legal rights to utilize the water. Due to the variability of regulations across regions, it is vital for developers of PSH projects to thoroughly examine the laws for a site of interest and identify the methods that exist to obtain water rights, as well as the quantity of water obtainable. For instance, in some cases water rights are organized and fulfilled by priority date, so water users who hold the oldest water rights are permitted to claim their water first, and any additional water is left to the junior water right holders. This variability in regulations means that there is not a single ideal water procurement strategy. It is possible that the strategy for obtaining water may involve leasing or buying water from an existing user, applying for a brand-new water

right, utilizing groundwater, and/or working directly with the appropriate authorities among many other possibilities.

It is recommended that developers select a project site that has access to a water supply (surface water or groundwater), available excess water, and where the laws provide a feasible means of obtaining the legal right to use the water. Selecting such a project site will enable developers to establish a clear method for obtaining water for the filling and refilling of the reservoirs. It is important to develop a water procurement strategy early in the development process for several reasons:

- Water is integral to the operation of the facility, and facilities typically require large volumes of water, which can be difficult to obtain; the quantity of water that can be diverted will control the length of time (which can be very long) needed to fill and refill the reservoirs, which will dictate the viability of obtaining water and the viability of the entire project; and each region has different regulations, exceptions, processes, and requirements that define the ability and quantity of water that projects use.

Environment

Environmental concerns must also be considered early in the siting process. Often, this process is overlooked during early site evaluation and only considered once development at a particular site has begun. But because environmental impacts can possibly extinguish any development, it is essential to evaluate the environmental status of a project site thoroughly and early in the site selection process. Important issues to consider may include threatened and endangered species, sensitive habitats, archeological and historical resources, erosion, and the presence of hazardous materials.

To identify and alleviate any environmental issues for a project site, it is recommended by Absaroka Energy to perform an early and thorough environmental analysis. In addition, it is possible and highly recommended to begin early mitigation measures for identified concerns. Certain mitigation measures may take the form of facility design decisions. A closed-loop PSH configuration allows for a facility to be built outside of natural water courses, minimizing impacts to riparian habitat, water resources, and native fisheries. Also, certain transmission line designs may reduce the impact to sensitive habitats and threatened and endangered species. In general, developers must fully consider environmental impacts during site selection, as this often determines the viability of the entire project and can influence the design of various facility features.

Transmission

Another important element of any PSH project is proximity to the transmission grid so the facility's services may access electrical markets while avoiding the burdensome costs of developing and constructing new transmission infrastructure. There are several aspects to be considered when searching for a site with nearby transmission: the distance to nearby lines, the voltage of the lines, the available capacity (if any) on the lines, the owner of the lines, method or processes of interconnection, and the origin and destination of the lines. In the ideal case, a project site would be selected with existing transmission lines, which are located in close proximity to the facility, are of an appropriate voltage for the PSH equipment or are suitable for a substation, have enough

available carrying capacity, serve markets that have a large demand for PSH services, and have a reasonable method of interconnecting with the project.

As may be expected, the development and deployment of a PSH facility is a lengthy, difficult, and complex process. Countless decisions and considerations go into designing a PSH facility, but site selection is possibly the most crucial factor that contributes to the success of a PSH project. As discussed above, there are many important requirements for selecting a PSH site. Successful development of a PSH project requires the developers to quantitatively and qualitatively evaluate the proposed project site in all categories. Although it may not be possible to fulfill all site selection criteria, it is still important for developers to carefully consider each and to assess the importance of each toward the overall success of the project.

-

C.2 Permitting and Licensing Process

In conjunction with project siting considerations, permitting and licensing practices can further decrease development timelines and increase the likelihood of the successful deployment of T/Q-PSH in the United States.

FERC has federal jurisdiction over the licensing of new hydroelectric projects in the United States. This licensing process was established decades ago in the Federal Power Act, and the process was designed for the construction and operation of more traditional reservoir dams or run-of-river hydro projects. Closed-loop PSH projects are different in their layout, impacts, and operations, and are ill-fitted for the current licensing process.

Currently, there are three licensing pathways to choose from when an applicant moves into the licensing phase of development: the Integrated Licensing Process (ILP), the Alternative Licensing Process (ALP) and the traditional licensing process (TLP). Beginning in 2005 [FERC, 18 CFR Part 5], the ILP became the default process for filing an application for an original, new, or subsequent license. For an applicant to use either the TLP or the ALP, they must ask and receive approval from the FERC.

- **ILP:** The ILP is intended to be a streamlined process by, "…providing a predictable, efficient, and timely licensing process" [FERC, 18 CFR Part 5]. The main differentiator between this path is that the process is led by FERC—the applicant plays a more participatory role in the effort.
- **TLP:** Unlike the ALP, the process and schedule under the TLP is led and driven by the developer. In utilizing the TLP, the applicant must complete and document a three-stage prefiling process. stages are:
- **ALP:** The ALP was introduced in 1997 to "…improve communications among affected entities" [FERC Order No. 596]. The process and schedule are still FERC-led but allow for the prefiling consultation process and environmental review process under the National Environmental Policy Act (NEPA). This allows for the preparation of a draft environmental assessment or draft environmental impact statement by a third-party contractor (chosen by FERC and funded by the applicant).

Each of the three licensing paths has benefits and drawbacks that must be weighed against the individual characteristics of a new PSH project. If the developer is willing to take on the full responsibility of the licensing process, the TLP allows for the most aggressive approach to both schedule and process management. The Reference Project was able to move through its licensing

process in just over three years, a notable achievement, though still outside the two-year expedited process that FERC is targeting.

Lessons learned from the FERC Licensing process for the Reference Project include:

1. Much attention is paid to the importance of selecting the best FERC licensing process for each proposed project. While process selection can be important, more important is the assessment of the critical factors and the key participants in the process: characteristics of the site and the potential for significant resource concerns, the applicant, and the stakeholders. In the case of the Reference Project, the initial strategic analysis concluded that the prescriptive nature of the ILP would actually have acted as a detriment to success. Given the initial assessment of the limited potential for project effects, the lack of federal land involvement, the apparent lack of Endangered Species Act (ESA) species/habitat, it was clear that agency involvement was likely to be limited primarily to state agencies and the USFWS. It was also clear that these agencies preferred a consultation process that did not require unnecessary time or effort, due to staffing limitations, and that neither the applicant nor the agency participants needed the discipline associated with ILP.
2. Absaroka determined that the TLP was the more appropriate process for the Reference Project, as it provided appropriate consultation opportunities without unnecessary structure, steps, or deadlines. By implementing a standard methodology of face-to-face engagement whenever possible, Absaroka was able to garner the necessary support from the agencies for the TLP, prepared its request to FERC to utilize the TLP, based on that support, the lack of any significant identified issues, and the apparent lack of controversy, and received FERC approval.
3. Once the TLP was approved, Absaroka sought FERC agreement to conduct early NEPA scoping. This was considered important by Absaroka, as it would ensure FERC staff were informed about the site, the proposed development concept, and the apparent lack of resource concerns. Absaroka would obtain FERC endorsement of the scope of analysis that would be required to support the license application. Early reconnaissance study efforts by Absaroka were valuable in providing FERC staff and the other agencies with site-specific information on which to base the conclusion that there was little potential for major resource impacts or for controversy to develop during the licensing process. Continuing its informal consultation with agencies and stakeholders, Absaroka prepared an Applicant-Prepared Draft SD1 to give FERC staff a starting point for FERC's official SD1. This draft document was shared with agencies to get their agreement that the scope of analysis was accurately reflected before filing the draft SD1 with FERC. Absaroka was able to gain full agency support for the request to FERC to conduct early NEPA scoping, and FERC was able to issue its SD1 quickly.
4. Keeping FERC staff fully apprised of the progress in addressing agency questions was also important in gaining comfort with FERC that staff resources should be committed to conducting the early NEPA scoping. It also had the benefit of getting FERC staff on-site so they could gain their own appreciation for the site location, characteristics, and lack of potential resource controversy. With FERC scoping helping to put sideboards on the resource questions that needed to be answered, and the results of the early studies conducted to characterize resource conditions, Absaroka was able to plan and execute a very modest study program in one field season.

5. The next regulatory step Absaroka thought would take more time than justified by the value added was the draft license application (DLA) step. Absaroka was convinced that, given the continual investment in face-to-face communications, a formal DLA development and review/comment step was unnecessary and that the engaged agencies would agree. FERC's regulations provide the opportunity to seek waivers from individual agencies from conducting specific regulatory steps that the agencies deem unnecessary [18 CFR 4.38(e) Waiver of Compliance with Consultation Requirements]. Absaroka confirmed with FERC staff that if Absaroka could get the agreement of all relevant agencies, then the DLA step could be waived. As important was FERC staff's commitment that if Absaroka could indeed get full agency support, FERC staff would not require a DLA of its own volition. The strategy used by Absaroka to gain agency support was to use an applicant-prepared environment assessment style and sharing it with stakeholders. With this continued investment in informal consultation, the agencies felt confident that all relevant concerns had been adequately studied and analyzed, and that a formal DLA step would not add sufficient value for the additional commitment of staff resources in formal review and preparation of comments. Thus, Absaroka was able to eliminate the formal DLA review/comment step and save substantial time in the overall prefiling process.
6. As of mid-2016, a Final License Application has been filed with FERC containing proposed mitigation measures and management plans that had been thoroughly vetted with the agencies. FERC staff conducted an expeditious review of the application resulting in minimal additional information requests. Because of the early NEPA scoping, during which FERC staff indicated their intent to prepare an environmental assessment and not an environmental impact statement unless some unexpected resource concern emerged during comments received on the accepted license application, FERC staff are currently preparing the environmental assessment.
7. Given the investment in early site characterization, face-to-face informal consultation throughout the prefiling period, frequent updates to FERC staff, early NEPA scoping, and a successful study program, Absaroka is confident that the environmental assessment will accurately reflect the hard work by Absaroka and the agencies and will not contain any surprises. All in all, from issuance of the first preliminary permit to the anticipated release of the EA and license has taken approximately six years. From filing of the notice of intent and pre-application document in April 2013, to anticipated release of the environmental assessment and license, is just over three years. While not as fast as a two-year process hoped for in the pilot licensing process, three years from notice of intent to license does show that with serious investment by the applicant in informal consultation, the cooperation of the resource agencies and flexibility by FERC staff in terms of process steps and sequence, the licensing process for a new closed-loop pumped storage project can be shortened considerably.

C.3 Equipment Selection Process

When starting a PSH project, the initial size of the project and selected equipment choice, which are required to submit the preliminary FERC permit application, are subject to change as the project matures. As project development progresses, the developer may find additional markets and equipment features that were not initially considered. Thus, the developer needs to be flexible when making the final equipment selection. To assist with the equipment selection, the developer can take a simple lean approach or a more comprehensive approach. A simplified approach involves the developer and a consultant knowledgeable with PSH technology selecting the equipment together. With a more comprehensive approach, the developer gains the support of all

project participants to collectively determine the equipment configuration using analytical and collaborative methods.

The comprehensive approach to equipment selection requires agreed-upon goals, selective matrix tools, and commitment to participation and meeting schedules deadlines. Each participating group has a defined division of work that is established early in the project development phase. For example, the turbine/generator equipment manufacturer will not participate in discussions related to the construction of the reservoirs, but will provide valuable information to the team about how long it will take the equipment to fill and drain the upper and or lower reservoirs and what equipment sizes are needed for the elevation differences between the upper and lower reservoir elevations (head). This equipment size will then be used by the civil contractor to determine the amount of excavation needed. In addition, the engineering firm will need to know what balance of plant equipment is required to support the operating turbine generator equipment, such as necessary oil lubrication systems, compressed air, auxiliary electrical components, control systems, and cable trays. All of this equipment requires space and connections, which are discussed with the civil contractor when designing the physical plant layout.

Analyzing and modeling the markets in which the PSH project will be participating is of utmost importance. Without a potential market and revenue stream, bankability of a project becomes a challenge. Once the market has been well-defined, matching the equipment to serve this market requires additional detailed analysis between the developer and their project team.

The four available PSH technologies come in different configurations and generate differently, which impact costs and also create different flexibility profiles that result in different value/revenue streams depending on the market. In addition, flexibility and reactivity are very important considerations for the future market thus transition speeds and response times for each of the four equipment options also need to be considered. This equipment evaluation process, as noted, requires complete collaboration with the comprehensive project team, and at the end, the completed matrix shown in Table C-1 allowed the developer to make the final equipment selection for the Reference Project.

Table C-1. PSH Equipment Selectivity Matrix Completed for the Reference Project

	Costs					Revenues					Main Interests	
400 MW PSH Configuration	Electrical & Mechanical	Submergence	Footprint	O&M	Refrences	Power	Efficiency	Arbitrage	Capacity	Ancillary Services	Flexibility	Reactivity
T-PSH (3 units)	-	+	-	-	-	+	-	+	+	+	+	+
C-PSH (3 units)	+	-	+	+	+	+					-	-
C-PSH (4 units)	+	-		+	+	+						-
Q-Pump + Pelton (3 + 3 units)	-		-	-	+	+	+	+	+	+	+	+
Q-Pump 2 stages + Francis (200MW)	-		-	-	+	+	+	+	+	+	+	+
Q-Pump 3 stages + Francis (200MW)	-	+	-	-	+	+	+	+	+	+	+	+
Q-Pump 2 stages + Francis (133MW)	-		-	-	+	+	+	+	+	+	+	+
Q-Pump 3 stages + Francis (133MW)	-	+	-	-	+	+	+	+	+	+	+	+
VS-PSH (3 units - all fully fed)		-	+	-		+	+	+		+	+	+
VS-PSH (3 units - 2 fully fed)		-	+	-		+	+	+		+	+	+
VS-PSH (3 units - 1 fully fed)	+	-	+			+		+		+	+	
VS-PSH (4 units - all fully fed)		-		-	+	+	+	+		+	+	+
VS-PSH (4 units - 2 fully fed)	+	-			-	+		+		+	+	
VS-PSH (2 STAGE 3 units - all fully fed)	-		+	-		+	+	+		+	+	+
VS-PSH (2 STAGE 3 units - 2 fully fed)			+		-	+		+		+	+	
VS-PSH (2 STAGE 4 units - all fully fed)	-			-	+	+	+	+		+	+	+
VS-PSH (2 STAGE 4 units - 2 fully fed)					-	+		+		+	+	

Utilizing a comprehensive team approach to for the equipment selection process enabled the developer to fully understand all necessary costs, revenue stream, risks, and opportunities. What was eventually learned through the process was that the quaternary configuration was less costly that the original ternary configuration, and still provided a proven technology and the desired flexibility. Additional lessons learned from the equipment selection process for the Reference Project include:

1. The equipment provider, GE/Alstom, was involved early in the development, design, and layout of the Gordon Butte PSH Reference Project. From the outset, the project's developer, Absaroka, requested an equipment configuration able to provide fast-acting operational capabilities throughout the unit's full operating range. Through the process described previously, the ternary configuration was identified as best suited for the project's unique site layout, powerhouse design, and desired operating requirements.
2. As the project design moved into a more granular phase, a second evaluation of the equipment selection was performed. This process resulted in the developer deciding to switch from the T-PSH to the Q-PSH configuration because the cost benefits of the quaternary configuration outweighed the ternary configuration
3. The geotechnical characteristics of the Gordon Butte PSH project site were such (the lower reservoir site is mixed shale, sandstone and siltstones) that an open pit powerhouse was deemed more feasible/constructible than a traditional cavern-style powerhouse. The initial equipment selection process that Absaroka and GE/Alstom resulted in a ternary equipment configuration. This was due to the fact that an adjustable speed unit would need to be set at a lower elevation, approximately 80-100 ft. lower, than a ternary unit which utilized a multistage pump. Working with the construction contractors, the cost/benefit analysis showed that the additional cost from excavating and constructing the powerhouse deeper to accommodate the AS-PSH units was equivalent to the additional cost of the more flexible and faster ramping ternary units. This is what led Absaroka to opt for the ternary configuration.
4. The second iteration of the equipment selection process was undertaken as the project design-build team started work on their more detailed front-end engineering design (FEED) of the

Gordon Butte PSH. It was revealed during this process that the project's 1,000 ft. of head resulted in a Pelton turbine and hydraulic coupler that were too large to be economically feasible for the project. Absaroka and GE/Alstom decided that a quaternary configuration was more suited to the Gordon Butte project. By utilizing the Q-PSH, the project will utilize pairs of Francis turbines coupled with variable-speed multistage pumps will preserve the flexibility and speed of the T-PSH, have the ability to provide frequency response and faster inertial response, the individual units will operate with higher efficiencies, maintain the ability to operate in a hydraulic short circuit, and eliminate the need for a hydraulic coupler.

5. Of concern with the ternary design was the size of the torque convertor, a size that has not yet been built, and the necessary size of the Pelton turbine, another size that has not been built. Not having the necessary references for these critical components added additional risks and compromised the project's bankability.
6. This final equipment selection maintained the original project output of 400 MW and provided the developer the ultimate plant flexibility of -400 MW to +400 MW. What was eventually learned through the process was that the original ternary configuration, though providing flexibility, the Quaternary configuration was less costly while still providing a proven technology (with existing projects to reference) and maintaining the desired flexibility. Though some compromises with the quaternary selection were made, these were eventually evaluated as lower risk than having the known references

Appendix D. Development of the T-PSH Dynamic Model

D.1 Dynamic Modeling of T-PSH (Dong et al. 2018; Dong et al. 2019; Dong 2019)

The team developed an improved model of T-PSH that includes: (1) the development of a new integrated governor-turbine model for T-PSH, representing the unique behavior of hydraulic short circuit (HSC) mode; (2) a mode switch module to continuously simulate the transition dynamic among three operation modes (generation mode, pumping mode, and HSC mode); and (3) detailed modeling of the gate valve and penstock-sharing feature based on industry feedback. In addition, the T-PSH model is implemented by using an Engineer's Program Control Language (EPCL)-based user-defined model in positive sequence load flow (PSLF), and, therefore, the model can be used to study the value of T-PSH in the Western Interconnection (WI). The T-PSH is studied in the WI system with different renewable contribution levels from 20% to 80%, and the T-PSH is potentially used in the wide-area control applications.

D.1.1 Overall Model Structure

In order to model performance, the T-PSH system is divided into many parts as shown in the block diagram in Figure D-1. Owing to evolution from C-PSH, the synchronous machine and excitation system in C-PSH modeling can still be used in the T-PSH system. Due to the new configuration and the additional HSC mode in T-PSH technology, the separated governor model used in C-PSH cannot be used. A new combination governor model must be created to model the most important feature of T-PSH in which both the turbine and pump work simultaneously.

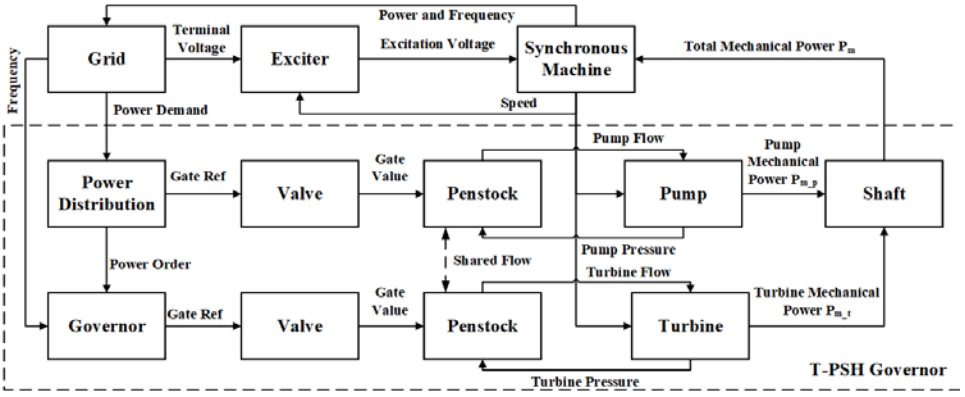

Figure D-1. Structure diagram of T-PSH system

D.1.2 Generator and Excitation Model

Since T-PSH technology retains the synchronous machine used in C-PSH technology, the model of the synchronous machine and its direct current (DC) excitation system in the C-PSH system model can be used in the T-PSH system model. When implementing the machine system used in the T-PSH system in the PSLF platform, the built-in salient pole synchronous machine and its DC exciter models are adopted. The introduction of these models is presented in this section.

D.1.2.1 Generator

The synchronous machine is the core of the entire T-PSH system and is used to convert electrical energy into kinetic energy in the pumping mode, or to convert kinetic energy into electrical energy in the generating mode. An existing three-phase salient pole machine model in the PSLF platform is used in this study. This model is called GENSAL (shown in Figure D-2), which means the salient pole synchronous machine is represented by equal mutual inductance rotor modeling (Concorda 2012; Kundur, Balu, and Lauby 1994). Additional parameters in this model are shown in Table D-1 and Table D-2.

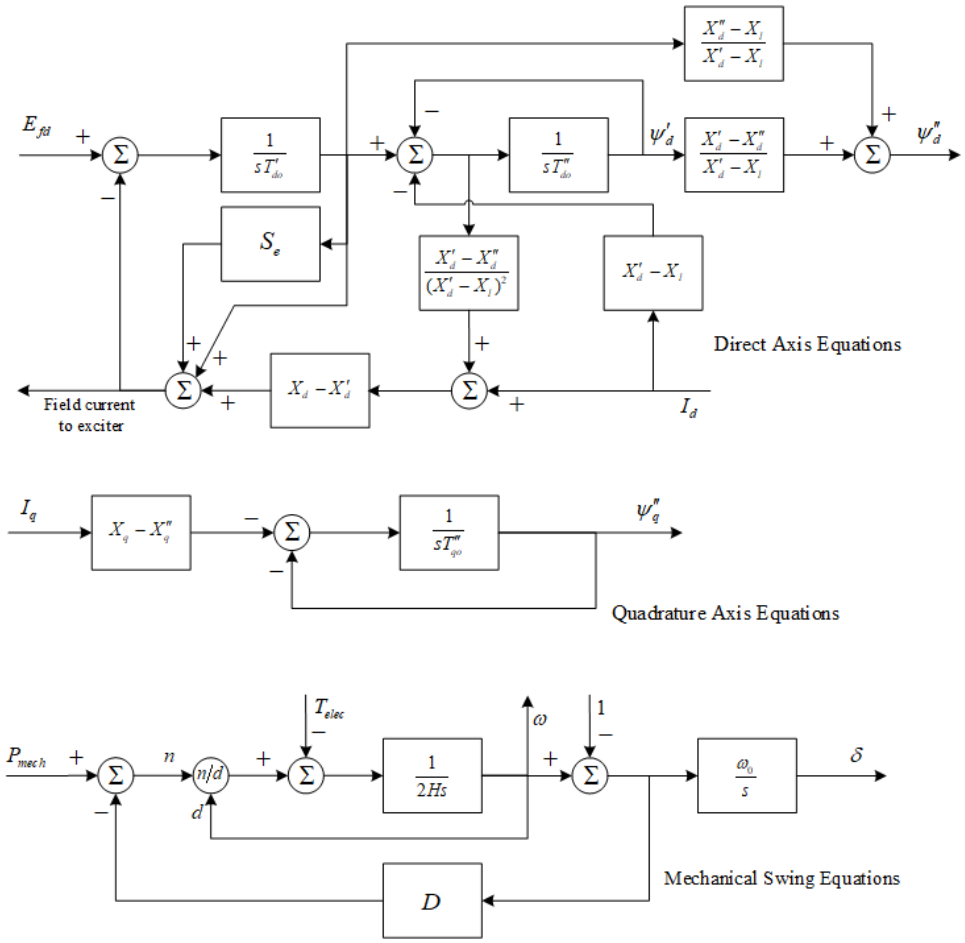

Figure D-2. Transfer function of GENSAL synchronous machine model

Table D-1. Parameters in the GENSAL Model

Parameter	Description	Units
T'_{do}	d-axis transient rotor time constant	sec
T''_{do}	d-axis sub-transient rotor time constant	sec
T''_{qo}	q-axis sub-transient rotor time constant	sec
X_d	d-axis synchronous reactance	p.u.
Xq	q-axis synchronous reactance	p.u.
X'_d	d-axis transient reactance	p.u.
X''_d	d-axis sub-transient reactance	p.u.
X''_q	q-axis sub-transient reactance	p.u.
Xl	Stator leakage reactance	p.u.
Ra	Stator resistance	p.u.
H	Inertia constant	sec
D	Damping factor	p.u.

Table D-2. Parameters in the Transfer Function

Parameter	Description	Units
Tr	Transducer time constant	sec
Ka	Voltage regulator gain	p.u.
Ta	Voltage regulator time constant	sec
Ke	Exciter field resistance line slope margin	p.u.
Te	Exciter field time constant	sec
Kf	Rate feedback	p.u.
Tf	Rate feedback time constant	sec

D.1.2.2 Exciter

The excitation system in the synchronous generator provides DC to the field winding, which induces three-phase voltages on the armature winding. Meanwhile, the additional functions of the exciter include voltage control, reactive power flow control, system stability enhancement, and generation system protection (Kundur, Balu, and Lauby 1994). In this T-PSH study, the IEEE (1968) Type 1 DC excitation system model is used to model the DC exciter. This excitation system is representative of a modern system in service. In the later IEEE standard (IEEE 1981), this IEEE (1968) Type 1 DC exciter has been modified to a Type DC1A DC excitation system. When implementing this excitation system in PSLF, the existing exciter model, IEEET1 (shown in Figure D-3), is used (Concorda 2012).

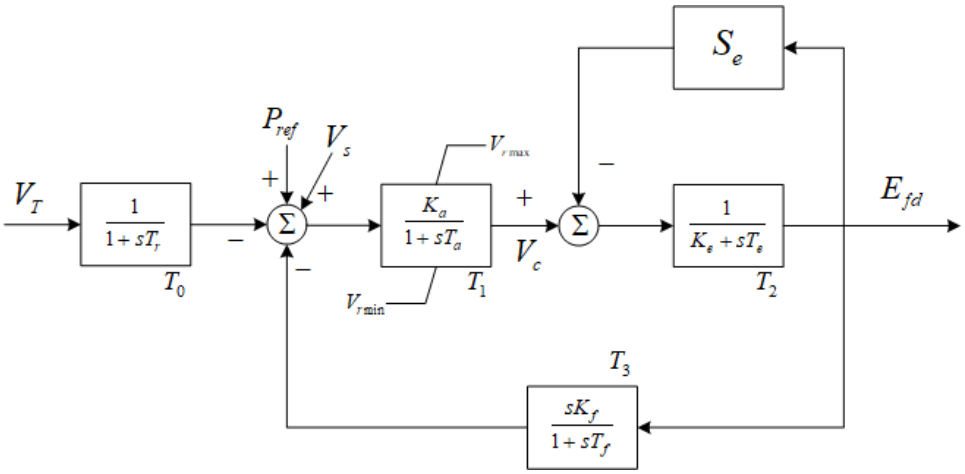

Figure D-3. Transfer function of IEEET1 DC exciter model

D1.3 Governor Control Model

D.1.3.1 Governor

Unlike the synchronous machine and exciter model, the governor model cannot directly use the C-PSH, due to the innovative structure of the governor in T-PSH system. A new dynamic governor model, whose diagram is shown in Figure D-4 is developed based on the HYGOV model. This dynamic model is a general hydropower turbine and governor model, which is universally used in hydropower generation modeling (Concorda 2012). Here, it will be used to model the turbine part of the governor. The model describes a straightforward hydroelectric plant governor with a simple hydraulic representation of the penstock with unrestricted headrace and tailrace and no surge tank (Koritarov et al. 2013d). To describe the pumping mode and HSC mode, an additional pump part with complete detailed water flow regulator and penstock system is added into the HYGOV model. A new function to describe the single shaft system with the turbine runner, pump runner, and synchronous machine connected is implemented in the model. Meanwhile, a distribution block is designed in this governor model to calculate and send the power reference to the turbine part and pump part, which can control or switch the operation mode of the T-PSH. In addition, a part is added to the shared-penstock hydro model to describe the water flow interaction between the turbine penstock and pump penstock during the HSC mode.

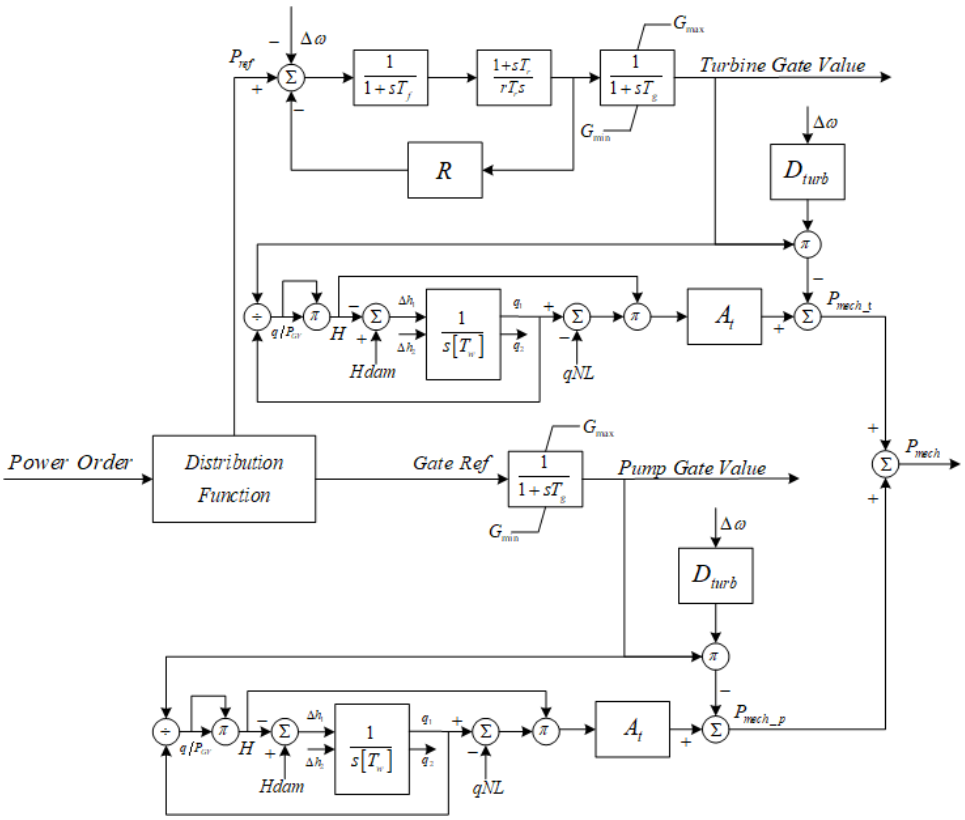

Figure D-4. Transfer function of governor model

D.1.3.2 Operation Mode Controller

As a combination governor model is used in T-PSH modeling, an operation mode controller is added to control the three T-PSH operation modes. In this controller, a pair of distribution coefficients are defined by

$$\begin{bmatrix} Tw_{tt} & Tw_{tp} \\ Tw_{pt} & Tw_{pp} \end{bmatrix} \cdot \begin{bmatrix} \frac{dq_t}{dt} \\ \frac{dq_p}{dt} \end{bmatrix} = \begin{bmatrix} \Delta H_t \\ \Delta H_p \end{bmatrix} \qquad (2)$$

where K_{d_t} is the distribution coefficient for the turbine part, K_{d_p} is the distribution coefficient for the pump part, P_{rate} is the rated capacity of the T-PSH unit, and P_{gen} is current power requirement of the T-PSH in HSC mode. These coefficients are set in the distribution block and share with the turbine and pump part the current working status of the T-PSH. The clutches and the gates will be controlled according to these coefficients to meet different operational needs in different operation modes. To control mechanical coupling between the turbine, pump, and shaft, this controller achieves a combination of operation of turbine and pump (separately or together) to generate a positive or negative mechanical power signal to the synchronous machine in the specific simulation case. This kind of design also allows a practical way for the customer to add any special operating situation in the future model updates or extend more function in the model.

According to these distribution coefficients, a power reference calculation function is defined in Equation 3 to generate the power order for each part during the initialization and the simulation.

$$\begin{cases} P_{gen\_pump} = -K_{d\_p} \times |P_{gen}| \\ Pd\_t|P_{gen}|_{gen\_turbine} \end{cases} \quad (3)$$

where P_{gen} is the active power of the synchronous machine in per unit, P_{gen_pump} is the power order of the pump part, $P_{gen\_turbine}$ is the power order of the turbine part, K_{d_t} is the distribution coefficient for turbine part, and K_{d_p} is the distribution coefficient for pump part. During the initialization, the power order for each part will be calculated according to the power demand from the grid and initial the T-PSH system. During the simulation, this power order will be updated in each simulation iteration.

In the generating mode, T-PSH is operated as a conventional hydropower plant with only the turbine part participating in the operation. The power reference for the governor is calculated by the setting power order in Equation 3, where K_{d_t} is equal to 1 and K_{d_p} is equal to 0. The droop controller in the governor can respond to the system variance dynamically by changing the gate value. The water flow in the penstock flows from the higher reservoir to the lower reservoir, shown in Figure D-5. The potential energy stored in the water is transferred into the kinetic energy of the shaft. Finally, the synchronous machine converts kinetic energy to electrical energy. Because of the droop controller, T-PSH in the generating model can achieve governor speed control, which means that it can provide frequency regulation service to a system to help stabilize the system under a contingency.

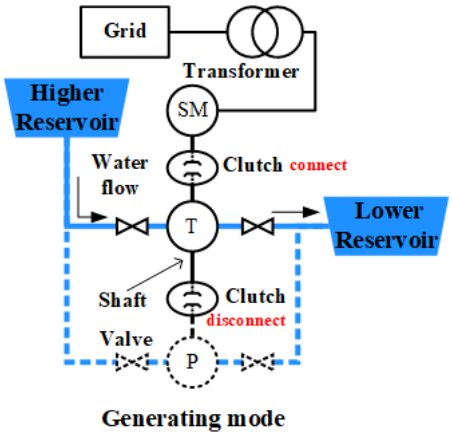

Figure D-5. Water flow of T-PSH in generating mode

In the pumping mode, T-PSH is operated as a fixed-speed pump, which is the same as C-PSH (i.e., only the pump is in operation). The desired gate value of the pump is calculated by the power order in Equation 3, where K_{d_t} is equal to 0 and K_{d_p} is equal to 1. The water flows from the lower reservoir to the higher reservoir as shown in Figure D-6. The electrical energy is absorbed by the T-PSH and transferred to potential energy, which is stored in the higher reservoir; however, different from the turbine part, there is no droop controller in the pump part. T-PSH in this pumping mode cannot participate in governor speed control because of its fixed power absorption during this operation. This means that in pumping mode T-PSH cannot respond to a system disturbance to provide any frequency regulation service.

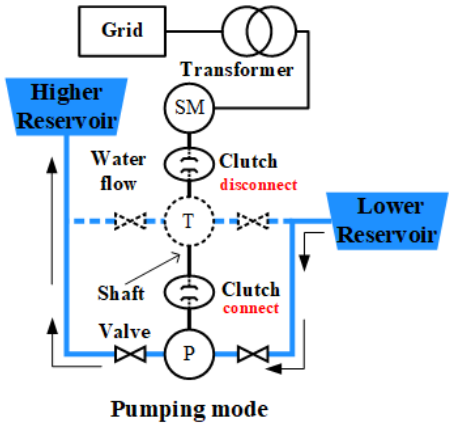

Figure D-6. Water flow of T-PSH in pumping mode

In HSC mode, both the turbine part and the pump part are in operation. The power order for each part will be calculated by K_{d_t} and K_{d_p}, shown in Equation 3, where K_{d_t} and K_{d_p} are satisfied according to the relationship shown in Equation 2. The net torque is a combination of variable turbine torque and fixed pump torque, resulting in a negative variable torque (absolute value of pump torque is larger than turbine torque). As a result, T-PSH behaves as a load to absorb power from the power grid. The water flow in this mode is from the lower reservoir to the higher reservoir, as shown in Figure D-7. This variable negative mechanical power output makes T-PSH in HSC mode respond to a system disturbance by an adjustment provided from the turbine part. In this mode, T-PSH can provide ancillary service in the pumping water, whereas the C-PSH cannot in pumping mode.

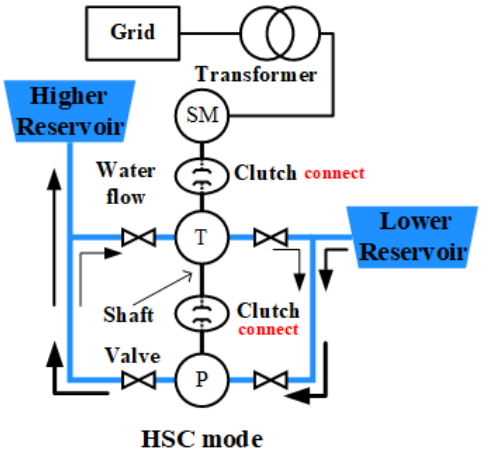

Figure D-7. Water flow of T-PSH in HSC mode

D.1.3.3 Sharing Penstock

Hydraulic short-circuit, as a new feature in the T-PSH system, occurs because the turbine runner and the pump runner work together. When T-PSH consists of a set of separated parallel penstocks, water flow in the pump part and the turbine part flow between the higher reservoir and the lower reservoir by themselves. Obviously, the direction of water flow in the two units, the pump, and the turbine are different. But the water flow in these parallel penstocks cannot affect each other, owing to the reservoir used in T-PSH system, which can be treated as an infinite water resource. As a

result, simply combine the turbine part and the pump part to achieve HSC mode. Under the control of the distribution block, the pump part is operated with a fixed output, whereas the turbine part provides variable output. The negative constant pump torque, countering the variable positive turbine torque, results in a variable net torque which is described in Equation 4.

$$P_m = P_{m\_t} + P_{m\_p} \qquad (4)$$

where P_m is the total mechanical power output of the governor, P_{m_t} is the mechanical power output of the turbine part, and P_{m_p} is the mechanical power output of the pump part. This function is added into the governor model to describe the combination of torque on the shaft. At the same time, there are some changes in the hydro model.

If a two-stage penstock structure is employed to save excavation costs, the HSC mode constitutes a circulating flow, as shown in Figure D-8. In this structure, the primary penstock is used to connect the reservoirs and chambers of T-PSH unit. A secondary penstock is split from the primary penstock to connect each chamber in the T-PSH unit. The water flow in the secondary penstock forms a circuit of water flows in HSC mode. The pump runner drives the water flow from the lower reservoir to the higher reservoir, as shown in Figure D-8 by the arrows from the bottom left to the upper right. Meanwhile, the turbine runner is driven by part of pumped water flow to generate torque, which is superimposed with the power on the shaft. The water flow through the turbine recombines with the water flow from the lower reservoir reflow into the pump. The water flow in the turbine part can be treated as a short-circuit water flow and will affect the whole water flow in the T-PSH system. As a result, a new water flow equation is designed to model this interaction, shown in Equation 5 (Koritarov et al. 2013c).

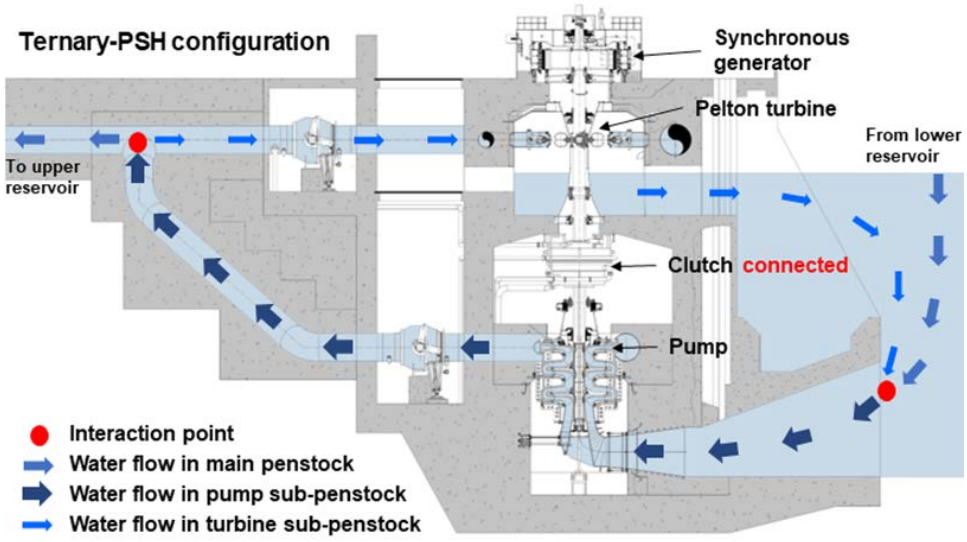

Figure D-8. Water flow in the HSC mode with two-stage penstock

Illustration from GE Renewable Energy

$$\begin{bmatrix} Tw_{tt} & Tw_{tp} \\ Tw_{pt} & Tw_{pp} \end{bmatrix} \cdot \begin{bmatrix} \frac{dq_t}{dt} \\ \frac{dq_p}{dt} \end{bmatrix} = \begin{bmatrix} \Delta H_t \\ \Delta H_p \end{bmatrix} \qquad (5)$$

where T_{w_pp} is the water time constant for the entire penstock length of the pump part, T_{w_pt} is the water time constant for the shared-penstock length from the pump part to the turbine part, T_{w_tt} is the water time constant for the entire penstock length of the turbine part, and T_{w_tp} is the water time constant for the shared-penstock length from the turbine part to the pump part; q_t, q_p are the turbine flows in per unit for the turbine part and the pump part; and ΔH_{w_t}, ΔH_{w_p} are the turbine head differences in per unit for the turbine part and pump part. Note that in HSC mode, T_{w_pt} and T_{w_tp} in the water constant matrix describe the interaction between two separate secondary penstocks whose water flow are in a different direction at the same time. If T-PSH only works in the generating or pumping mode, this water time constant is still suitable by only setting a value for T_{w_tt} or T_{w_pp} and setting the other three elements as zero. If T-PSH works in the HSC mode without shared-penstock, T_{w_pt} and T_{w_tp} are set at zero to remove interaction between secondary penstocks.

D.1.3.4 Implementation in PSLF

After finishing the T-PSH modeling, system implementation on a commercial power system software is the next step, because currently there is no T-PSH model existing in a simulation platform. The T-PSH system must be implemented in the GE PSLF, both in power flow analysis and dynamic simulation. Since there is no existing dynamic model of the governor for T-PSH system, the governor model needs to be developed by using EPCL in a user-defined model.

PSLF is a package of programs developed by GE for studying power system transmission networks and equipment performance in both steady-state and dynamic environments. PSLF is a power system software platform commonly used in large-scale power system planning with a large number of data to demonstrate the system performance effectively and accurately. The power flow analysis can be performed on systems with up to 80,000 buses. This capability makes the study analysis and simulation of the wide-area system (e.g., the WI) possible.

The user-defined dynamic model is a subprogram used in a dynamic model simulation developed and written by the user. This allows users to customize some models that are currently not available in the dynamic model library. The user-defined model is developed by using the EPCL, which is a built-in programming language in PSLF and is part of the PSLF software.

EPCL is usually used for two purposes: (1) customized function as a script to run a set of sequence commands; and (2) to develop a user-defined dynamic model. Customized function is typically used to control PSLF, such as running multiple simulation cases. The EPCL application is used to implement a user-defined model. Different from the customized function, the EPCL user-defined dynamic model must work with the PSLF C code model called 'epcmod.' This C code model is the bridge between the EPCL dynamic model and the PSLF core. Because of this, the EPCL model must be written in a fixed structure. The user deploys the EPCL language to implement custom functions under the structure of the epcmod model. An inherent simulation order is shown in Figure D-9. Five blocks of code, except 'NTWK,' which is executed in the PSLF core, are needed in the EPCL user-defined model. Each stage is explained as follows Concorda (2012):

- INIT: dynamic model initialization
- SORC: dynamic model network boundary source conditions calculation

- NTWK: network boundary calculation (execution in PSLF core)
- ALGE: secondary variables calculation
- RATE: state variable derivative calculation
- OUTP: output variables setting.

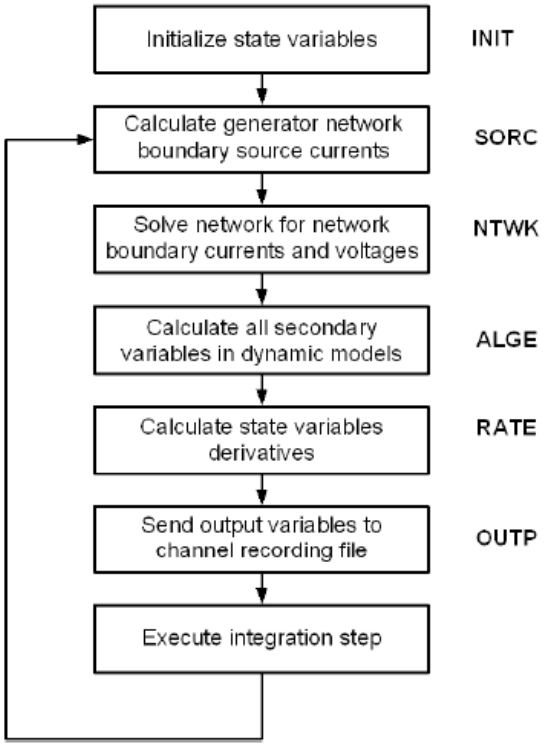

Figure D-9. Flow Chart of a dynamic simulation

Illustration from Concorda (2012)

```
Algorithm 2: EPCL model structure
   Input: Network Parameters
   Output: Output Channel
 1 switch @mode do
 2 |   case RATE do
 3 |   |   calculate state variable derivative;
 4 |   |   break;
 5 |   case ALGE do
 6 |   |   calculate secondary variables;
 7 |   |   break;
 8 |   case SORC do
 9 |   |   calculate dynamic model network boundary
   |   |    source conditions;
10 |   |   break;
11 |   case OUTP do
12 |   |   Send output variables to record channels;
13 |   |   break;
14 |   case INIT do
15 |   |   Initial state variables;
16 |   |   break;
17 |   end
18 end
```

Figure D-10. Pseudocode for structure of EPCL model

For one dynamic simulation case, the initialization is executed once at the beginning of the simulation. After that, all other five substeps are executed in a fixed order and repeat until the end of the simulation. If there is more than one EPCL model in a simulation case, all EPCL models will be first initialized together, followed by sequential execution. Different from the single EPCL model, the execution of a multimodal case obeys a preset order, which is defined as a number from 0-49 in a parameter table and is treated as a sequence table for the compiled EPCL model. This number must be unique for each EPCL user-defined model. If an EPCL model is used several times in one simulation case, the same assigned number should be used. During the simulation, the PSLF core will call the blocks of code in the EPCL model, according to their fixed order shown in Figure D-11. These blocks of structure in an EPCL model are implemented by using the function of multiple choices switch function.

T-PSH system is modeled as two electric machines. The machine connected to the turbine and pump is modeled by a generic equal mutual inductance rotor synchronous machine model with the IEEE Type 1 excitation system model (IEEE Committee 1968). The governor in this system is developed by an EPCL user-defined model.

D.2 Q-PSH Employing Full-Converter-Based Machines

Compared with other PSH technologies, Q-PSH combines several characteristics from C-PSH and AS-PSH technologies. A dual-machine, dual-shaft system is used in Q-PSH, shown in Figure D-12.. In this configuration, the synchronous machine and its exciter are placed to operate as the turbine directly connected to the grid. Another synchronous machine operating as the adjustable speed pump is connected to the grid through a full-size converter. The whole Q-PSH system is controlled by the distribution block in the governor. The power order (reference) generated by distribution block is sent to the pump system and turbine system separately. The adjustable-speed pump and conventional turbine unit are operated simultaneously during HSC mode. Various algorithms can be developed to deploy frequency regulations on the grid. The frequency regulation

can be achieved in all modes of operations (pump, turbine, or HSC). The whole system is modeled and introduced in this section 7.

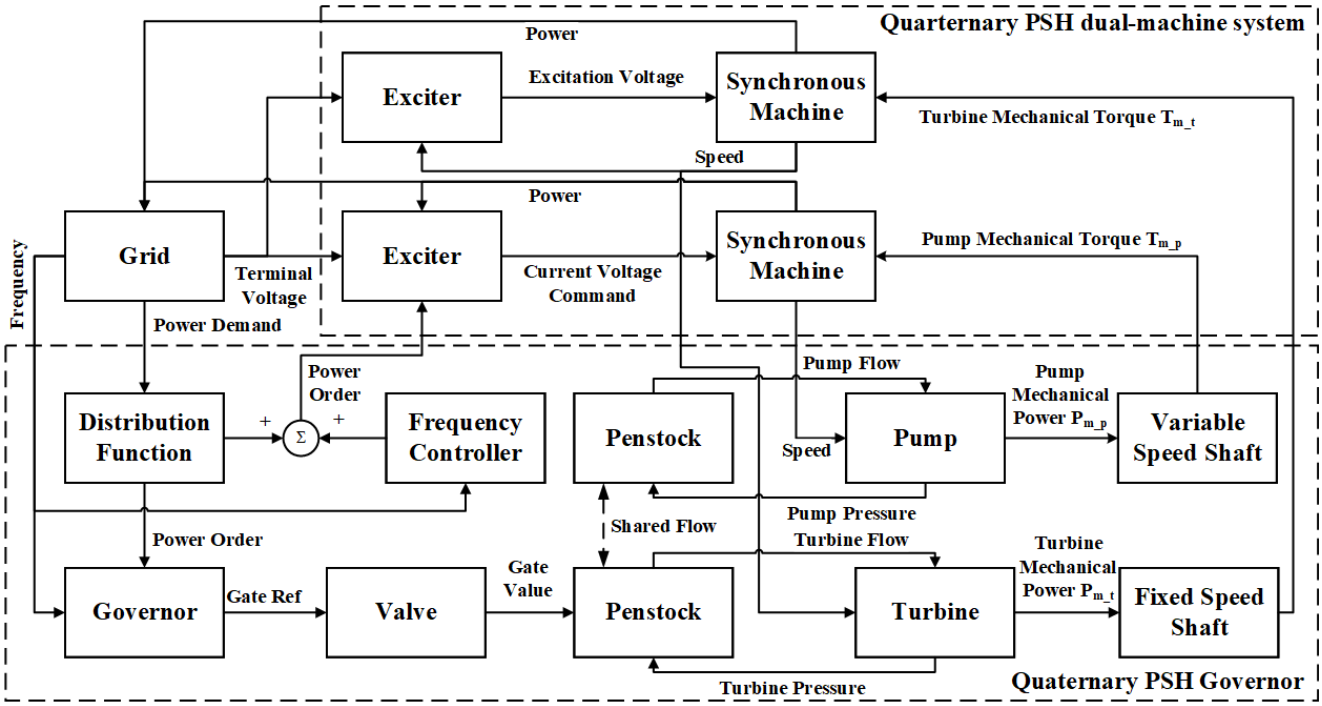

Figure D-11. Structure Diagram of Q-PSH system

D.2.1 Generator and Converter Model

In the quaternary configuration, two electrical machines with their shaft system and runner system are placed in separate chambers, as shown in Figure D-12.

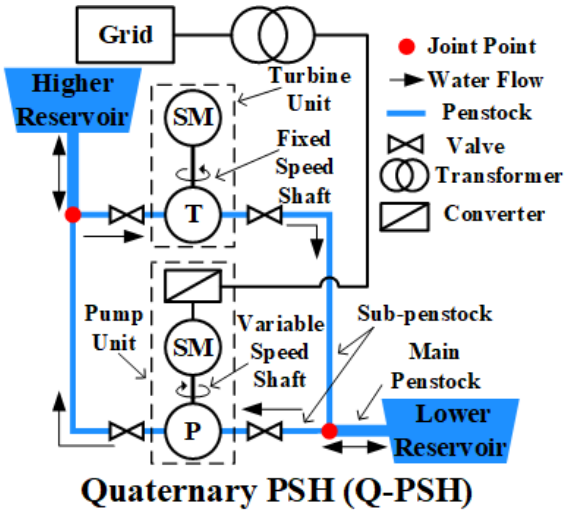

Figure D-12. Diagram of Q-PSH

In our Q-PSH system, a grid-connected synchronous machine system is modeled. In the pump part, an adjustable-speed pump is modeled as a full-power converter connected to the AC motor

(a similar concept used in the Type 4 wind turbine model). This model simplifies the mechanical dynamics and flux dynamic to reflect the rapid response of the power converter (Concorda 2012; MacDowell et al. 2011). The power orders for each machine system are sent by distribution function in the governor model, which makes the two machine systems electrically coupled.

D.2.2 Governor Control Model

As introduced previously, a full-size converter machine system is used in the pump system. A conventional permanent magnet synchronous machine is connected to the grid through a full-size converter. This type of system used in the dynamic modeling of the wind turbine can be used in adjustable-speed pump dynamic modeling; however, the governor used to describe the hydraulic characteristic of the pump system still needs to be developed.

D.2.3 Mechanical and Hydraulic System

In the adjustable-speed pump system, there is a characteristic curve to describe the relationship between water head, water flow, and shaft speed (Liang and Harley 2010; Volk 2013; Girdhar and Moniz 2011). In the curve shown in Figure D-13, the relationship could be approximated by a quadratic polynomial (Hacobian and Yee 1978).

$$H_d = a_0\omega^2 + a_1\omega|Q_d| + a_2{Q_d}^2 \qquad (6)$$

where a_0, a_1 and a_2 are coefficients for curve fitting, H_d is the dynamic water head, Q_d is the water flow, and ω is the shaft speed. In this function, when there is a certain value of dynamic water head, the relationship between water flow and shaft speed can be obtained. Because of this, the change in water flow is only affected by the shaft speed. In addition, in the pumping mode, the gate is only used to open or close the penstock and does not control the water flow, which is always used in hydro generation.

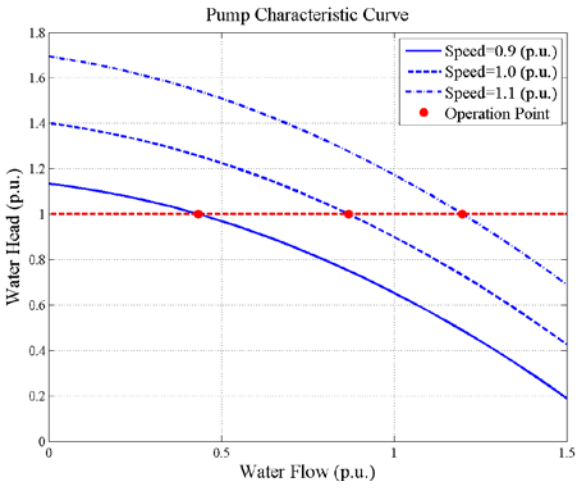

Figure D-13. Pump characteristic curve

After implementing the pump performance curve, mechanical power output can be expressed as:

$$P_{mech} = \frac{H_d Q_d}{\eta} where \quad Q_d = \frac{H_0 - H_d}{sT_w} \qquad (7)$$

where P_{mech} is mechanical power output in per unit, H_d is the dynamic water head, Q_d is the water flow, η is the pump efficiency, H_0 is the water head at the reservoir, and T_w is the hydraulic time constant. In this function, the hydraulic time constant is used to model the single penstock. In order to model the shared penstock in Q-PSH operation, the hydraulic time constant will be replaced by a matrix, which will be introduced later in this section.

Combined with Equation (5) and Equation (6), the shaft speed is the only input for the dynamic model of the pump hydraulic part. A swing equation describes the mechanical dynamic related the shaft speed to the net torque, as shown in Figure D-14 (Kundur, Balu, and Lauby 1994).

$$\dot{\omega} = \frac{1}{2H}\left(\frac{P_{mech}-P_{elec}}{1+\omega}\right) \quad (8)$$

where ω is the shaft speed, H is inertia, and P_{mech} and P_{elec} are mechanical power and electrical power separately. When there is a disturbance in the power system, there will be a temporary imbalance between the supply and demand. In the generator, there is an imbalance between electrical power and mechanical power, thus developing a transient in the speed, and in the acceleration of the rotor.

D.2.4 Frequency Control System

After using a distribution block, the machine system operates at a set point. As in any inverter-based resource, the power converter (in the pump system) acts as a buffer between the grid and the electrical machine. Thus, it cannot directly respond to the grid event. The power converter can be controlled through the distribution block to make pump system respond to the frequency variance on the grid. A set of controllers is built into the pump governor to adjust the pump output power responding to the system requirements.

An inertia controller (shown in Figure D-14) is added into the control system to provide inertia response from the pump system (Morren, Pierik, and De Haan 2006; Morren et al. 2006). Different from traditional electric machine system, an inverter-based adjustable-speed pump is not directly connected to the grid. Thus, it does not contribute to the inertial response as in a conventional grid-connected synchronous machine. By adding the inertia controller, the pump system can be made to have a virtual inertial response when system contingency occurs on the grid.

In addition, a primary frequency controller (Figure D-14) is added to help pump system give primary frequency response after the frequency event in the system (Knuppel et al. 2011). When there is a frequency variance in the power grid, these auxiliary controllers enable the full-converter machine-based pump to respond to the frequency event like the conventional rotating machine system, providing the inertial response and the primary frequency response.

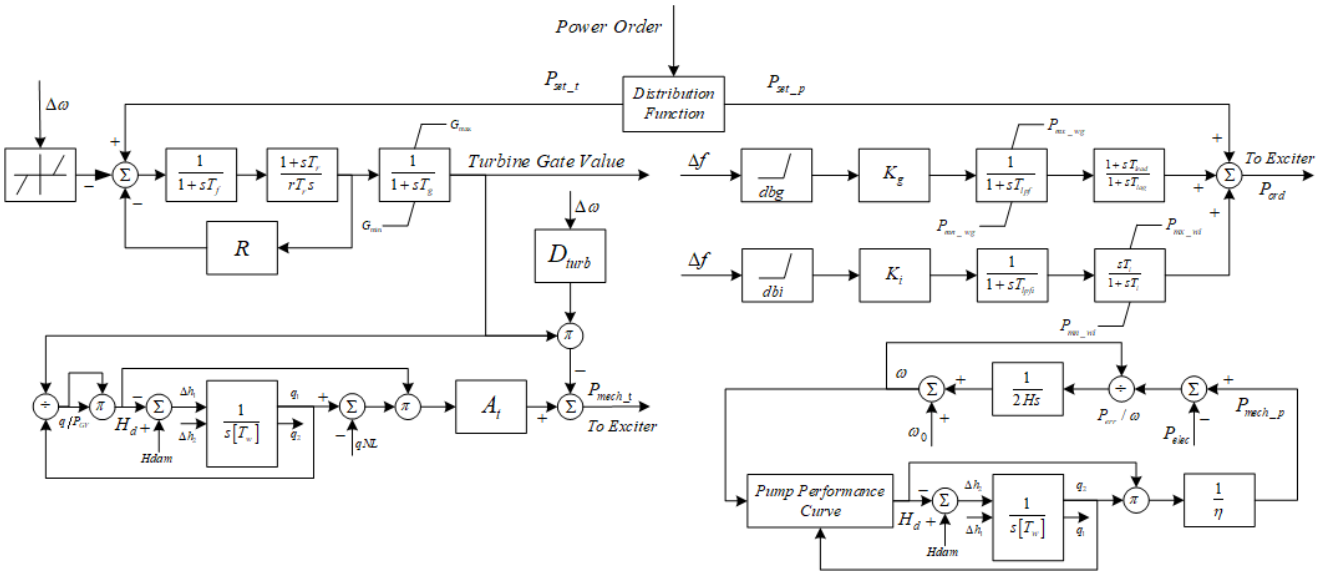

Figure D-14. Transfer function of Q-PSH governor system

D.2.5 Turbine System Modeling

In the turbine system, a conventional hydro synchronous generator system model is used to describe the generator and its exciter. Different from the pump part, the hydropower generation governor model can be used in the turbine system. Based on a generic standard hydro turbine governor model used in a hydropower simulation, a turbine part governor model is modified and built to work with a machine model (Concorda 2012). In this governor-turbine model, detailed modeling of the gate, which includes the injector and deflector, is described. The description of the shared-penstock situation is also added to model the hydraulic short-circuit mode in detail.

D.2.6 Sharing the Penstock Model

Since Q-PSH uses the same penstock structure as T-PSH technology, the penstock model used in the Q-PSH governor is same as in T-PSH functions.

D.2.7 Implementation in PSLF

The Q-PSH system is modeled as two electric machines. The machine connected to the turbine is modeled by a generic equal mutual inductance rotor synchronous machine model Kundur, Balu, and Lauby 1994) with the IEEE Type 1 excitation system model (IEEE Committee 1968). The machine connected to the pump is modeled by the GE full converter wind turbine model with its control system (Concorda 2012; Liang and Harley 2010; Clark, Miller, and Sanchez-Gasca 2010). The governor and dual-machine controller in this system is developed by an EPCL user-defined model.

D.2.8 AS-PSH Employing Full Converter-Based Machines

AS-PSH, as an electrical innovation, adopts wind turbine technologies. In the doubly-fed induction generator (DFIG) AS-PSH technology, the original synchronous machine used in C-PSH is replaced by the DFIG. The DFIG is connected directly to the grid, and the converter is used as the DFIG's AC exciter. Another type of AS-PSH is the full converter AS-PSH. In this technology, the synchronous machine in the C-PSH system is kept, and the machine is connected to the grid

through a full-size converter. This design has a wider range of speed adjustment and power factor, compared to DFIG-based AS-PSH. This part shows the development of a dynamic model of full converter AS-PSH in the GE PSLF platform, based on the GE Type 4 full converter wind turbine technology. A new governor is developed that can be operated in both generating mode and pumping mode. In this governor mode, the mechanical and hydraulic parts are designed as two subsystems, which are responsible for different operation modes. The operation of these two sets of subsystems is controlled by an operation mode controller designed to send power order and the control signal to the whole full converter AS-PSH system. Furthermore, a set of frequency controllers is deployed in the governor to control the output of the converter, providing frequency regulation capability to the whole system. In addition, the wicket gate system and the penstock system in the new governor model are modeled in detail, according to the real date from the manufacturer, and have the capability to simulate with different sets of parameters.

D.2.9 PSLF Model

The detailed dynamic model of full converter AS-PSH (Type 4 AS-PSH) is presented in D-15. In this configuration, the synchronous machine with its full-size converter is modeled as the machine system. The exciter in this system is the converter controller, which is used to send the power order from the governor to the converter. In the governor, an operation mode controller is designed to control the operation mode and calculate the power order. A set of frequency controllers is deployed to improve the performance of the frequency response. Further, there are two different sets of mechanical and hydraulic subsystems to be used in generating mode and pumping mode separately, which will be controlled by the operation mode controller.

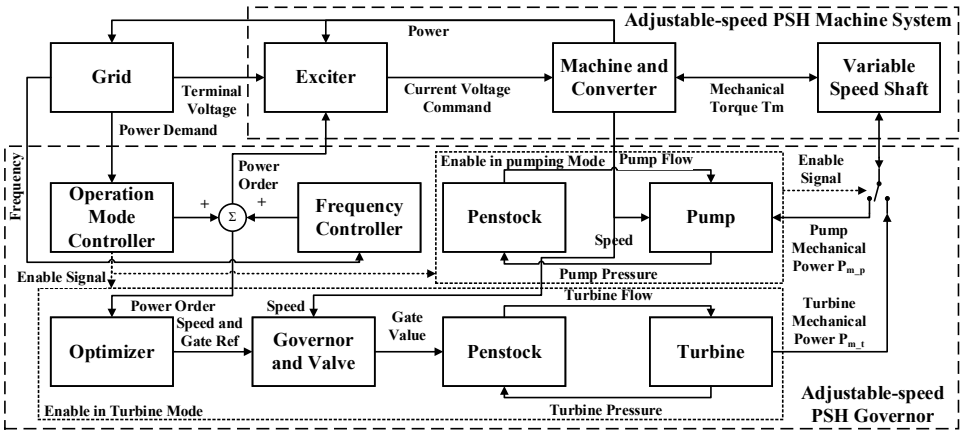

Figure D-15. Diagram of Type 4 AS-PSH

In Type 4 AS-PSH system, the synchronous machine is connected to the grid through a full power converter. These machine and converter systems are modeled by a simplified generator model that does not have mechanical dynamics and a flux dynamic to reflect the rapid response of the power converter controlled by the high-level command (the same concept as the Type 4 full converter wind turbine model) (MacDowell et al 2011; Clark, Miller, and Sanchez-Gasca 2010). The bridge between governor and generator system is the converter controller, which is modeled as an exciter in the PSLF. Different from traditional generator system, the exciter in full converter AS-PSH does not provide field voltage, but instead sends the active power and reactive power order, which is generated by the governor.

In order to study all operation modes of Type 4 AS-PSH, a universal governor is designed for both generating mode and pumping mode. In this governor, the operation mode controller and frequency controllers are the universal subsystems used in generating mode and pumping mode; however, because of the different physical characteristics of these two operation modes, the mechanical and hydraulic parts are modeled separately and controlled by the operation mode controller.

The operation mode controller is designed to control the Type 4 AS-PSH operation mode and send power order to the machine system. The enable signal is generated by this controller and is sent to the rest of the governor to initialize the system with the required operation mode. The power order is calculated by Equation 9:

$$P_{ord} = K_d \times |P_{demd}| \quad where \begin{cases} K_d = 0 \ standstill \\ \frac{P_{rate}}{P_{init}} \geq K_d > 0 \ generating \\ -\left|\frac{P_{rate}}{P_{init}}\right| \leq K_d < 0 \ pumping \end{cases} \tag{9}$$

where P_{ord} is the reference power (power orders) sent to the power converter of the Type 4 AS-PSH, K_d is distribution constant, P_{demd} is the power demand from the system, P_{rate} is the rating power output for the Type 4 AS-PSH unit, and P_{init} is the initial value of the power output of Type 4 AS-PSH unit. Note that in the initialization, the distribution constant K_d is equal to a positive one for generating mode or a negative one for pumping mode to make Type 4 AS-PSH be initialized by the system power demand.

In a Type 4 AS-PSH system, the converter acts as a buffer between the power system and the electrical machine. The power order of converter (a constant order) is set by the operation mode controller, which cannot make the converter respond to the frequency event if one occurs in the system. A set of frequency controllers is designed as a universal part (used in two operation modes) to adjust the power order and meet the system frequency requirements.

A primary frequency controller and inertia controller are built into this frequency control system, shown in Figure D-16 (Morren et al. 2006). Different from the traditional synchronous machine, in a Type 4 AS-PSH system, the participation of the converter hinders the electrical machine inertia response. The inertia controller is added to emulate the virtual inertia response. In addition, the primary frequency controller no longer works with the electrical machine like the C-PSH system, but it provides the primary frequency response to the converter directly.

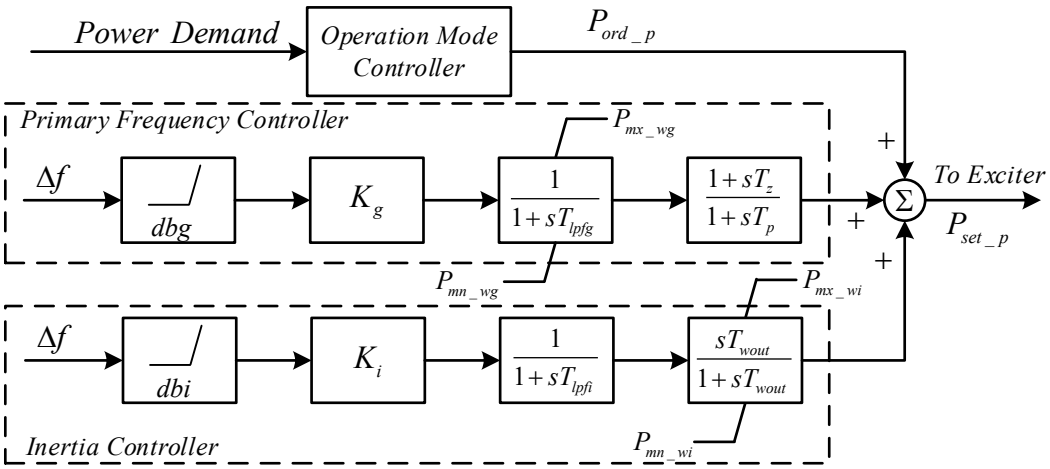

Figure D-16. Transfer function of governor system frequency controller

When a Type 4 AS-PSH is operating in generating mode, a Pelton turbine system is enabled by the operation mode controller. In this part of the system, which is shown in Figure D-17, the hydraulic and mechanical system is modeled based on a generic conventional hydropower governor. The detailed gate system with an injector, deflector, and tunable transition time, are fully considered. In a Francis turbine, a droop controller, used for adjustment of (wicket) gate value, is also included in this turbine system. Moreover, several new blocks are developed based on the requirement of the Type 4 AS-PSH in generating mode.

Since the Type 4 AS-PSH does not work in synchronous speed, optimization functions are designed to provide system-optimized speed reference and gate reference to track maximum efficiency. Two linear functions are expressed in Equation 10 to show the relationships among two references (speed and gate), power order and water head (Koritarov et al. 2013b).

$$\omega_{ref} = aP_{set} + bH + c$$
$$G_{ref} = cP_{set} + eH + f \qquad (10)$$

where ω_{ref} and G_{ref} are references for shaft speed and gate, respectively, P_{set} is the setting power (power orders) sent from governor to the power converter of the Type 4 AS-PSH, H is the water head, and a to f are coefficients for real date curve fitting. When the size of the reservoir is sufficiently large, and the power adjustment is only for a very short duration, the change of water level, the water head can be treated as a constant during the simulation. It is worth noting that the setting power (power reference or power order) used for these optimization functions is bypassed during the inertial response—from the inertia controller, which prevents unnecessary excessive change in two references. In addition, these optimization functions are only used in daily normal operation. When there is a contingency in the system like load tripping, these functions will be disabled to let the Type 4 AS-PSH respond quickly and be enabled again after the system completes the short-term power regulation.

In addition, a swing equation (11) is placed in the governor model to describe the dynamic relationship between shaft speed and net torque, which is removed in the simplified generator model (Kundur, Balu, and Lauby 1994).

$$\dot{\omega} = \frac{1}{2H}\left(\frac{P_{mech}-P_{elec}}{1+\omega}\right) \quad (11)$$

where ω is the shaft speed, H is inertia, P_{mech} and P_{elec} are mechanical power and electrical power separately. When there is a mismatch between the mechanical power and the electrical power, like a contingency occurring in the power system, the transient speed will change as reflected in the acceleration or deceleration on the rotor.

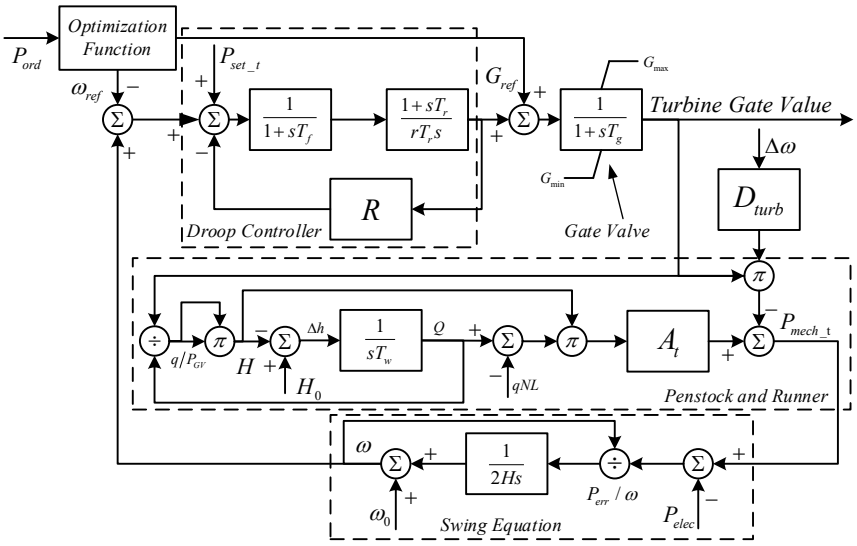

Figure D-17. Transfer function of governor system turbine part

Like the turbine part, the pump system is only enabled in AS-PSH when operated in the pumping mode. Unlike the turbine system, the gate system in the pumping mode is modeled as an on/off function, not to control the water flow. Thus, there is no droop controller and gate function built into the pump system, shown in Figure D-18.

Although there is no gate to control water flow, a characteristic curve is used to describe the relationship among water head, water flow, and shaft speed (Volk 2013). This curve, always called the pump curve, could be approximated by a quadratic polynomial, shown in Equation 12 (Liang and Harley 2010).

$$H = a_0\omega^2 + a_1\omega|Q| + a_2Q^2 \qquad (12)$$

where H is the dynamic water head, Q is the water flow, ω is the shaft speed, and a_0, a_1, and a_2 are coefficients for curve fitting. As indicated previously, when the water head changes slightly, it can be treated as no change during the simulation. The relationship between the speed and water flow can be found, which shows that in the pumping mode, the Type 4 AS-PSH changes the size of water flow only by adjusting the shaft speed. Because of this, the shaft speed is the only input for the pump system. The mechanical power output of the pump system is directly controlled by shaft speed. To get the shaft speed, the same swing function as in the turbine system is also added.

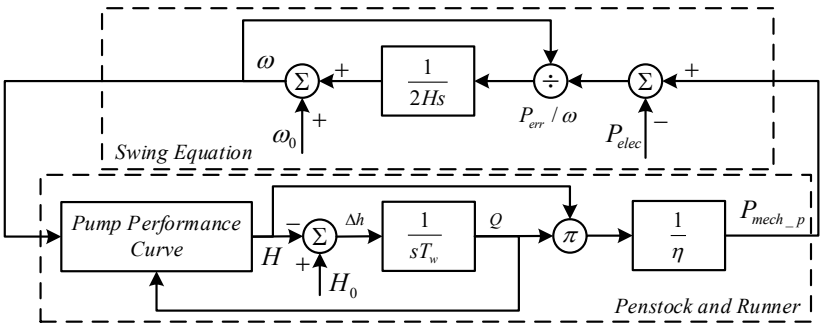

Figure D-18. Transfer function of governor system pump part

D.2.10 PSCAD Model (Kim et al. 2019)

An AS-PSH can be implemented from a PSH employing a full-scale converter with a synchronous machine. An AS-PSH is a physical transformation of a conventional PSH unit in which the synchronous machine of the PSH unit is connected to a power system through converters, thereby achieving continuous control of the variable speed operation of the turbine and pumping modes. Thus, an AS-PSH unit can provide flexible services as a functional extension of the PSH unit. An AS-PSH unit is mainly classified into three parts: a governor with an optimizer, penstock dynamics, and converter controllers.

Figure D-19 shows the configuration of an AS-PSH unit. An AS-PSH unit normally optimizes its rotational speed and gate position to maximize efficiency at a given power reference, P_{ref}. To achieve this, an optimizer, which calculates the optimum speed and gate position based on the power reference, is used to determine the speed reference, ω_{ref}, and gate reference, G_1. A typical function of an optimizer can be found as linear equations, and it can be written as:

$$\omega_{ref} = 1.25(|P_{ref}| - 0.8) - 0.25(h_0 - 0.8) + 0.95 \qquad (13)$$

$$G_1 = (|P_{ref}| - 0.8) - (h_0 - 0.8) + 0.8 \qquad (14)$$

where h_0 is the head level.

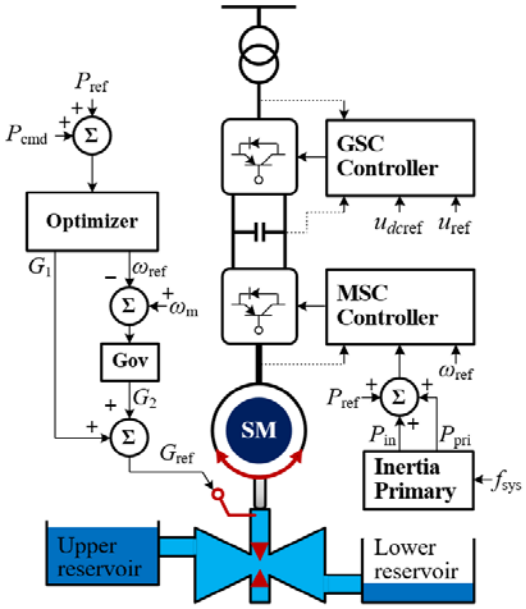

Figure D-19. Configuration of an AS-PSH

Once ω_{ref} and G_1 are determined, the governor, which is based on a proportional–integral–derivative controller in series with the pilot and distribution valves, adjusts its gate reference, G_{ref}, as shown in Figure D-20. G_{ref} is transformed into mechanical input power using a table function, and it is transferred through a penstock, as shown in Figure D-21. Mechanical power through a penstock, P_m, can be written as (Nanaware, Sawant, and Jadhav 2013):

$$P_m = A_t h(q - q_{nl}) - \beta \Delta\omega \quad (15)$$

where A_t, h, q, q_{nl}, β, and $\Delta\omega$ are the turbine gain, head at the water surface, water flow, no load flow, proportionality gain, and speed deviation, respectively.

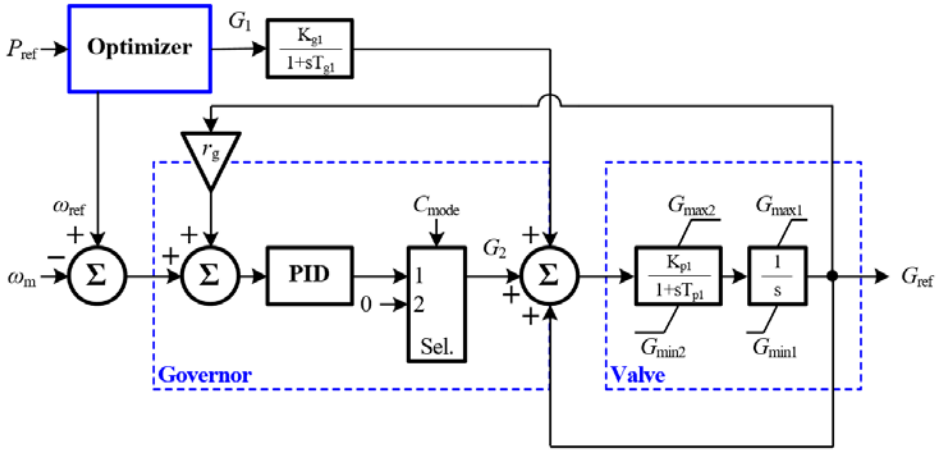

Figure D-20. Governor and valve model of an AS-PSH

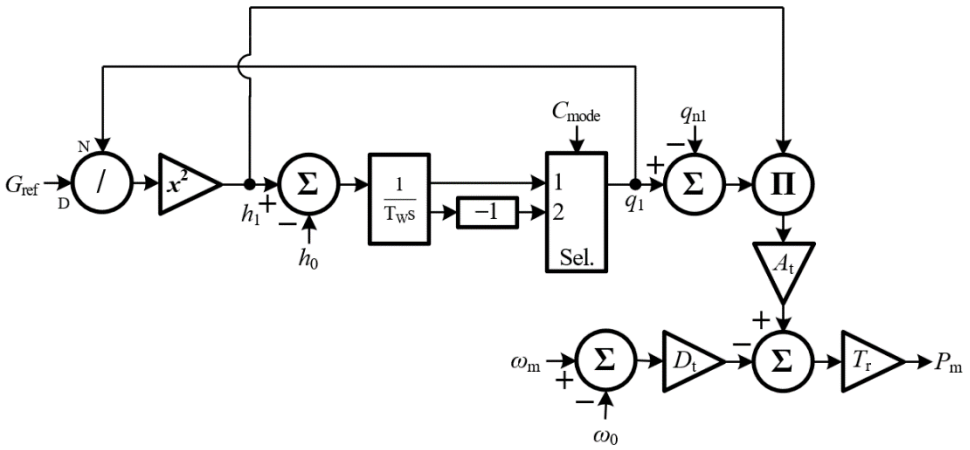

Figure D-21. Penstock model of an AS-PSH

q through a penstock can be given by (Choo, Muttaqi, and Negnevitsky 2008):

$$q = G\sqrt{h} \qquad (16)$$

As the water flow moves through a penstock, P_m is transferred to a mechanical power, driving the synchronous permanent magnet machine.

The converter controller of the AS-PSH unit consists of the machine-side converter controller and grid side converter controller. A frequency control loop is implemented in the machine-side converter controller, as shown in Figure D-22. DC-link voltage and terminal voltage control loops are implemented in the grid-side controller. The frequency controller determines the active power reference, Pref_AS, by adding three active power references: inertia control reference, Pin; primary control reference, Ppri; and Pref from the optimizer. Pin and Ppri are adjusted by the system frequency. In the current control loop (shown in Figure D-23), the d-axis current reference, Id_ref, is obtained from an active power error through a proportional-integral (PI) controller. Further, the AS-PSH distinguishes its modes of operation—a turbine mode and pumping mode—by the control mode signal (Cmode). For the turbine mode, Cmode is set to 1, and it is set to 2 for pumping mode.

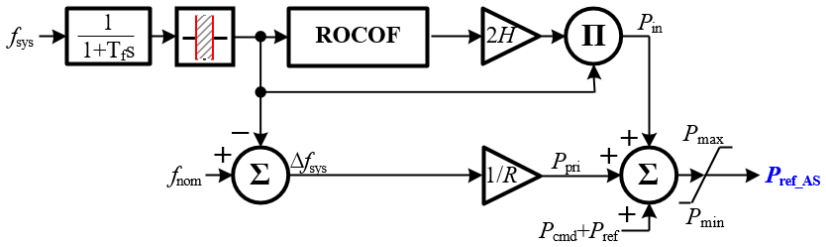

Figure D-22. Frequency control loops in the machine-side converter controller

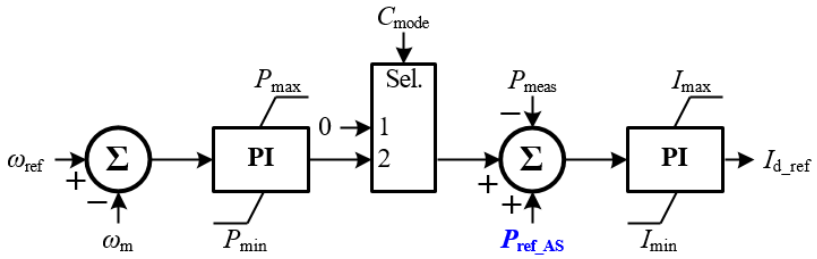

Figure D-23. Current control loop in the machine-side converter controller

D.2.11 Dynamic Model of Energy Storage (PSCAD) (Kim et al. 2019)

Energy storage devices have diverse forms of physical realizations and operational characteristics. Applications of energy storage devices in power systems vary widely based on system characteristics and needs. A battery energy storage device is mainly used to reduce the operational cost of overall storage, which is high because of the battery's high energy density; however, because of its slow response, it cannot provide frequency support. Fortunately, supercapacitors (SCs) feature a fast charging/discharging characteristic that can satisfy a power density application, but they are unable to provide long-term energy. Thus, SC-based energy storage systems (SCESSs) can be considered as an option to provide a short-term ancillary service in a power system.

Figure D-24 shows the configuration of a SCESS, comprising a DC-DC converter and voltage source converter (VSC). The bank of SCs can be represented by its equivalent capacitance, C_{eq}, and resistance, R_{eq}.

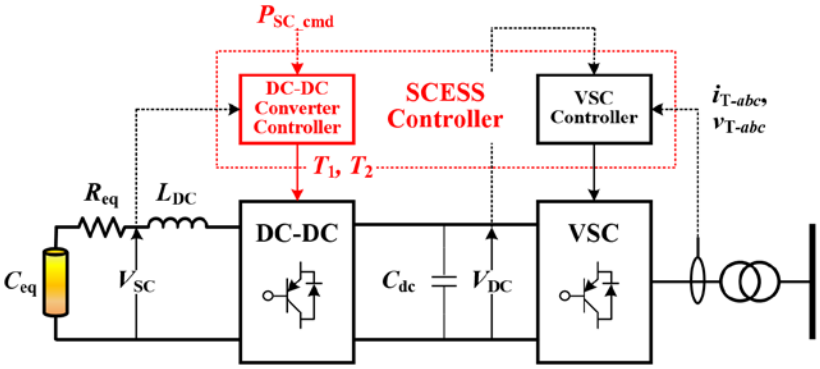

Figure D-24. Configuration of a SCESS

Short-term energy storage can be achieved by using SCs. SCs are electrochemical capacitors that exhibit high energy density compared to conventional capacitors, reaching values of thousands of farads (F) (del Toro García et al. 2010). Their nominal voltage is relatively low. Thus, a series of SCs is needed for high voltage applications. The energy, W, stored in a capacitor is directly proportional to its capacitance, C, and the square of DC voltage, V, across the capacitor:

$$W = \frac{1}{2}CV^2 \quad (17)$$

Super capacitors have voltage limits. Exceeding these can cause a dielectric breakdown, resulting in permanent damage. Thus, the maximum energy, W_{max}, that the capacitor can store can be calculated from the maximum capacitor voltage, V_{max}. The charging and discharging characteristics of SC energy storage can be controlled so that constant current or constant power

output can be achieved. The decay of capacitor voltage at constant power discharge can be calculated using the following basic capacitor equations:

$$I_D = C\frac{dV}{dt} = \frac{P}{V} \qquad (18)$$

where I_D and P are the discharging current and discharging power, respectively. After a simple mathematical transformation from Equation 18, the following integral equation can be derived:

$$\int VdV = \frac{1}{C}\int Pdt \qquad (19)$$

Then, from Equation 19, the voltage decay profile versus time at a given initial voltage, V_{max}, and discharge power, P, can be written as

$$V = \sqrt{V_{max}^2 \frac{2P}{C}} \qquad (20)$$

Figure D-25 shows example voltage decay profiles for a 20-*F*, 1,000-V capacitor bank discharging at 1-, 2-, and 3-MW constant power, respectively. In this example, a 20-*F* capacitor with an initial voltage of 1,000 V can potentially inject 1 MW into an electric grid for 10 seconds, at 2 MW for 5 seconds, and at 3 MW for 3.3 seconds. A similar equation can be derived for the charging process when the capacitor storage is being charged at constant current:

$$V = \frac{I_C}{C}t \qquad (21)$$

where I_C is the constant charging current. According to Equation , the capacitor voltage will increase linearly until the maximum allowed voltage level is reached. Figure D-25. shows an example of the voltage profiles for the same 20-*F* SC bank during constant current charging for three different charging currents: 1,000 A, 2,000 A, and 3,000 A.

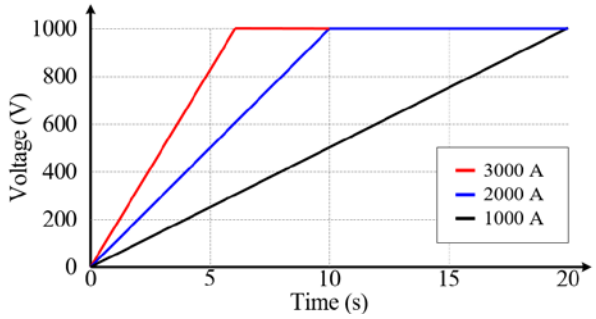

Figure D-25. Characteristics of the SC voltage decay for a 20-*F* SC at three different discharge powers

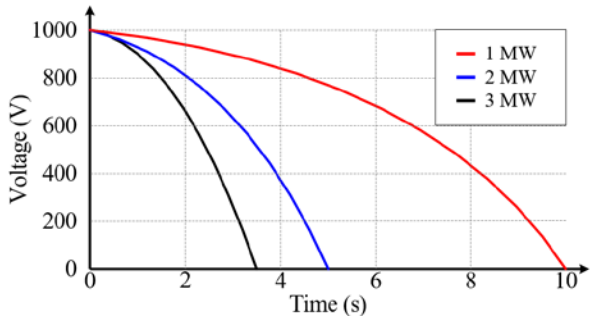

Figure D-26. Characteristics of the SC voltage rise for a 20-*F* SC at three different charging currents

For the control of the SCESS in Figure D-24, the SCESS controller consists of a DC-DC converter and VSC controllers. The former provides charging/discharging power flow from the SC, and the latter maintains the DC-link voltage (VDC) as a constant. Figure D-27 shows the control scheme for the DC-DC converter. The DC-DC converter is connected to the SC on the left side. The controller receives the power command, P_{SC_cmd}, from an external controller. Then, the operation modes—buck or boost—of the DC-DC converter is automatically determined by the sign of P_{SC_cmd}; in detail, the mode signal, M, can be 0 or 1 for the boost or buck, respectively. Therefore, the SC can be charged or discharged. The on-off signal for the converters, S_{on}, is to enable or disable the converter and is obtained depending on V_{SC} by:

$$S_{on} = \begin{cases} 1, & V_{\max} < V_{SC} < V_{\min} \\ 0, & otherwise \end{cases} \quad S_{on} = \begin{cases} 1, & V_{\max} < V_{SC} < V_{\min} \\ 0, & otherwise \end{cases} \tag{22}$$

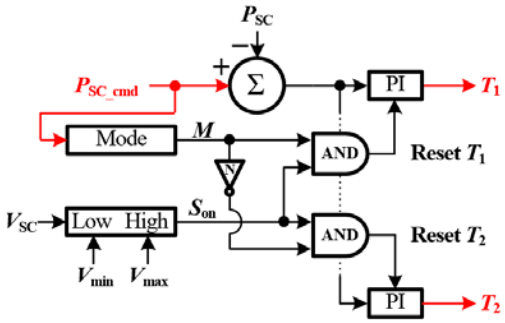

Figure D-27. Control scheme for the DC-DC converter

Once P_{SC_cmd} and the mode are set, then the PI controller for an applicable mode processes switching signals through P_{SC_cmd}.

Figure D-28 shows the control scheme for the VSC in Figure D-24. The controller is designed based on the PI controllers to regulate the DC-link voltage and the reactive power or current at the terminal of the SCESS.

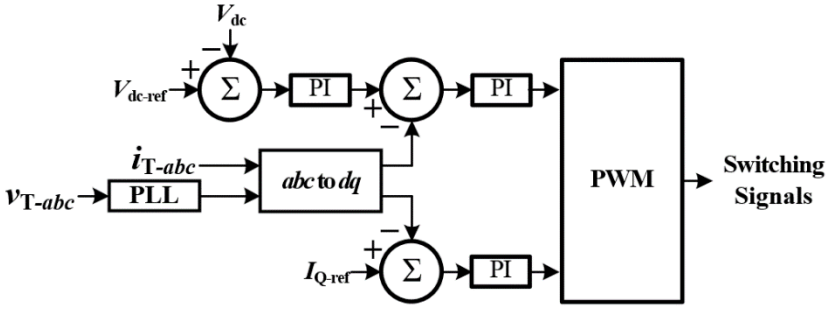

Figure D-28. Control scheme for the VSC

Appendix E. System Protection and Controls (PSCAD)

E.1 Grid Faults and Disturbances

Grid faults and disturbances are common in an interconnected large system because of the exposure of power system components to natural forces. As most of the transmission distribution network consists of overhead lines, the exposure to wind, lightning, fallen trees, and wild vegetation may touch or create a path for the short circuit to the ground. Similarly, the substation, transformer, and switchyard are in the open air. The exposure to rain, hail, and dust exposes high voltage components to the open air, creating corona losses and leakage current paths, affecting the integrity of the component or communication lines, due to induced electromagnetic interference or radio interference.

The impact of disturbances or faults on the customer are usually measured by the level of the voltage and frequency deviations (e.g., under/over normal values, dips, surges, and oscillations). Disturbances and faults can affect the power system and may result in a quick temporary disturbance, a prolonged underdamped event, a cascading event, or even a total blackout. The response of the system depends on the location, effectiveness of the system protection to isolate the fault, and the effectiveness of the control system to damp out the impact of the disturbance. How far is the fault from the generating station? Which lines will be disconnected from the grid in order to isolate the fault? Will the line removal will affect many people? The duration of the disturbance is another consideration; for example, two lines may touch the branch of a tree, and a short circuit current will flow through generating heat, burning and charring the branch, and causing the short circuit to cease to flow. This is also called a temporary, self-clearing fault. If the duration is short enough, the system will return to the initial stable operating point.

E.2 Ride-Through Capability

Fault ride-through limits for voltage and frequency in the North American Electric Reliability Corporation (NERC) standard PRC-024 are shown in Figure E-1. Note that the frequency requirement varies for different interconnections. In general, when the operating point is in the envelope between the upper limit and lower limit, generating assets are expected to "ride through" faults that occur within the operating envelope (i.e., the units are expected to stay connected to the grid).

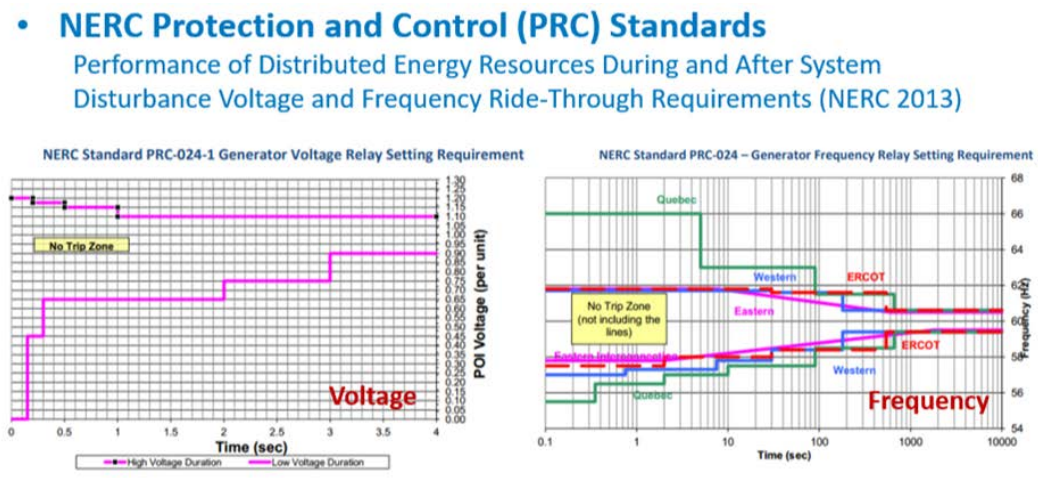

Figure E-1. Voltage and frequency ride-through as listed in NERC Standard PRC-024

The PSH must also comply with the ride-through capability standard stated by NERC, the regional reliability council, and local utilities. The key point of this requirement is to make sure that a small supply-demand imbalance caused by a disconnection of line, generator, or loads does not create additional supply-demand imbalances due to further disconnections.

E.3 Frequency Regulation

Frequency regulation is accomplished by maintaining the supply-demand balance. Any deviation will change the grid frequency, and the change is influenced by the size of imbalance. The ROCOF is proportional to the level of inertia available on the grid. The level of inertia is determined by the size of the kinetic energy available in the rotating masses in the system, including the direct connected rotating generators and motor loads. The frequency regulation is usually accomplished by the governor control where a linear controller is used to increase the incoming power to the grid in proportion to the frequency deficit. For a conventional power plant (e.g., gas turbine, diesel engine) to increase its output power, fuel must be increased (gas or diesel) to the combustion process.

Figure E-2 shows the progression of grid frequency changes for a generation loss contingency. Thus, the demand exceeds the supply; however, as kinetic energy cannot be changed instantaneously, the first contribution to supplement for the loss of generation comes from the inertial response, where the kinetic energy in the rotating masses slowed down to give part of the kinetic energy to the grid. As the rotating speed in a generator is directly proportional to the frequency, the change in the rotational speed is shown as the frequency dip. If the level of inertia is large, the ROCOF will be low; otherwise, the ROCOF will be high (a steep decline of frequency). The governor action takes place from the time governor detects the frequency deviation on the grid. Note because the response time of the governor is not very fast, the corrective action cannot be brought instantaneously. The frequency nadir (lowest frequency) on the grid is affected by the size of the inertia in the system, the response time, and the droop (sensitivity) setting of the governor. The first period of the response (between the loss of the generator to the lowest-frequency grid) is called the arresting period. The second period of the frequency change occurred during the rebounding period where the contribution from the governor responses starts to take place. The next period of the response is also called the recovery period, when the automatic generation control takes action to correct the grid frequency to a normal value (60 Hz).

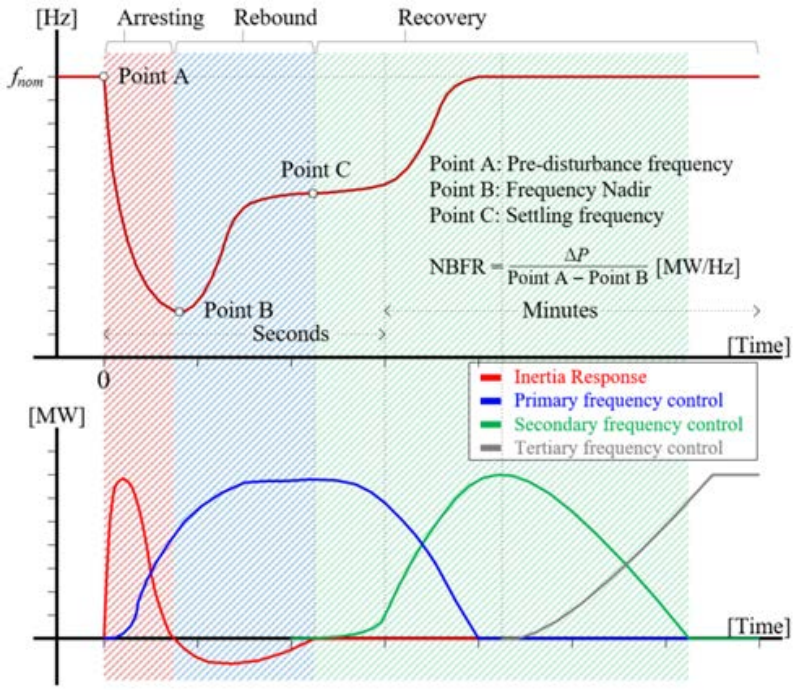

Figure E-2. Typical grid-frequency behavior during supply-demand imbalance

In a power system, especially a small isolated system, the level of inertia is limited; fortunately, many of the loads are flexible in nature. Thus, the variability of renewables is more tolerable. The variability in renewables is often unexpected, even though the technology forecasting renewables is presently sophisticated and advanced. While it is very easy to curtail the renewable generation to allow down-regulation, the up-regulation in most renewables is not possible. For example, if there is not enough wind, the level of generation cannot be increased. Or if there is a cloud passing the PV arrays, the level of generation cannot be maintained constantly without energy storage in the PV system.

E.4 G.3.1 Voltage Regulation

Good voltage regulation is very important in a power system at any voltage level—at the generating station, at the transmission network, and at the distribution network. For example, at a constant frequency, an undervoltage operation will result in underflux operation. In an induction motor, this means that the motor will operate at higher slip, higher loss, and higher temperature, and may lead to overheating—and worse, to winding insulation failure. On the other hand, for an overvoltage operation, the magnetic flux in the induction motor will be saturated. This leads to higher core losses, and higher core temperature may lead to eventual winding insulation failure, as well.

The voltage drop in a line is affected by the phase angle and magnitude of the line current, the magnitude of the reactance, and the magnitude of the resistance. Figure E-3 describes the impact of the line reactance X and the line resistance R.

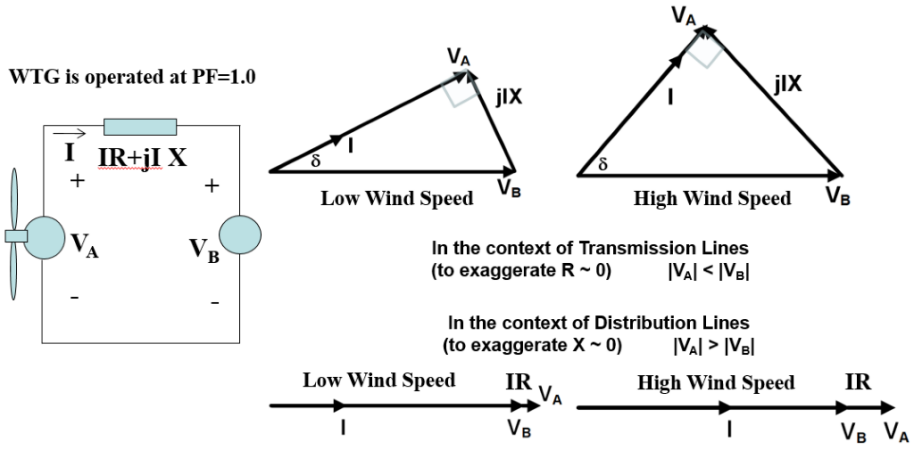

Figure E-3. Simplified per-phase equivalent circuit and phasor diagram illustrating voltage regulation

As can be seen Figure E-3, a simplified system consists of two buses: the sending end (Bus A), where the wind turbine is connected, and the receiving end (Bus B). Two different levels of X/R are illustrated, and a unity power factor is assumed. For example, in a transmission system, the X/R ratio is very high, so the size of the reactance X is much larger than its resistance R. As illustrated in Figure E-3, the voltage at the terminal of the wind turbine is affected by the voltage drop IX. The higher the wind speed (higher output current), the higher the power angle and the lower the terminal voltage V_A; however, it is easy to see that by changing the phase angle of the current with respect to the terminal voltage of the wind turbine, the terminal voltage V_A can be increased. That is why controlling the reactive power at the sending end will help regulate the voltage V_A.

In an urban distribution network where the buses are very close to each other, the lines are shorter and the X/R is very low, or, to exaggerate, X ~0. As can be seen from Figure E-3, the voltage at the sending end is higher as the wind speed increases (higher output current).

E.5 Grid Code

The surge in variable generation from wind prompted the development of formal technical interconnection procedures and standards for wind power systems in the United States. FERC's 2003 order (FERC Order No. 2003) proposed a Large Generator Interconnection Procedure and a Large Generator Interconnection Agreement (LGIA) for all generators with a generation capacity greater than 20 MW, but made no distinction between synchronous and variable-speed generators (Zavadil et al. 2005). In response, the wind industry, including the American Wind Energy Association and Western Electric Coordinating Council, developed proposals for interconnection standards and guidelines specific to wind generation. In June 2005, FERC issued Order No. 661, requiring public utilities to include technical requirements and standard procedures for the interconnection of large wind-generating plants in their large generator interconnection procedures and LGIAs (70 FR 47093). The requirements address low voltage ride through (LVRT) capability, SCADA capability, and power factor design criteria. After that, the American Wind Energy Association and NERC jointly proposed changes to the LVRT standard, and FERC issued Order No. 661-A in December 2005, updating the LVRT provision in Order No. 661 (USFER Commission 2005).

In 2012, NERC's Integration of Variable Generation Task Force released a special assessment of its Interconnection Requirements for Variable Generation to address voltage and frequency ride-through, reactive and real power control, and frequency/inertial response criteria specific to the technical characteristics of variable generation (NAER Corporation 2012). Recommendations from the Integration of Variable Generation Task Force to update standards and procedures are currently being implemented. In compliance with NERC and FERC standards, regional reliability organizations have established regional versions of the grid codes. The two regional grid codes studied here are from ISO-NE and ERCOT. These two regional grid codes were studied because both have relatively high wind installation targets, designed their grid codes after extensive studies, and are representative of subnational grid codes. In November 2009, ISO-NE released the Technical Requirements for Wind Generation Interconnection and Integration as part of its wind integration study, commissioned "in anticipation of significant wind generation development" (GE Energy Applications and Systems Engineering 2009). Prepared by GE, EnerNex, and AWS Truepower, the study makes specific recommendations for ISO-NE's wind interconnection policies and practices. ERCOT has incorporated many technical requirements for WPPs into its Nodal Operating Guides, which specify practices for the ERCOT system with NERC standards and ERCOT Nodal Protocols. In July 2010, ERCOT released a summary of the significant WPP requirements in its region that specified the three requirements placed on wind turbine generators in ERCOT "above and beyond their general responsibilities as interconnected generators": voltage ride-through, reactive support, and frequency response (Lasher 2010).

Appendix F. DTC Supplemental Information

F.1 FACTS

The power system has traditionally been controlled by mechanically operating switches, and, recently, Flexible Alternating Current Transmission System (FACTS) has introduced a new methodology to improve the performance of the existing system. FACTS is defined by the IEEE as, "a power electronic based system and other static equipment that provide control of one or more AC transmission system parameters to enhance controllability and increase power transfer capability" (FACTS Terms & Definitions Task Force 1997).

These systems have been deployed across the globe at various locations for solving power system transmission issues like reactive power management, voltage profile maintenance, oscillation damping, and power flow control. These controllers help increase the power transmission capability without having to invest in land and in transmission infrastructure with minimum investment. Recent interest in the smart grid and renewables has opened up new opportunities for integration of FACTS controllers with energy storage systems and renewables (Joshi 2019).

A FACTS controller is used to generally characterize the various power electronic circuit topologies or equipment that perform a certain function, such as current control, power control, and other functionalities. In general, FACTS is a relatively new technology, with the principal role of enhancing controllability and power transfer capability in the AC system. FACTS involves conversion or switching power electronics in the range of few tens to a few hundred MW (Hingorani and Gyugyi 1999).

F.2 Inverter based resources

Inverter-based resources (IBRs) are different from the conventional synchronous generator. To understand the difference, both the synchronous generator and IBRs will be reviewed.

The Conventional Synchronous Generator

To simplify the illustration, the armature resistance of the synchronous generator is assumed to be negligible compared to the synchronous reactance (X_s). In a synchronous generator, the real power (P) and the reactive power (Q) are not completely independent. In a conventional generator, usually, to raise the output power (real power), the fuel input to the prime mover is increased. But the change in real power (P) will affect the terminal voltage because of the changes in the voltage drop across the synchronous reactance (IX_s). Thus, the automatic voltage regulator continuously regulates the field current to adjust the internal voltage (E_f). By increasing or decreasing the internal voltage (E_f), the terminal voltage (V_t) will be regulated as the output power changes.

The output of the synchronous generator can be expressed as:

$$P_{3\phi} = \frac{3|V_t||E_f|}{|X_s|} \sin\delta = P \sin\delta_{max}$$

$$P \frac{3|V_t||E_f|}{|X_s|}_{max}$$

$$Q_{3\phi} = \frac{3|V_t||E_f|}{|X_s|} \cos\delta - \frac{3|V_t|^2}{|X_s|} \; VAR \qquad (23)$$

The real power (P) is usually controlled or set according to the demand; it is also adjusted by the so-called governor that will change the real power linearly with the frequency deviation. This linear control of the governor is set to a certain value (droop). For example, it is common to set the droop as 5% to adjust the real power output automatically as the frequency deviates from the rated value. A 5% droop means that the drop of 5% of frequency will give an additional boost of 100% rated power. Keep in mind that the allowable frequency deviation is very small. For example, from the NERC-PRC024, it is shown that the allowable frequency range within ERCOT is $\pm$3% for up to 500 seconds. This means the response time of the governor action must be quick (within minutes) to adjust the real power. The response time in a conventional power plant is limited by the response time of the governor action from the time it sensed the frequency deviation to the actual change of the real power desired. This is limited by the time-constants of the governor, the fuel injection, and the sensors.

The voltage and reactive power control are directly adjusted by the field excitation, where an increase in the field excitation current (DC) will increase the internal voltage (emf E_f). This, in turn, will increase the reactive power output power of the generator. In short, the reactive power output of the synchronous generator can be increased by controlling the field current (I_f), which in turn will increase the magnitude of the emf voltage (E_f) (which also increase the terminal voltage (V_t) of the generator). The time it takes from sensing the voltage deviation to actually producing the desired terminal voltage is limited by the response time (time constants) of the sensors, the field winding (which has actually long-time constant F_{lu}/R_f), and the field voltage regulator.

The IBR

IBR (PV, wind) generators are usually controlled by the output current, using current-controlled pulse width modulation. Thus, the control of real and reactive power is easier to manage. In addition, it is usually controlled based on the reference phasor angle of the grid voltage.

To simplify the illustration, the voltage and current phasors are shown in Figure F-1, where the synchronous reference frame q-axis is synchronized to Phase A of the grid voltage ($V_{s.} = 0$). As shown in Figure F-1, the real and reactive power can be controlled independently by controlling the output current components, I_{ts} and I_{ds}, respectively. This is easily accomplished by the control action of the power converter connected to the grid side of IBRs. Another important aspect of the IBR control is that the response time is practically instantaneous, so the time constant of the fuel injection, or the mechanical time constant due to the inertia of the rotating mass, does not appear in an IBR system.

The real and the reactive power can be easily controlled, and the equations can be expressed as

$$P = 3\ V_{ass}\ I_{qs} \text{ and } Q = 3\ V_{os}\ I_{ds}$$

It is generally controlling real and reactive power in an inverter-based resources is independent and instantaneous. That is why the IBRs offer a very fast and flexible control of P and Q instantaneously and independently.

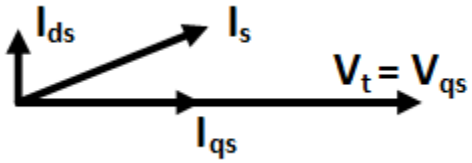

Figure F-1. V_t, I_d, and I_s phasor representation

Capability and Flexibility

As described in the previous subsection, the real power and reactive power of IBRs (PV, Wind, advanced PSH) can be controlled independently and instantaneously. The response to the real power command is not impeded by the time constant of the fuel injection or mechanical and thermal time constant. Similarly, the response to the reactive power command is not impeded by the time constant of the field winding and excitation circuit of a synchronous generator.

Figure F-2 shows a comparison of capability curve between a synchronous generator and an IBR (see also Section 2.1.2.2). Note that the limitation bounds which appear on a synchronous generator (armature/stator current heating limit, and the field winding heating limit) disappear in an IBR generator, and this extends the operating area significantly.

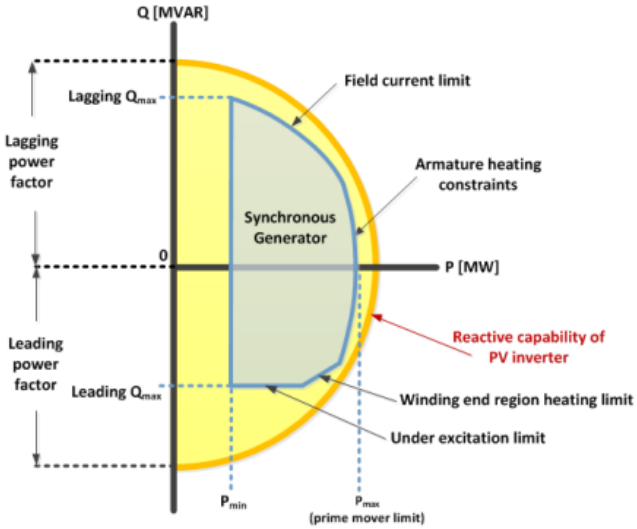

Figure F-2. Capability curve comparison between the conventional synchronous generator and IBR

The proposed CAISO reactive capability for asynchronous resources is shown in Figure F-3. The vertical axis is the real power output, and the horizontal axis is the reactive power output. The positive value of the reactive power output indicates that the VAR is produced by the resource, and negative value of the reactive power output means that the VAR is absorbed by the resource. Positive VAR usually means that the generator provides reactive power to increase the voltage at the point of injection (where the generator is connected), while the negative VAR means to absorb reactive power from the grid, thus reducing the voltage at the point of injection. The dynamic reactive power capability ensures the ability to quickly adjust the reactive power at a specified output power up to its limit. It is also shown for two different sets of power factor (power factor =

± 0.985 and power factor = ± 0.95), where the lower power factor (a larger reactive power Q) range is desirable for weaker grid interconnection.

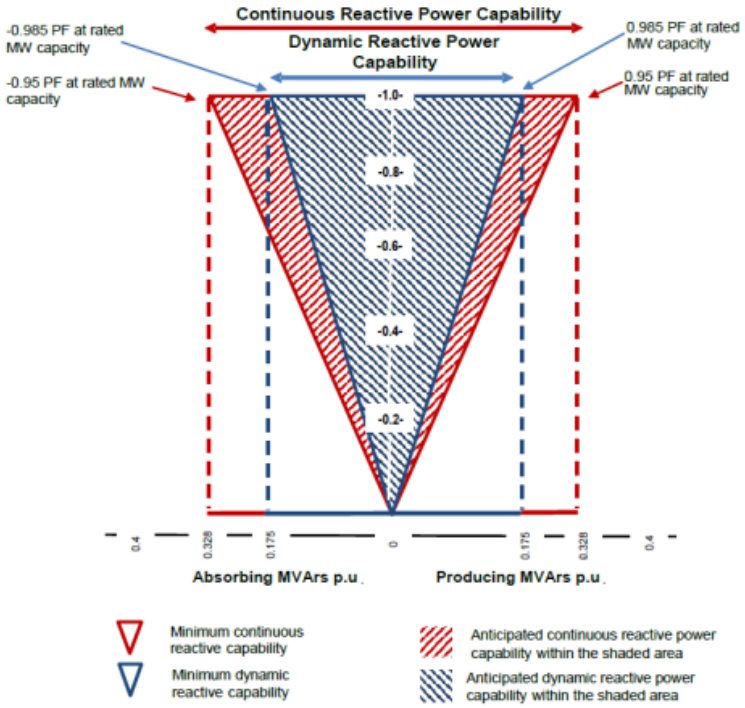

Figure F-3. Proposed CAISO reactive capability for asynchronous resources

Appendix G. WI Frequency Response Under High Renewable Penetrations

One of the more challenging stability situations in the WI is when it is minimally loaded with significant amounts of the needed energy being supplied by variable generation. The 2022 Light Spring (LSP) scenario standardized planning case was developed for testing grid performance under such conditions (low load, high renewables).

The LSP model is implemented in GE's PSLF platform. It contains approximately 117 GW of online generation, 367 GW of total capacity, more than 19,000 buses, and has a system inertia of 2.89 (Tan et al. 2018). More than 4,000 generators are represented, each with their own dynamic model which was derived from real data. The contribution of total online renewable is 23.51%, (Figure G-1), and this model provides an ideal foundation for studying the performance of T-PSH under challenging system conditions.

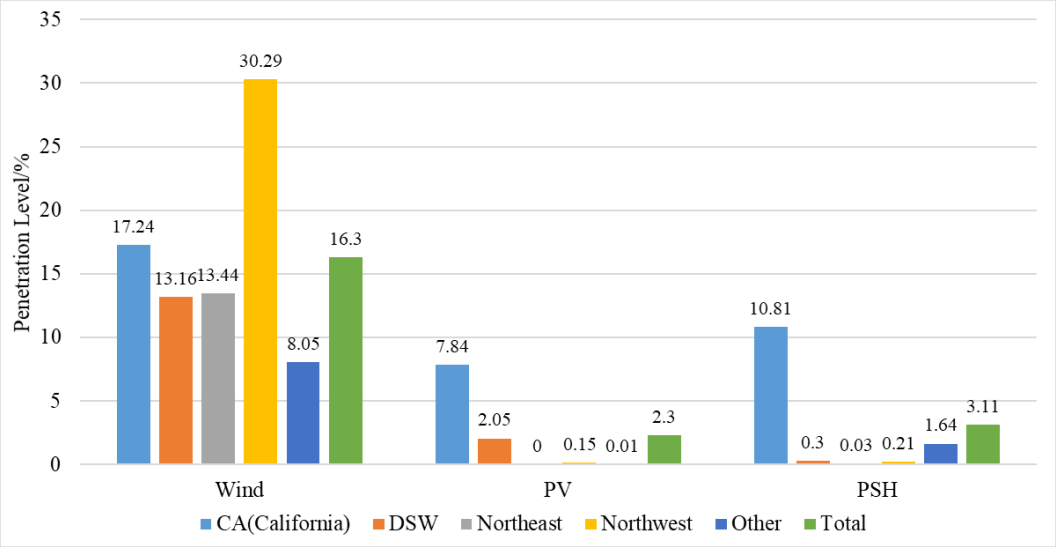

Figure G-1. Percentage of renewable energy contribution level in each area

G.1 The Role of PSH in WI Frequency Response Under High Renewable Penetrations

This section summarizes the analysis of T-PSH performance under increasing amounts of variable renewable energy, where C-PSH performance serves as the baseline.

To setup the test environment, four renewable penetration test models were required and derived from the WI LSP model described in the previous section. The renewable contribution levels, which varied from 20% to 80%, were created by selectively replacing traditional power plants by PV plants (Liu et al. 2018). The first change was to replace the fossil fuel power plants, the second was the hydropower plants, and the last was the nuclear plants. This replacement was based on existing PV resource data and PV technical potential estimation in the National Solar Radiation Database (Tan et al. 2018; Tan et al. 2017). The detailed contribution parameters are shown in Figure G-2 and Table G-1, in which the contribution level of the wind power remained basically the same, and the penetration level of solar energy increased linearly. The remaining penetration comes from the PSH units when implemented in these cases. In PSLF, only the dynamic models of these thermal power plants were replaced by a GE Type 4 wind power plant model, as suggested

in (Clark, Walling, and Miller 2011; Miller et al. 2015). As synchronous machines were gradually replaced by PV generation units, the system equivalent inertia decreased linearly with the increase in renewable contribution level, as shown in Figure G-2 Especially, the system equivalent inertia is calculated below:

$$H_{sys} = \frac{\sum_{i=1}^{n} H_i \times S_i}{S_{sys}} \qquad (24)$$

where H_i is inertia of the i^{ts} synchronous generator, S_i is the rating capacity of the i^{t} synchronous generator, and S_{assy} is the rating capacity of grid.

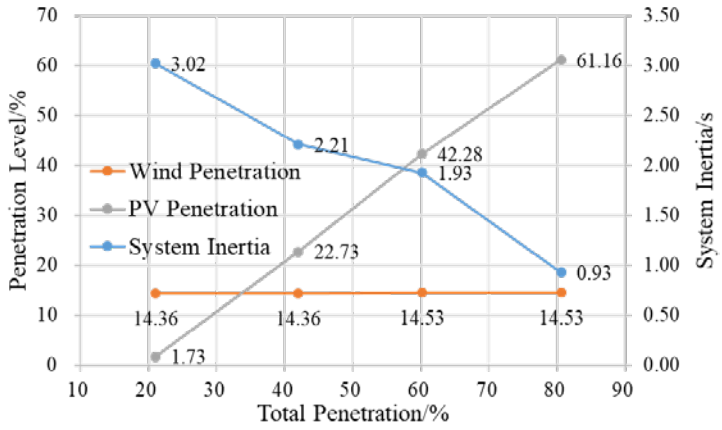

Figure G-2. System Contribution and Inertia in Each Case

Table G-1. System Contribution and Inertia of Different Contribution Cases

Case	System Inertia	Wind Contribution	PV Contribution	PSH Contribution	Total Contribution
20% case	3.02	14.36%	1.73%	4.94%	21.03%
40% case	2.21	14.36%	22.73%	4.94%	42.02%
60% case	1.93	14.53%	42.28%	3.35%	60.16%
80% case	0.93	14.53%	61.16%	4.92%	80.61%

The next section describes the baseline C-PSH study that was performed. It is followed by a comparison of how T-PSH and Q-PSH performed under the same grid conditions.

G.2 Developing a C-PSH WI Frequency Response Baseline

Before studying the performance of T-PSH under an extremely high renewable contribution level, the system with C-PSH in pumping mode was analyzed to provide a reference baseline. The N-2 contingency used previously was applied at 10 seconds in each contribution case (Tan et al. 2018). To find out the frequency response of C-PSH units under different contribution levels, all protective devices in the WI system were disabled. To more accurately show the frequency response of the whole system, the system frequency was calculated by using the center of inertia (COI) frequency, expressed below:

$$f_{coi} = \frac{\sum_{i=1}^{n} H_i \times f_i}{\sum_{i=1}^{n} H_i} \qquad (25)$$

where H_i is inertia of the ith area and f_i is frequency measured in the ith area. The frequency was measured at a randomly selected bus with the highest voltage level in each area.

The frequency results shown in Figure G-3 illustrate that the system's frequency response declined with increasing contributions of renewable energy. Figure G-4 shows that there is a larger overshoot after a frequency event when the system has a higher contribution level. This overshoot in electrical power results is related to the frequency dip. After that overshoot, the results illustrate that the C-PSH units themselves cannot adjust their output by using a governor in the pumping mode. The frequency regulation was provided by the limited number of synchronous generators. Contributing to increasing poor frequency response are reduced system inertia, the slow response of traditional synchronous plants, and a limited number of frequency regulation providers. To make matters worse, C-PSH units, as part of the synchronous plant in the system, cannot respond to the frequency event when in the pumping mode. In the 80% case, the frequency nadir was lower than the set point, 59.5 Hz, of the first stage of underfrequency load shedding, and the protective devices would have triggered load shedding in the 80% contribution level case. Therefore, a certain degree of power outage would have occurred in the 80% renewable penetrated WI system case. Although the 60% contribution case was spared from protective load shedding, the frequency nadir shown in Figure G-5 indicates that the nadir was very close to the set point of the underfrequency load shedding. Because of this, the WI system with C-PSH units whose renewable contribution level was higher than 60% will not survive this N-2 contingency.

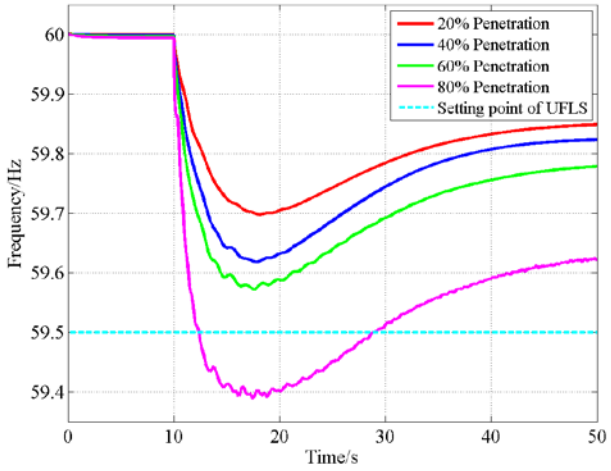

Figure G-3. COI Frequency responses of C-PSH units under different renewable contribution levels

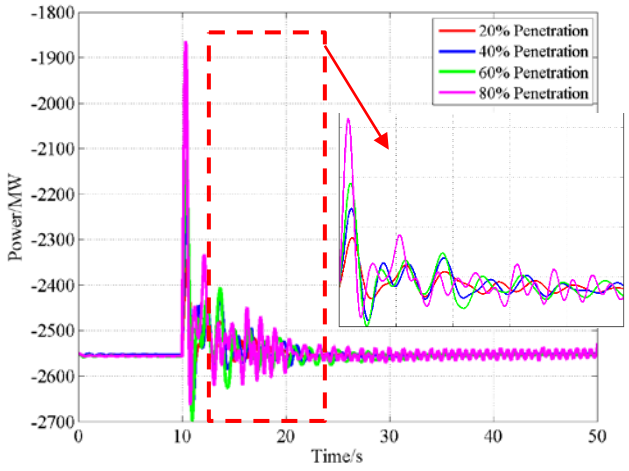

Figure G-4. Electrical power output of C-PSH units under different renewable contribution levels

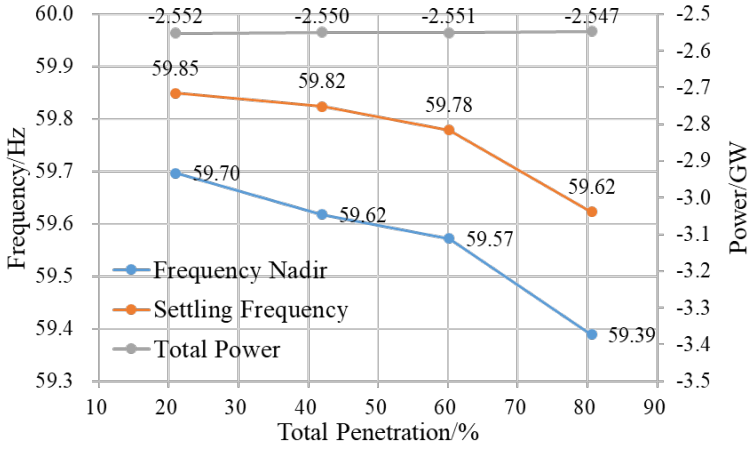

Figure G-5. Frequency nadir, settling frequency, and total power outputs of the C-PSH in each case